universität wien

MASTERARBEIT / MASTER'S THESIS

Titel der Masterarbeit / Title of the Master's Thesis

„Assessment of binding characteristics of antibodies against polysaccharide antigens in human serum“

verfasst von / submitted by

Kai Sauerwein BSc

angestrebter akademischer Grad / in partial fulfilment of the requirements for the degree of

Master of Science (MSc)

Wien, 2019/ Vienna, 2019

Studienkennzahl lt. Studienblatt / degree programme code as it appears on the student record sheet:	A 066 862
Studienrichtung lt. Studienblatt / degree programme as it appears on the student record sheet:	Masterstudium Chemie UG2002
Betreut von / Supervisor:	Univ.-Prof. Mag. Dr. Margit Cichna-Markl

Dedication

This thesis is dedicated to my wife Stefanie, who showed me how to buckle down and work. Let this be a small paragraph within the story we write together. It is dedicated to my mother, who sparked the interest for all things within me, my uncle who introduced me to science and guided me along the way and the rest of my family, who supported me financially , mentally and also professionally until this point in my life. I hope to return what was given.

Declaration

I declare that this thesis was composed by myself, that the work contained herein is my own except where explicitly stated otherwise in the text, and that this work has not been submitted for any other degree or processional qualification. Parts of this work have been published (*1–3*).

Acknowledgements

Special thanks to Professor Wolf and Professor Cichna-Markl for many hours of discussion and guidance while working on this thesis. I would also like to acknowledge Professor M. Eibl and thank all members of the Immunology Outpatient Clinic for allowing me to conduct my research and providing any assistance requested especially Christoph Geier, MSc and Ing. Hüseyin Akyaman. I also thank Professor M. Fischer for advice and guidance regarding SPR analysis.

Contents

1 Introduction **7**

1.1 Kinetic description of the antigen-antibody binding event 9

1.2 Determination of association and dissociation rate constants (k_a and k_d) using SPRS 10

1.3 Determination of dissociation equilibrium constant (K_D) using ELISA 15

1.3.1 The Hill equation as the regression model used to calculate K_D 16

1.4 Isoagglutinins and anti PNV23 antibodies 17

2 Methods **19**

2.1 Surface plasmon resonance spectroscopy (SPRS) - analysis of blood group A or B antibodies 19

2.2 PNV23 ELISA 21

2.3 Anti blood group A ELISA 21

2.4 Determination of Anti-A/B Antibody Titers by the DiaMed-ID Micro Typing System 22

2.5 Data analysis 22

3 Results **23**

3.1 Surface Plasmon Resonance spectroscopy 23

3.1.1 Establishment of isotype specific quantification of anti polysaccharide antibodies within serum 23

3.1.2 Establishment of avidity estimation of anti polysaccharide antibodies in serum by SPRS 34

3.1.3 Final Workflow 40

3.1.4 Application 40

3.2 Anti-A/B ELISA 44

3.3 Anti-PNV23 IgG titration ELISA 45

3.3.1 Establishment of data analysis 46

3.3.2 Consideration of Hill coefficient 50

3.3.3 Independence of K_D from the serum antibody concentration . 51

3.3.4 Variation of PNV23 antigen concentration for coating 51

3.3.5 Repeatability 55
3.3.6 Could difference in optical density measured after different incubation periods serve as a substitute for calculation of K_D ? 56
3.3.7 Shorter incubation period of serum sample tested in ELISA . 57
3.3.8 Summary 57
3.3.9 Application 60

4 Conclusion and Discussion **64**

A Abstracts **74**
A.1 Abstract - english 74
A.2 Abstract - german 75

B Publications **76**

Chapter 1

Introduction

To diagnose immunodeficiencies with predominant antibody deficiency like common variable immodeficiency (CVID), agammaglobulinemia or selective deficiency of immunoglobulin isotypes the concentration of immunoglobulin within serum is routinely determined. Their physicochemical properties like the affinity of the antibody to its antigen and hence the strength of the antigen-antibody bond is not routinely taken into account. This is mostly due to the absence of assays to determine antibody affinity that can be integrated into an everyday diagnostic routine even in the immunology laboratory. However the heterogeneity of patients with presumed antibody failure calls for additional criteria to further separate them and enable the design of a more specific therapy (*4*). The aim of this master thesis is to describe a routinely applicable method to allow for screening of large patient cohorts. The bioanalytical challenge consists of finding a method and form of analysis that is suitable for measurement of serum samples, which constitute a highly complex matrix since the limitation of costs, expenditure, sample volume and duration does not allow for purification of the analyte (e.g. anti-polysaccharide antibodies) for each sample by affinity chromatography or likewise. An intensive treatment would also most likely compromise the integrity of the sample and introduce analysis bias.

SPRS has been the gold standard for determination of binding characteristics of receptor ligand pairs, or antigen-antibody interactions (*5–10*). Alternatively Syedbasha *et al* described a protocol to determine the dissociation equilibrium constant using a direct Ligand-Receptor interaction assay for ELISA, which in contrast to SPRS is inexpensive and does not require special laboratory equipment (*11*). In brief the receptor is immobilized to the plate at a constant concentration and different concentrations of ligand are added afterwards. After addition of secondary antibodies and substrate the resulting optical density is measured and plotted against concentration. The data points are regressed applying the commonly used Hill-equation and K_D is read as concentration at half-maximum binding. This assay is based on previously described methods by Rosenbluh et al and Levin et al

(*12*, *13*). Eble et al presented an equation tailored specifically to the binding curve yielded by titration ELISA assays (*14*), proving that the dissocation equilibrium constant can be calculated from titration assays. However this equation was only applied to a monovalent binding system meaning that both receptor and ligand exhibit only one binding site. It was to be determined if this equation works for antigen-antibody binding curves. In addition to avidity determination solely based on analysis of binding curves generated by ELISA a method relying on addition of chaotropic reagents such as ammonium thiocyanate or urea were presented (*4*, *15*). For this the ratio of bound to unbound antibody is plotted against the molar concentration of the chaotropic agent. The avidity index is interpolated from this plot and is defined as the molar concentration of thiocyanate that corresponds to 50 % binding (*4*). This assay is based on the ability of the antigen-antibody complex to withstand attack by a chaotropic agent, which means the disruption of hydrogen bonds. However antigen-antibody interactions are not only based on hydrogen bonds, but also electrostatic interactions, van der Waals forces and hydrophobic interactions. Thus an assay based on chaotropic disruption estimates how much the antigen-antibody interaction is based on hydrogen bonds for a given antibody in the strict sense. This certainly correlates to the avidity of said antibody but since it is the least precise estimate for an in-vivo avidity, this approach was not pursued any further. In this study surface plasmon resonance spectroscopy (SPRS) and enzyme linked immunoabsorbent assay (ELISA) are used to determine the avidity of antibodies against polysaccharide antigens. Explicitly IgG antibodies against blood group A and B polysaccharide antigens and 23-valent anti-pneumococcal capsular polysaccharide vaccine are the analytes of choice. The primary difference between the two methods is the time-dependence of the antibody binding reaction. With SPRS real-time binding events can be determined, which means that the increase and decrease of antigen-antibody complex (AbAg) is displayed in a time-dependent manner. ELISA on the other hand only measures a signal after the binding reaction reached equilibrium. Both methods complement each other since SPRS is better suited for determination of reaction rate constants, whereas ELISA provides the reaction equilibrium constant.

1.1 Kinetic description of the antigen-antibody binding event

The formation of the antigen-antibody complex (AbAg) can be described by equation 1.1, whereas dissociation of said complex follows equation 1.2.

$$\mathrm{Ab} + 2\,\mathrm{Ag} \rightleftharpoons \mathrm{AbAg_2} \tag{1.1}$$

$$\mathrm{AbAg} \rightleftharpoons \mathrm{Ab} + \mathrm{Ag} \tag{1.2}$$

For both reactions an equilibrium constant (association equilibrium constant K_A) based on the law of mass action can be formulated (equations 1.3, 1.4). For AbAg formation this constant is called association equilibrium constant (K_A), for dissociation of said complex this constant is called dissociation equilibrium constant (K_D) (equations 1.3, 1.4).

$$\mathrm{K_A} = \frac{[\mathrm{AbAg_2}]}{[\mathrm{Ab}] \cdot [\mathrm{Ag}]^2} \tag{1.3}$$

$$\mathrm{K_D} = \frac{[\mathrm{Ab}] \cdot [\mathrm{Ag}]}{[\mathrm{AbAg}]} \tag{1.4}$$

Both reactions consist of the same two parts; the association and dissociation happening at the same time. To formulate reaction rates (the association rate constant k_a and the dissociation rate constant k_d) both reactions can be considered separately (equation 1.5, 1.6)

$$\mathrm{Ab} + 2\,\mathrm{Ag} \xrightarrow{k_a} \mathrm{AbAg_2} \tag{1.5}$$

$$\mathrm{AbAg} \xrightarrow{k_d} \mathrm{Ab} + \mathrm{Ag} \tag{1.6}$$

This shows that association is a reaction of third order, whereas dissociation is a reaction of first order. Accordingly the reaction rate for association is described by equation 1.7 and for dissociation by equation 1.8.

$$v = \frac{-\mathrm{d}[\mathrm{AgAb}]}{\mathrm{dt}} = \mathrm{k}_a \cdot [\mathrm{Ab}] \cdot [\mathrm{Ag}]^2 \tag{1.7}$$

$$v = \frac{-\mathrm{d}[\mathrm{Ag}]}{\mathrm{dt}} = \frac{-\mathrm{d}[\mathrm{Ab}]}{\mathrm{dt}} = \mathrm{k}_d \cdot [\mathrm{AbAg}] \tag{1.8}$$

For the purpose of assessing the affinity of antibodies determination of K_D is more applicable, because the physical intepretation of equation 1.4 is simple. If knowing K_A is of importance it can be calculated by equation 1.9 (*16*).

$$\mathrm{K_A} = \frac{1}{\mathrm{K_D}} \tag{1.9}$$

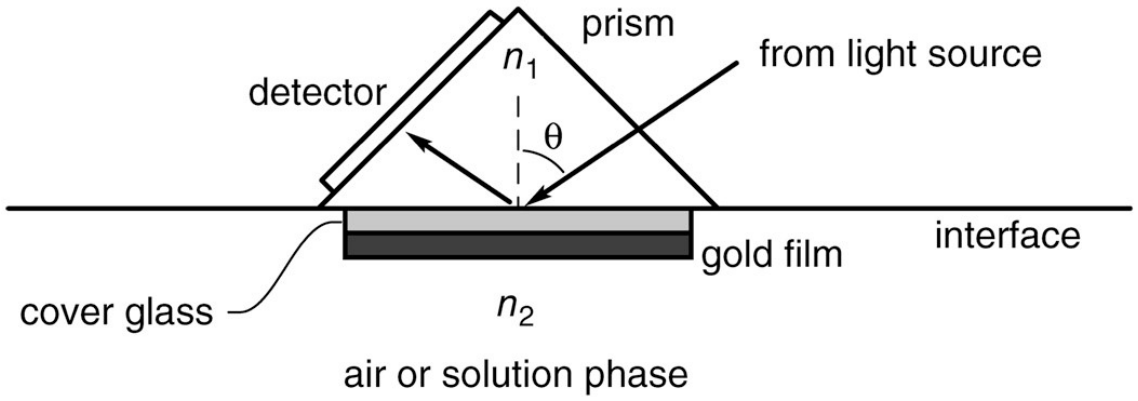

Figure 1.1: Schematic presentation of the sensor used in surface plasmon resonance spectroscopy; n1: Medium with higher refractive index; n2: Medium with lower refractive index; θ: incident angle; total internal reflexion (TIR) within n1 occurs if θ is greater the θ_c (critical incident angle) ($sin(\theta_c) = n2/n1$) leading to surface plasmon resonance; adsorption at medium n2 changes the refractive index of the medium, changing the angle at which SPR occurs; measuring the change of PR angle allows for detection of association or dissociation of macromolecules to the surface (*17*).

1.2 Determination of association and dissociation rate constants (k_a and k_d) using SPRS

When a light beam hits a half circular prism at an incident angle θ greater than the critical incident angle θ_c total internal reflexion occurs, meaning that all the incoming light reflects within the prism (figure 1.1). Evanescent waves are formed in the process and if the prism is coated with a film of noble metal such as gold the electrical field interacts with the free electron constellations in the gold surface namely shell and conduction band electrons. In this way the photons are absorbed and the energy is transferred to the electrons turning them into surface plasmons. These are quanta of plasma, a surface electromagnetic wave whose propagation is confined to the metal dielectric interface (*17*). During this conversion the energy and momentum of the photon have to be conserved. If the momentum of the incoming light (photon) matches the characteristic momentum of plasmons, depending on the nature of the conducting film and the properties of the medium on either side of the film among other things, resonance occurs. The angle at which surface plasmon resonance occurs is dependent upon the refractive index of the media on either side of the metal film. Adsorption at the side opposed to the prism changes the refractive index of the media (n_2), thus changing the angle at which surface plasmon resonance occurs. The measurement of the change of surface plasmon resonance angle allows for detection of association and dissociation of e.g. biomolecules to the surface (figure 1.2).

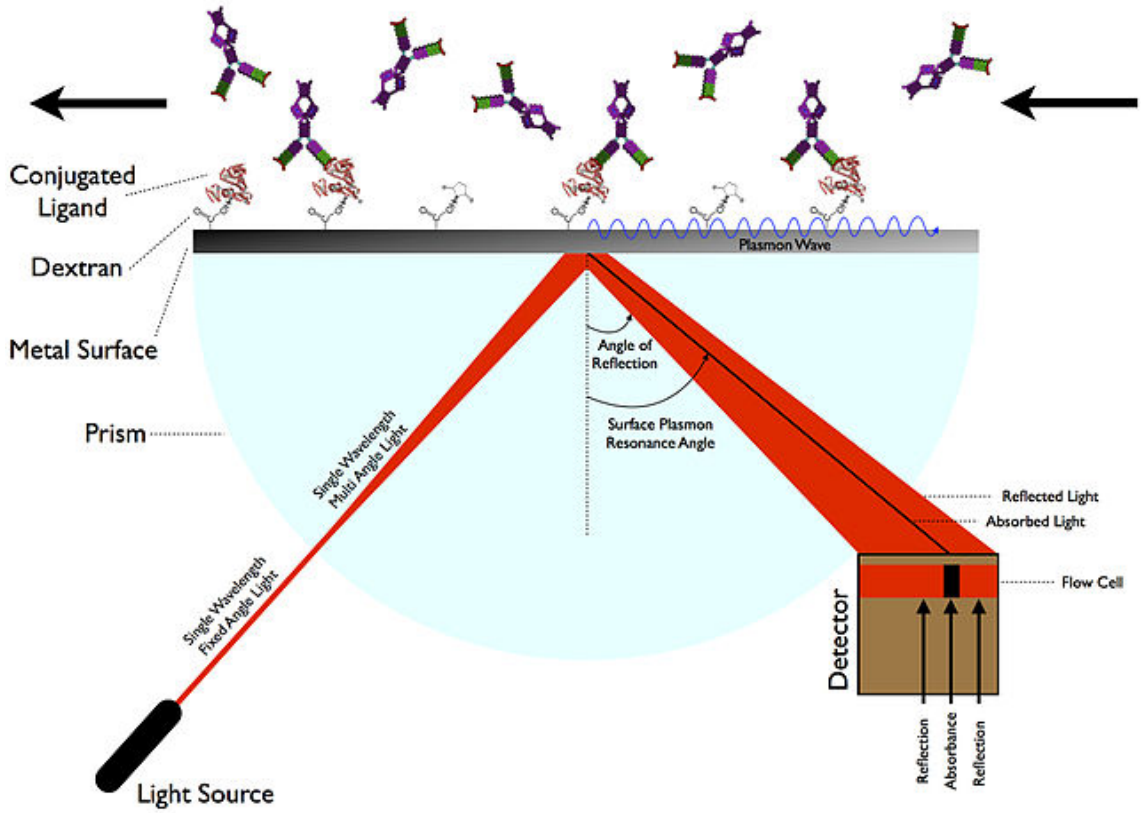

Figure 1.2: Ad- and desorption of antibodies to antigens immobilized onto the dextran/metal surface under a constant stream of aqueous buffer. This process changes the surface plasmon resonance angle, which is recorded and transformed into a sensorgram. This sensorgram can be analyzed to yield association and dissociation rate constants of the binding reaction (*18*).

To achieve association of biomolecules a capture molecule is immobilized onto the surface. For this the surface is functionalized using different functional groups (see figure 1.2). In this study a CM5 chip with a carboxylated dextran surface is used. EDC (1-ethyl-3-(3-dimethyl-aminopropyl)carbodiimide hydrochloride) is used to activate carboxyl groups and adding N-hydroxysuccinimide leads to formation of amine-reactive esters. The capture molecules (blood group antigens) are derivatized with primary amino groups and thus a peptide-like covalent bond is formed to immobilize the antigen (*19*).

In SPRS measurements the analyte (e.g. antibody) flows constantly over the surface containing the immobilized capture molecule (e.g. antigen) for a distinct period of time. After a set period of time, injection of analyte stops and only buffer flows over the surface. As long as the buffer contains analyte, resonance units (RU) increase and for buffer only RU decrease, depicting the association and dissociation reactions (figure 1.3). The uniqueness of this method becomes apparent when looking at the association and dissociation rates (equation 1.7, 1.8 vide supra). The continuous stream of analyte leads to its concentration being constant, since it is continually replenished, if mass transfer limitation is minimized. This means that the concentration of analyte equals the concentration of the provided solution at all times during association. In other words excess of analyte is guaranteed at all times, if the initial concentration is chosen accordingly. This ensures the actual association and dissociation are the rate determining steps for the reaction. The increase of response units is given by the difference of association to dissociation (equation 1.7, 1.8) (*20–22*).

The initial concentration of capture molecule available for ligand binding equals the concentration that was immobilized, which decreases when binding occurs, slowing the increase of response units down and inevitably leading to establishment of a steady state, which persists as long as analyte is injected. When injection of analyte stops analyte starts to dissociate and is continuously removed from the surface by the buffer stream. Thus association does not contribute to the change of RU anymore and the decrease of response is only given by the maximal response times the dissociation constant (equation 1.8). Figure 1.3 shows a sensorgram as recorded by SPRS depicting association, steady state and dissociation. In SPRS the affinity or equilibrium dissociation constant is calculated by equation 1.12. It is not determined directly. During association every analyte molecule has to reach the binding surface through diffusion; the delay this diffusion causes is called *mass transport limitation* (MTL) (figure 1.4). This can be described by equation 1.10. MTL occurs if the analyte binds faster to the surface than it can diffuse to it, creating a shortage of analyte at the interaction surface and diffusion thus becomes the rate determining step. So reducing MTL is a matter of excess of analyte. Excess can be established

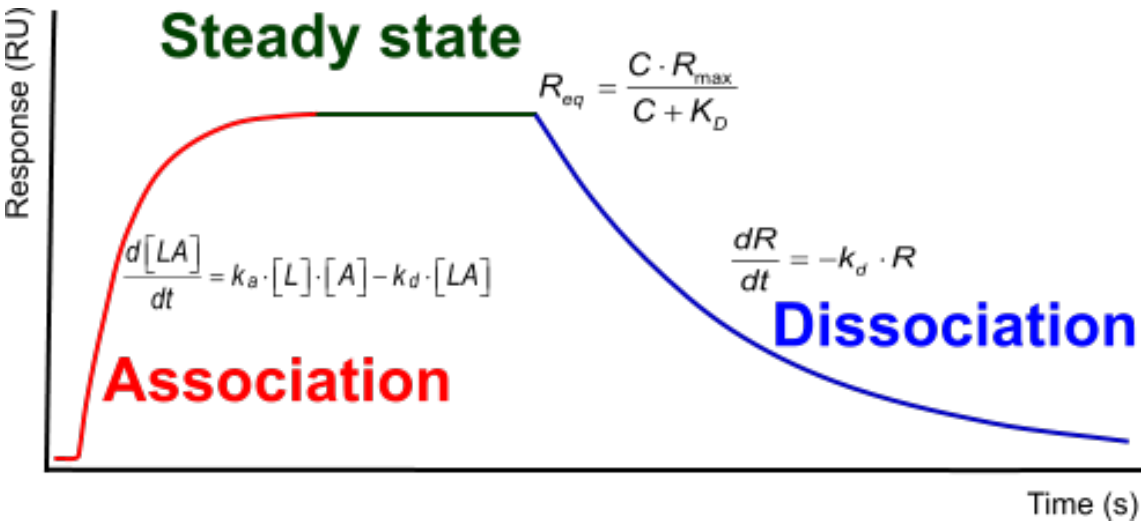

Figure 1.3: Sensorgram as recorded by SPR spectroscopy and equation describing association, steady state and dissociation curve (source: <https://www.sprpages.nl/kinetics> , 15.02.2019)

by either increasing concentration of analyte or decreasing concentration of surface bound capture molecule. As mentioned above determination of antibody avidity in patient serum by methods that require antibody purification is not feasible. This means that the concentration of antibody within its matrix cannot be increased, which leaves only alteration of immobilized capture molecule.

$$\mathrm{A(bulk)} \xrightarrow{k_T} \longrightarrow \mathrm{A(surface)} + \mathrm{L} \xrightarrow{k_a} \mathrm{LA} \tag{1.10}$$

Moreover mass transfer is influenced by the diffusion coefficient of the analyte, flow cell dimensions and the flow rate. The diffusion coefficient is constant for a given flow cell and flow rate can be increased to reduce MTL. To assess the degree of MTL the curvature of binding curves must be considered (figure 1.5). Kinetic parameters calculated from curves lacking curvature reflect more the mass transfer rate than the actual binding kinetics (*23*). If the diversity of the matrix for different samples is high, which is the case for serum samples, unspecific binding becomes an issue. To eliminate this problem the antibody of interest has to be purified before assessing its avidity, thereby essentially reducing the complexity of the matrix to almost zero. This however is highly costly both in time and financial resources and requires high volume of each sample, making it a non-feasible choice if establishment of avidity as a routinely determined parameter is the goal. Instead the issue can be minimized by ensuring conditions that are as close to physiological as possible and carefully considering the antigen-antibody relationship from a biological point of view. Physiological conditions are approximated firstly by ensuring physiological conformation of antibody and antigen. This can for instance be achieved by leaving

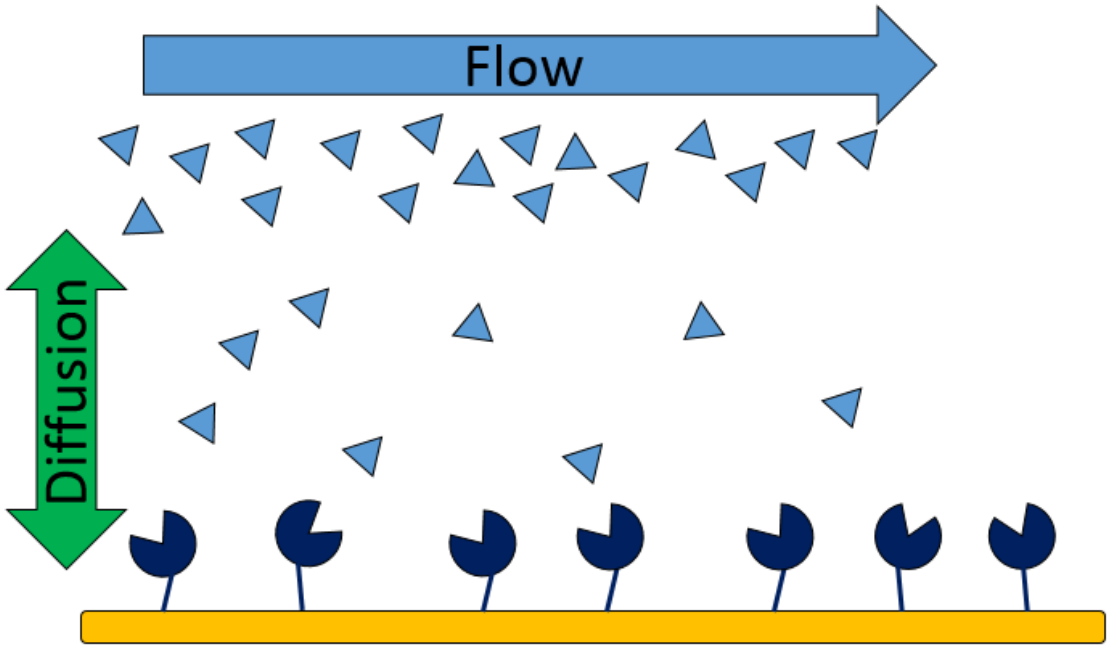

Figure 1.4: Depiction of diffusion of analyte molecules to binding surface (source: https://nicoyalife.com/blog/3-ways-to-limit-mass-transfer-effects/, 15.02.19)

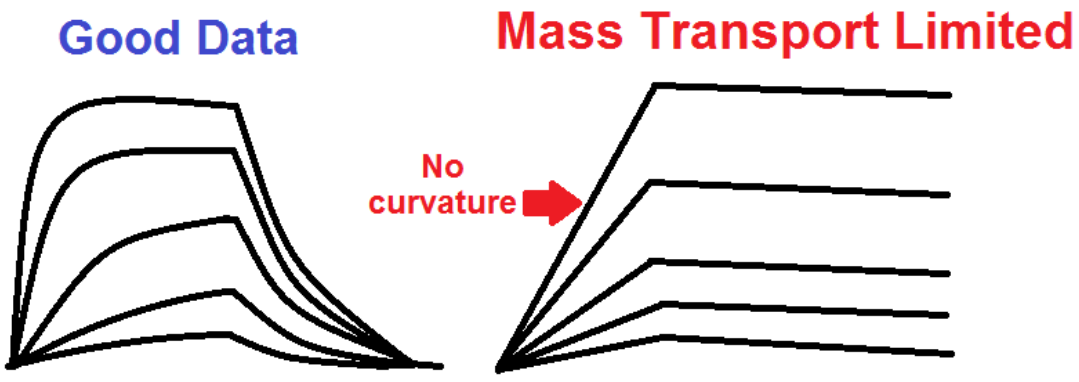

Figure 1.5: Binding curves without (good data) or with (Mass Transport Limited) influence of MTL (source: https://nicoyalife.com/blog/3-ways-to-limit-mass-transfer-effects/, 15.02.19)

them in their natural environment (i.e. serum) or by immobilization of the antign through a separately introduced functional group like primary amines, so that the actual binding site remains unaffected. Secondly under physiological conditions there is not a plethora of molecules in human serum that bind to a given antigen in addition to the antibody. Generally for antigens only the respective antibody and molecules from the innate immune system are to be considered. For instance for carbohydrate as antigens, mannan-binding lectin (MBL) can lead to unspecific binding. However, this oligopeptide is not known to bind to blood group polysaccharides. If a molecule like LPS is the antigen unspecific binding must be considered more carefully. Using SPRS has the benefit of minimizing unspecific binding, because all interactions take place under a constant flow of sample over the immobilized antigen. This puts an additional pressure onto ligand binding removing those ligand bindings with lesser affinity, characteristic for unspecific binding (*24*).

1.3 Determination of dissociation equilibrium constant (K_D) using ELISA

When the association and dissociation reaction of AgAb (equation 1.1) reaches equilibrium, reaction rates of formation and dissociation of AbAg are equal. The reaction is balanced and no change in concentration of AgAb is observable. In contrast to steady state no further input of energy is required to maintain this status. In this case equation 1.11 and subsequently the dissociation equilibrium constant K_D can be formulated.

$$\mathrm{k}_a \cdot [\mathrm{Ag}] \cdot [\mathrm{Ab}] = \mathrm{k}_d \cdot [\mathrm{AgAb}] \tag{1.11}$$

$$\frac{\mathrm{k}_d}{\mathrm{k}_a} = \frac{[\mathrm{Ag}] \cdot [\mathrm{Ab}]}{[\mathrm{AgAb}]} = \mathrm{K_D} \tag{1.12}$$

According to equation 1.4 K_D is given in units of concentration, thus it can be equated to measures of concentration. With ELISA either [Ab] or [Ag] is kept constant by immobilization, corresponding [Ab] or [Ag] is to be determined (analyte) and [AbAg] is the measure. Then the analyte is correlated to the measure and interpolated. This yields a sigmoidal curve where the upper asymptote represents the maximum optical density that can be achieved for the given ELISA system, also called maximum binding (B_{max}). B_{max} is also represented by the sum of [AbAg] and [Ab] or [Ag] (whichever is immobilized). So to assess K_D using ELISA the concentration of analyte (Ab or Ag) equaling K_D must be determined. According to equation 1.11 if K_D equals [Ab] for instance [AbAg] equals [AG] (equation 1.12). For this the ratio of [AbAg] to [AbAg] + [Ag] equals $\frac{1}{2}$ (equation 1.13). Since [AbAg] represents the number of occupied binding sites and [Ag] the number of unoccupied

binding sites, their sum is equal to all available binding sites and thus equal to B_{max} (equation 1.14). So if in equation 1.13 B_{max} is substituted for [AbAg] + [Ag] it becomes apparent that if K_D equals [Ab], [AbAg] equals $\frac{B_{max}}{2}$ (equation 1.15, 1.16) (*25*).

$$\text{if } \mathrm{K_D} = [\mathrm{Ab}] \text{ then } [\mathrm{AbAg}]{=}[\mathrm{Ag}] \tag{1.13}$$

$$\text{if } [\mathrm{AbAg}]{=}[\mathrm{Ag}] \text{ then } \frac{[\mathrm{AbAg}]}{[\mathrm{AbAg}] + [\mathrm{Ag}]} = \frac{1}{2} \tag{1.14}$$

$$[\mathrm{AbAg}] + [\mathrm{Ag}] = \mathrm{B_{max}} \tag{1.15}$$

$$\text{if } [\mathrm{Ab}] = \mathrm{K_D} \text{ then } [\mathrm{AbAg}] = \frac{\mathrm{B_{max}}}{2} \tag{1.16}$$

In practice this means that [AbAg] (the measure) needs to be plotted against different concentrations of Ab to determine B_{max} by nonlinear regression. Thereupon [Ab] must be read at $\frac{B_{max}}{2}$ to yield K_D. For practical and financial purposes the aim of this thesis is to figure out if titer and Kd can be calculated from the same binding curve so that only one measurement has to be performed, thus greatly increasing the applicability of the method for diagnostical purposes in a routine laboratory.

1.3.1 The Hill equation as the regression model used to calculate K_D

To interpolate the data points of optical density for given dilutions a nonlinear regression model must be chosen. The primary criteria for this is a low determination coefficient yielded by the respective model. The Hill equation was originally designed to describe the binding of molecular oxygen to hemoglobin, which has four oxygen binding sites, but it can be adapted for all multivalent receptors. If there is only one binding site this equation becomes the *Michaelis-Menten equation*. In the case of a titration-based ELISA K_d ought to have the same unit as antibody concentration does, which is *dilution factor*, which represents actual conentration of antibody thus *total antibody*. The measurand is optical density representing *bound antibody*. The ratio of bound antibodies to total binding sites (θ) can also be expressed by equation 1.17.

$$\theta{=} \frac{[\mathrm{AbAg}]}{[\mathrm{Ak}]^{+}[\mathrm{AbAg}]} \tag{1.17}$$

Formulating Equation 1.4 as equation 1.18 and substituting [AkAg] in equation 1.17 yields equation 1.19, which represents a common formulation of the Hill equation.

$$[\mathrm{AkAg}] = \frac{[\mathrm{Ab}][\mathrm{Ag}]}{\mathrm{K}_d} \tag{1.18}$$

$$\theta = \frac{[\mathrm{Ag}]}{\mathrm{K}_d + [\mathrm{Ag}]} \tag{1.19}$$

Substituting OD as dependant variable y and Dilution as independent variable x in equation 1.19, yields the final equation 1.20.

$$\mathrm{y} = \mathrm{OD} = \frac{\mathrm{y}_{\max} \cdot \mathrm{x}}{\mathrm{K}_d + \mathrm{x}} = \frac{\mathrm{OD}_{\max} \cdot \mathrm{Dil}}{\mathrm{K}_d + \mathrm{Dil}} \tag{1.20}$$

This is based on the assumption that only one binding site of the antibody binds to its antigen leading to the Hill coefficient n equaling 1. If both binding sites bind to antigen equation 1.20 becomes equation 1.21 (*26*, *27*).

$$\mathrm{OD} = \frac{\mathrm{OD}_{\max} \cdot \mathrm{Dil}^2}{\mathrm{K}_d + \mathrm{Dil}^2} \tag{1.21}$$

In this case K_D is the macroscopic dissociation constant and equals K_d^2, which is the microscopic dissociation constant (*11*). Whether the Hill coefficient is to be considered or disregarded when calculating K_D is further explored in this thesis.

1.4 Isoagglutinins and anti PNV23 antibodies

Wolfram, Sauerwein et al described production, structure and role of natural antibodies and pneumococcal polysaccharides as follows (see Appendix B for full text): „Isoagglutinins, i.e., antibodies against carbohydrate epitopes that form the AB0 antigens on red blood cells (RBCs), are considered prototypic natural antibodies. Natural antibodies are produced in the absence of overt external antigenic stimulation early in life in all healthy individuals with a functional immune system, presumably as a product of germline gene segment assembly (*28*). Therefore, they show low affinity to many microbial pathogens and certain cross-reactivity, even to some self-antigens (*28–31*). Antibodies to carbohydrate epitopes share certain characteristics with natural antibodies, e.g., the absence of extensive class switching and affinity maturation due to absent T-cell help (*32*). The appearance of isoagglutinins can be explained by inapparent stimulation particularly from intestinal bacteria because antigens cross-reactive with blood group oligosaccharides are widely distributed in the environment (*28*, *33*, *34*). A or B blood group individuals develop anti-B or anti-A antibodies, respectively O blood group individuals produce both anti-A and anti-B antibodies, while AB blood group subjects have neither anti-A nor anti-B because they express both antigens on their RBCs.

The human ABO blood group antigens are oligosaccharide moieties formed on precursor backbones by glycosyltransferases (*31*, *35*). Blood group O individuals

have carbohydrate structures named H-antigen terminated in the sequence alpha-Fuc(1,2)Gal. The blood group A antigen is then formed from the H-antigen by an N-acetylgalactosaminyltransferase that uses a UDP-N-acetylgalactosamine (GalNAc) donor, and the blood group B antigen is formed by a galactosyltransferase that uses a UDP-galactose (Gal) donor to convert the H-antigen (*31*). The human A and B blood group antigens differ from each other only in the substitution of an acetamino for a hydroxyl group on the terminal saccharide residue, and this substitution can be differentially recognized by specific antibodies (*21*, *28*, *31*).

In addition to their role as a first line of defense against infection, natural antibodies have been shown to play an important role in the initiation of autoimmunity (*29*, *34*, *36–38*). Natural antibodies reacting with self-antigens were initially considered to represent breakdown of tolerance, thus functioning as a template for the generation of pathogenic autoantibodies produced through a process of clonal selection, somatic hypermutation, and class switching driven by antigen (14). More recently, these antibodies have been attributed an additional role in the prevention of autoimmune disease, e.g., by inhibiting activation of the adaptive immune system by molecules released from apoptotic cells that could facilitate autoimmune events (*37*, *38*). Since the titer of anti-blood group AB0 antibodies varies between individuals, a modulated production of those antibodies in response to environmental antigens (e.g. immunization) is plausible. B cells could thus recognize shared carbohydrate epitopes due to structural similarities in saccharide composition, e.g., between microbial polysaccharides (e.g. pneumococcal polysaccharides, PnPs) and blood group A/B antigens, which could also have an effect on blood group anti-A/B specific antibody production after PnP-immunization. Previous findings indicate shared epitopes between blood group oligosaccharides and pneumococcal capsular polysaccharides, as antibodies cross-reacting with human erythrocytes and pneumococcal antigens have been described (*33*) "(*1*). As natural antibodies have been shown to play an important role in the initiation of autoimmunity (*29*, *34*, *36–38*), concerns have been raised that vaccination might lead to the development of autoimmune disease (*39*). As part of this thesis the effect of Pnp vaccination on isoagglutinin production (e.g. antibody titers and binding characteristics) in healthy controls and patients with type I diabetes mellitus, a frequent autoimmune disease, was investigated.

Chapter 2

Methods

2.1 Surface plasmon resonance spectroscopy (SPRS) - analysis of blood group A or B antibodies

Both anti-A and anti-B antibodies were measured simultaneously on one chip surface (CM5-chip) using a four channel Biacore T200 device. This method was already described in the paper published by Wolfram, Sauerwein et al but is cited below for better readability: „The dextran hydrogel layer on the CM-5 sensor chip was used to form a hydrophilic environment for the attachment of blood group A or B trisaccharide amine derivative, preserving the blood group antigens in a non-denatured state (18). This allows for measurement of antigen−antibody binding under almost physiological conditions.

Amine-labeled blood group A and B trisaccharides (Dextra Laboratories Ltd., Reading, UK) were immobilized on CM5 sensor chips (Biacore, GE Healthcare) according to standard protocols (*21*). In brief, the CM-5 sensor chip surface was activated with 100 μl of 0.05 mol/l N-hydroxysuccinimide (Sigma Aldrich, St. Louis, MO, USA) and 0.2 mol/l N-ethyl-N'-dimethylaminopropylcarbodiimide (Sigma Aldrich) injected into the buffer stream of HBS-EP (0.01 mol/l HEPES buffer, pH 7.4, containing 0.15 mol/l NaCl, 3 mmol/l EDTA, and 0.005% (v/v) surfactant P20).“(*1*). A flow rate of 10 μl/min for 600 s was chosen. 100 μl of 1 mol/l ethanolamine-HCl (pH 8.5) was used to inactivate residual active ester groups on the sensor surface and thus achieving a stable baseline. Immobilization onto Gold/Dextran surfaces of Flow cell one (FC-1) and three (FC-3) were performed without trisaccharide and served as blank during binding analysis. 1 mg/ml blood group A trisaccharide was immobilized onto the surface of FC-2 and 1 mg/ml blood group B trisaccharide were immobilized onto the surface of FC-4. „For binding analysis, crude serum was diluted by half with HBS-EP and injected in FC-2 and FC-4 for 180 s at a flow rate of 10 μl/min. The flow-path was $2-1$ and $4-3$. To determine IgM and IgG levels

of A- and B-bound antibodies, anti-human IgG Abs [polyclonal aHIgG (γ-chain), Sigma-Aldrich, St. Louis, MO, USA] and anti-human IgM [polyclonal aHIgM (μ-chain), Sigma-Aldrich, St. Louis, MO, USA] were injected for 180 s at a flow rate of 10 μl/min directly after the serum sample. For measurement of anti-A/B antibodies RU at report point *stability* (Figure 3.2) and for levels of IgM/IgG anti-A/B antibodies levels at report point *enhance level* (see Figure 3.2) relative to baseline were recorded. After determination of response units of IgM and IgG anti-A/B antibodies, the chip was regenerated twice with 50 mmol NaOH for 30 s at a flow rate of 10 μl/min with a stabilization period of 5 s after the second regeneration to reach the same baseline as prior to the measurement. For kinetic measurement, an association time of 200 s and dissociation time of 800 s was chosen.

To compute an affinity constant K_D the concentration of IgG antibodies in microgram per milliliter must be known, thus RUs for different concentrations of monoclonal anti-A IgG (clone 9A, Abcam, Cambridge, MA, USA; clone NaM87-1F6, BD Pharmingen, San Jose, CA, USA) were measured (Figure 3.12, Panel 1)). Thus an increase in response units derived from anti-A/B IgG measurements in patient serum could be correlated with microgram per milliliter of anti-A/B IgG antibody by regression analysis in order to calculate the respective concentration of IgG anti-A/B (Figure 3.3, Figure 3.12, Panel 2)). Subsequently two dilutions of patient serum, concentrated and diluted by half, and a blank were measured (Figure 3.12, Panel 3)), and the resulting binding curves were used to calculate KD (computed as KD = kd/ka) using the BIAevaluation software from GE Healthcare. To fit the association/dissociation curve, a 1:1 binding model was chosen. The molecular weight of the analyte was assumed to be 150,000 Da (IgG). To assess the quality of the calculations, controls within the software were used. No external calculations were performed nor parameters added. Furthermore, as an internal control to test before each measurement was started, anti-blood group A or B IgM mAbs (anti-A murine monoclonal Abs clone MH04 and A3D3, anti-B murine monoclonal Abs clone NB1.19, NB10.5A5, and NB10.3B4, Ortho-Clinical Diagnostics, Neckargemünd, Germany), and anti-blood group A IgG mAb (clone 9A, Abcam, Cambridge, MA, USA; clone NaM87-1F6, BD Pharmingen, San Jose, CA, USA) were used to guarantee optimal chip performance and full recovery.“(*1*)

2.2 PNV23 ELISA

96-Well plates were coated using Pneumovax(R) 23 (PNV23) vaccine as antigen to measure antibody response to the PnP vaccination. PNV23 is a liquid vaccine consisting of a mixture of purified capsular polysaccharides from Streptococcus pneumoniae types (1, 2, 3, 4, 5, 6B, 7F, 8, 9N, 9V, 10A, 11A, 12F, 14, 15B, 17F, 18C,

19F, 19A, 20, 22F, 23F, and 33F). Each 0.5 mL dose of vaccine contains 25 micrograms of each polysaccharide type in isotonic saline solution containing 0.25% (v/v) phenol as a preservative. For immobilization of the antigen the vaccine was diluted using a bicarbonate puffer at pH 9.6 of 96 Well-plate (F8 Maxisorb NUNC-Immuno Mod plate, Thermo Scientific, Nr.468667) to reach a concentration of 250 μg/ml. 50μl of solution were added to the wells and incubated over night at 4 °C. Then the wells were washed with PBS + 0.05% (v/v) Tween20 and remaining binding sites blocked using PBS + 2% (v/w) BSA for 2 hours at 37 °C. For storage the plates were frozen at -20 °C. To perform analysis serum samples and a serum pool were diluted 1:20, 1:160, 1:640 and 1:2560, added to the plates and incubated for one hour at room temperature. Three dilutions (1:50, 1:100, 1:200) of serum pool were additionally measured to normalize the optical density. Following this plates were washed using PBS + 0.05% (v/v) Tween20 and a secondary anti human IgG antibody (biotinylated anti-human IgG (Vector Laboratories, Nr. BA3080; Firma Szabo Scandic)) (0.5μg/ml) was added. Again after one hour of incubation, plates were washed and streptavidin and Biotin (Vector Laboratories, Nr. pk-4000; Firma Szabo Scandic) were added for half an hour to enhance the signal. At last the plates were cooled at 4 °C for 10 minutes and 100 μl of ABTS substrate were added and repeatedly measured at 450nm until concentration 2 of the serum pool reached an optical density of one and then data was collected. OD was plotted against the dilution factor and nonlinear regression using the Hill-equation was performed. Titers were determined as the dilution factor at OD = 0.5 and K_D as the dilution factor at half-maximum binding (Bmax/2) as described above. $1/K_D$ was calculated to positively correlate avidity and magnitude of avidity parameter, making its interpretation simpler. This yields reciprocal K_D in units of dilution factor.

2.3 Anti blood group A ELISA

Amine-labeled blood group A trisaccharides were immobilized onto a maleic anhydride activated 96-Well plate. 50 μl of a solution with varying concentrations (see Results) were added to the plate and incubated over night at 4 °C. After washing with PBS + 0.05% (v/v) Tween20, which served as washing buffer for all washing steps, 200 μl of a five percent solution of bovine serum albumin were added to block remaining unspecific binding sites and incubated overnight at 4 °C, however the contents of blocking solution were also subjected to optimization (see Results). The plates were stored at -20 °C. For analysis a mouse anti-A antibody (abcam, HE-193) served as positive control and to calculate a calibration curve, due to no antibody of human origin being available. 50 μl were added and incubated for one hour at room temperature. After washing 50 μl of an anti-mouse IgG antibody (5 μg/ml)

(Thermo-Fisher, 31430) was added to quantify isotypes. Finally 100 μl of ABTS substrate were added and optical density was measured at 450nm.

2.4 Determination of Anti-A/B Antibody Titers by the DiaMed-ID Micro Typing System

„Titers of blood group anti-A and anti-B antibodies were determined by the DiaMed-ID Micro Typing System (Biorad Lab. Inc., Hercules, CA, USA) used according to the manufacturer's protocol. The ID-Card 50520 (NaCl) was used to measure IgM, while the ID-Card 50531 [LISS/Coombs containing poly-specific anti-human gamma globulin (AHG) serum] was used to determine IgG in addition to IgM. The serum samples were serially twofold diluted with 0.9% (w/v) saline solution starting with 500 μl serum and 500 μl saline solutions. Also, 25 μl of each dilution were pipetted into a single column of the microtube gel card, and 50 μl of DiaMed-ID-DiaCell ABO/I-II test cell suspensions A1 or B (Biorad Lab.) was added. ID-Card 50520 (NaCl) cards were incubated at room temperature for 15 min, the ID-Cards (LISS/Coombs) at 37°C, and thereafter centrifuged in a DiaMed-ID-Centrifuge 24 S for 10 min at 910 rpm. Results were read immediately after centrifugation and were subdivided into positive and negative results. The titer that led to visible agglutination of erythrocytes dispersed in the gel was selected positive.“(*1*).

2.5 Data analysis

Data analysis was performed using the BIAEvaluation software (GE Healthcare) and Microsoft Excel and statistical analysis was performed using Microsoft Excel, R and Prism 6 (Graphpad). All figures were drawn using Graphpad Prism 6. Study groups were analysed for statistically significant differences using the non-parametric two-tailed Mann-Whitney U-Test and statistically significant correlation between two parameters was calculated using the non-parametric two-tailed Spearman test, except where specified differently.

Chapter 3

Results

3.1 Surface Plasmon Resonance spectroscopy

3.1.1 Establishment of isotype specific quantification of anti polysaccharide antibodies within serum

The isotype-specific anti-polysaccharide antibody assessment using SPRS is based on a second injection with secondary antibodies without regenerating the chip-surface. Thus the primary antibodies were still attached to the immobilized antigen and a second layer of antibodies forms that changes the angle of surface plasmon resonance maximum absorption further. Figure 3.1 shows an exemplary sensorgram depicting both injections. A slight dissociation of primary antibodies happens before the injection of secondary antibodies, which means that the sum of response units of isotypes is expected to be higher than those of total primary antibodies, depending on the degree of dissociation. The corresponding analysis software determines report points at which response units are read. The report point *stability* is used as a measure for total antibodies and *enhance level* for isotype quantification (figure 3.2 (*1*)).

Choosing secondary antibodies (aHIgM and aHIgG)

Introducing a secondary antibody can lead to an increase in unspecific signal, because it binds to the surface to some degree. To minimize this effect polyclonal anti-IgG antibodies of different specificities, e.g. directed against the heavy chain of IgG (γ-chain) (10 and 1 μg/ml) (Sigma-Aldrich, Product number: I3382) and the whole IgG molecule (Sigma-Aldrich, I2011) and two polyvalent anti-IgG sera (Coombs C3d: Biorad, Article Number: 14710, Coombs Diamed: Diamed, REF: 107910) were compared using blood group A+ and 0- serum from healthy controls (table 3.1). This was only conducted for IgG since both isotype specific antibodies

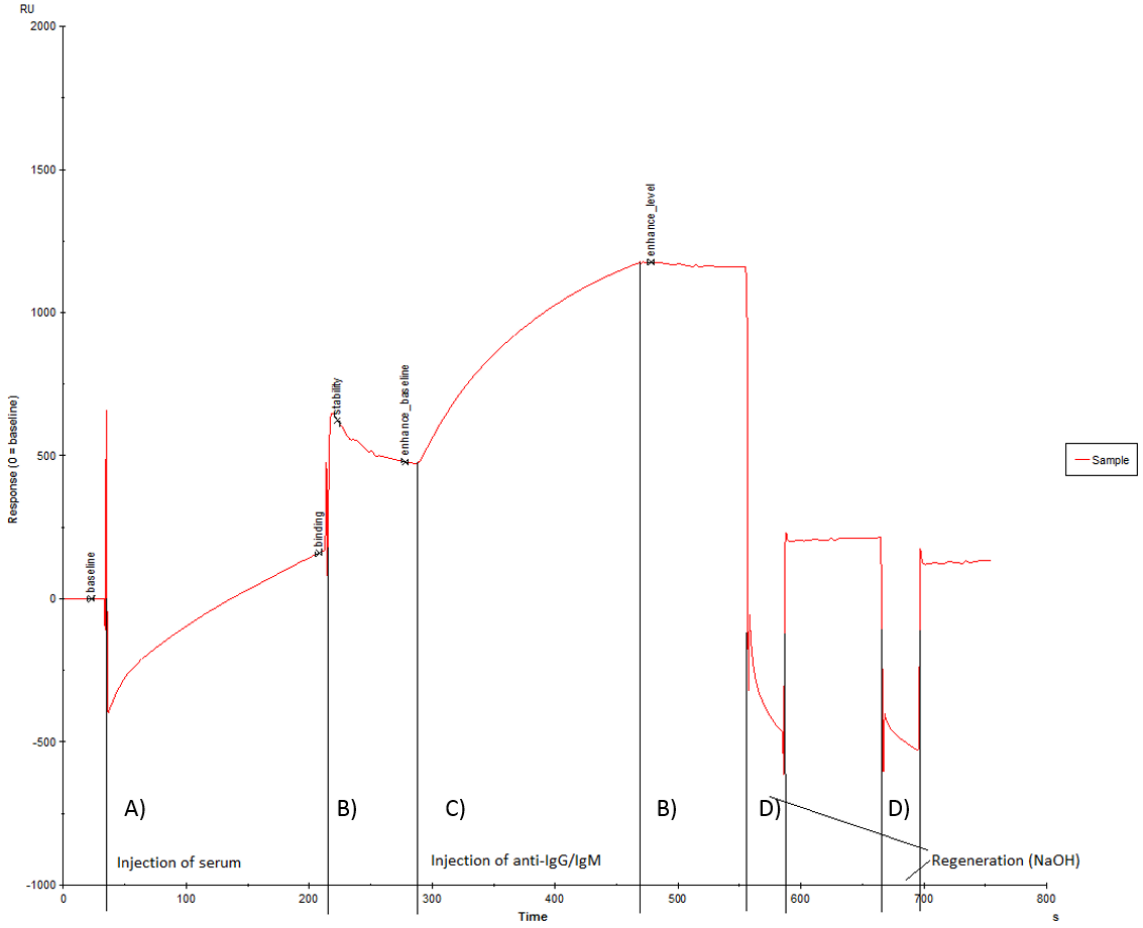

Figure 3.1: Example for sensorgram as recorded by Biacore T200 A) Injection of sample (in this case serum) and following increase in RU due to binding of trisaccharide A/B antibody B) Injection of flow buffer (HEPES) and slight dissociation of bound antibody C) Injection of secondary antibody anti-IgG/IgM to quantify bound levels of IgG/IgM D) Removal of bound antibody with NaOH to regenerate sensor chip

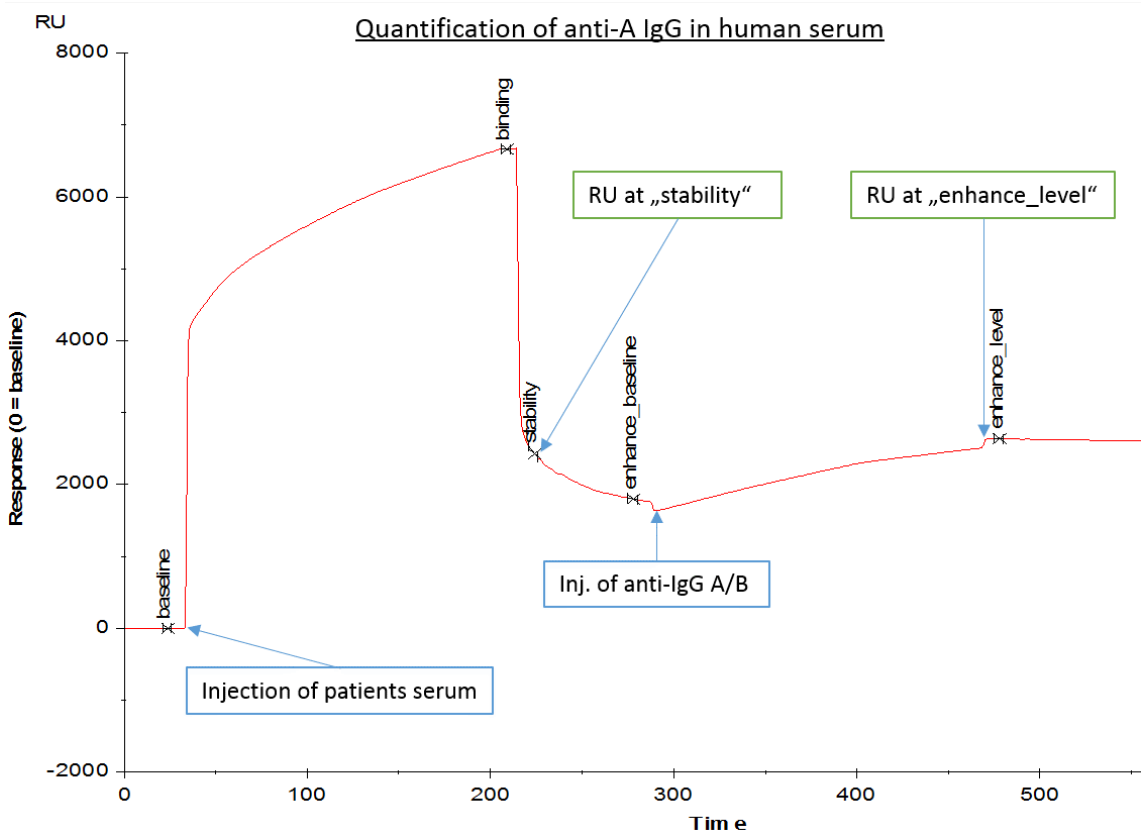

Figure 3.2: „Exemplary binding curve of quantification of anti-A IgG antibodies in human serum, as generated by BIAevaluation software (GE Healthcare). Injection of human serum was followed by a second injection of anti-IgG; response units (RU) at *stability* were recorded to assess the concentration of anti-A blood group antibodies, while response units at *enhance level* were representative for anti-A IgG concentration. The x-axis gives time in seconds, and the y-axis represents response units (RU).“(*1*)

have to be of the same nature and derived from the same species for comparability in any case. A specific isotype signal requires elevated IgG-levels only if total levels are elevated too. This criterion was met by 10 μg/ml of anti-γ-chain IgG, which was used henceforth. For isotype quantification of IgM two concentrations (10 and 100 μg/ml) of anti-IgM directed against the μ-chain of the antibody were compared. Both showed specific signals, thus 10 μg/ml was chosen due to comparability to IgG and lower costs (table 3.2). For IgM isotype-specific quantification the process was repeated using a μ-chain specific anti-human IgM secondary antibody (table 3.2) using the equialent concentration of 10 μg/ml and comparing it to 100 μg/ml. This analysis was performed only for trisaccharid A antigen.

Calculation of calibration curve

To correlate response units as measured by SPRS to actual units of concentration (g/l) several concentrations of a monoclonal anti-A IgG antibody were measured and a calibration curve was computed (figure 3.3). However it is generally advised to express quantities determined by SPRS as response units when dealing with serum or samples of similar complexity. Alternatively the concentration of the analyte in g/l within serum can be determined using a different method and then a calibration curve using serum itself can be computed. However for the present analyte the establishment of such an assay failed (see below).

Comparison of anti-A/B isotypes as determined by SPRS to the Diamed MicroTyping system

To verify the experimental setup, the isoagglutinin titers of healthy controls were determined using a common method (Diamed Micro Typing system). For this micro typing cards and an experimental setup containing NaCl or polyclonal anti human IgG serum (LISS/Coombs) were used. Total anti-A/B concentration as determined by SPRS was correlated to titers (figure 3.4) detected in the presence of NaCl only and IgG response units to LISS/Coombs titers (figure 3.5). This showed that both methods do correlate with high statistical significance ($p < 0.0001$) (figure 3.4, 3.5). The superior solution and sensitivity of SPRS is shown in figure 3.6 and 3.7, where all measured RUs for a given titer are depicted. The fact that SPRS outputs continuous values, while titers are semiquantitative (because only values increasing by a factor of two are possible) further contributes to its higher resolution, sensitivity and ultimately precision and accuracy.

Table 3.1: Comparison of Coombs Serum C3d, Coombs Diamed and a whole molecule anti-human IgG with two concentrations 10 μg/ml and 1 μg/ml) of a γ-chain specific anti-human IgG antibody to quantify isotypes of anti blood group A/B antibodies bound onto the surface where Blood group trisaccharides A/B (tris. A/B) were immobilized to serve as antigen. To achieve this four serum samples of healthy controls were injected first, followed by a second injection of secondary antibodies before regeneration of the chip surface was performed. *Total* represents the response units after injection of primary blood group antibodies, correlating to non-isotype specific concentrations. *IgG* represents response units after the second injection correlating to IgG-isotype specific quantity of primary blood group antibodies. A specific isotype signal requires elevated levels of IgG only if total levels are elevated too. 10 μg/ml of γ-chain specific anti-human IgG was used for further analysis since it met this criterion.

		tris. A		tris. B	
Sample	Sec. AB	Total	IgG	Total	IgG
			[RU]		
	Coombs C3d				
HC1		1561.8	586.8	47.0	-12.6
HC2		809.0	337.1	137.5	9.7
HC3		188.5	180.2	510.2	7.2
HC4		1717.9	411.5	565.5	57.3
	Coombs Diamed				
HC1		1545.0	287.1	57.0	-16.7
HC2		806.7	124.2	143.5	-2.2
HC3		180	48	516.3	-56.3
HC4		1689.9	120.6	558.9	-12.7
	αHIgG (whole mol.)				
HC1		1664.1	3089	47.8	18.3
HC2		984.8	1827.7	142.5	136.3
HC3		395.8	1063.0	516.4	333.7
HC4		1864.6	2732.4	539.6	677.7
	αHIgG (γ-chain spec.) 10 μg/ml				
HC1		1485.4	1609.8	50.0	0.1
HC2		1698.6	1478.7	579.5	372.0
HC3		760.2	788.3	137.4	71.0
HC4		173.3	288.4	520.2	130.0
	αHIgG (γ-chain spec.) 1 μg/ml				
HC1		1596.0	173.2	53.4	-6.9
HC2		801.4	69.7	139.0	-2.1
HC3		187.0	49.2	518.0	-41.2
HC4		1663.1	9.4	549.2	41.3

Table 3.2: Comparison of two concentrations (10 and 100 μg/ml) of μ-chain specific anti human IgM to quantify isotypes of anti blood group A/B antibodies bound onto the surface where Blood group trisaccharide A (tris. A) were immobilized to serve as antigen. To achieve this four serum samples of healthy controls were injected first, followed by a second injection of secondary antibodies before regeneration of the chip surface was performed. *Total* represents the response units after injection of primary blood group antibodies, correlating to non-isotype specific concentrations. *IgM* represents response units after the second injection correlating to IgM-isotype specific quantity of primary blood group antibodies. A specific isotype signal requires elevated levels of IgM only if total levels are elevated too. Both concentrations of the tested antibody met this criterion, so for better comparibility the concentration equal to the secondary anti human IgG antibody was chosen (10μg/ml)

Sample	Sec. AB	tris. A	
		Total	IgM
		[RU]	
	αHIgM (μ-chain spec.) 10 μg/ml		
HC1		446.0	122.4
HC2		1910.8	-354.1
HC3		964.2	164.4
HC4		736.5	155.6
	αHIgM (μ-chain spec.) 100 μg/ml		
HC1		252.9	265.2
HC2		1964.1	-230.3
HC3		781.7	425.9
HC4		652.3	379.0

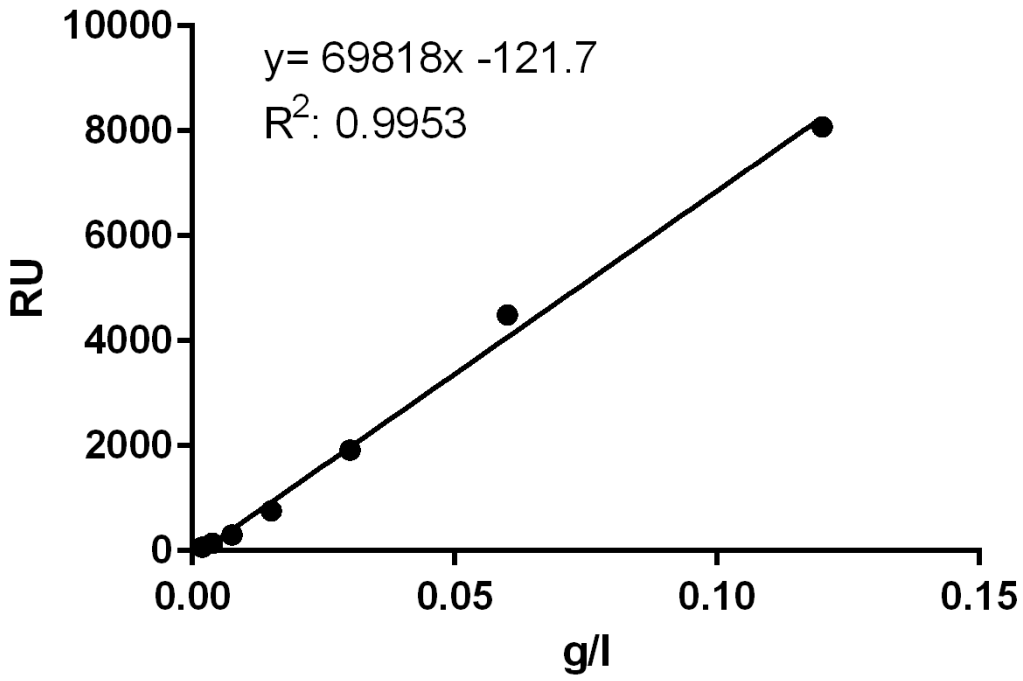

Figure 3.3: Seven different concentrations of anti-A IgG (clone 9A, Abcam, Cambridge, MA, USA; clone NaM87-1F6, BD Pharmingen, San Jose, CA, USA) were measured and their concentration plotted against RUs. Linear regression yields a function to calculate concentration in g/l from given RUs.

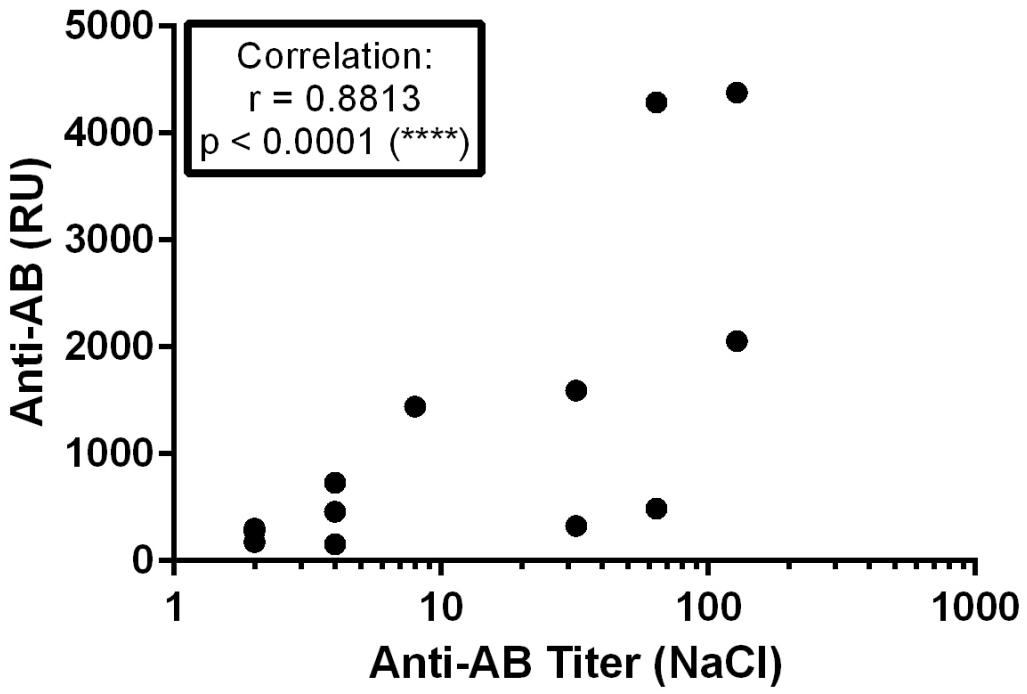

Figure 3.4: Correlation of total anti-A/B antibodies as determined by SPRS to titers detected by NaCl cards for the Diamed Micro Typing system. RUs and titers correlate with statistical significance, however the range of RUs for a given titer is wide.

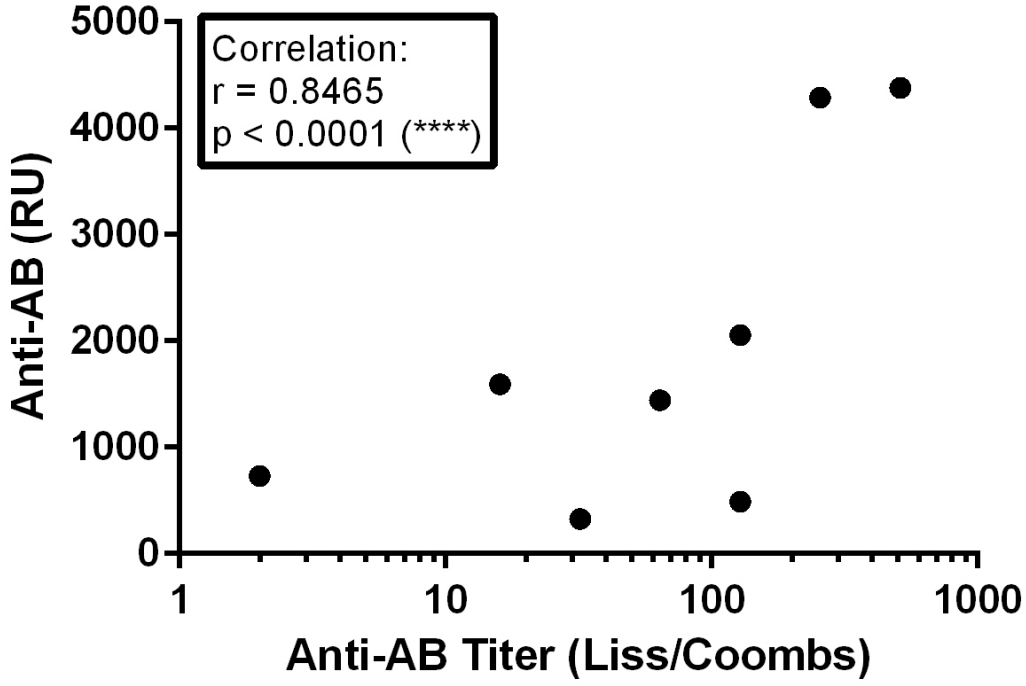

Figure 3.5: Correlation of anti-A/B IgG antibodies as determined by SPRS to titers detected by LISS/Coombs cards for the Diamed Micro Typing system. RUs and titers correlate with statistical significance, however the range of RUs for a given titer is wide.

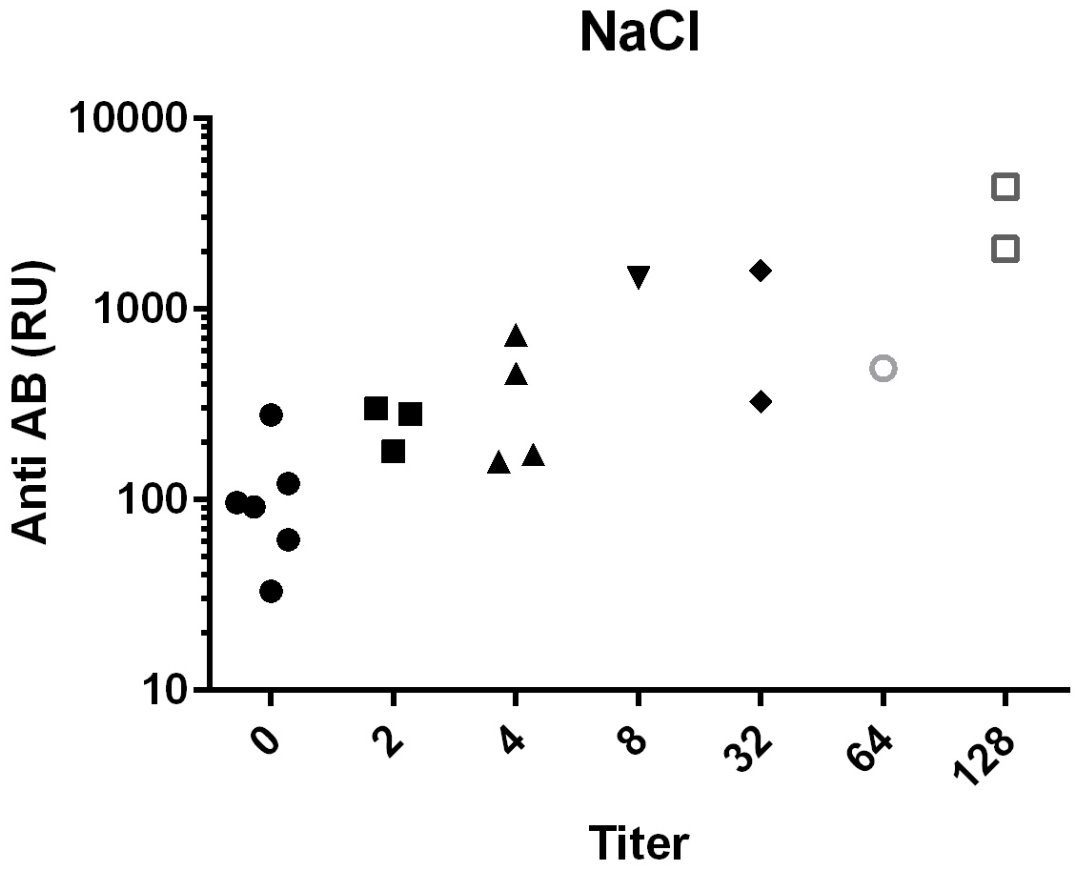

Figure 3.6: Response units as measured by SPRS were plotted against titers as measured by the DiaMed MicroTyping system using NaCl cards to evaluate resolution and sensitivity of both methods. RUs do correlate to titers (see figures 3.4, 3.5), however the RUs for a given titer vary heavily with the variation being greatest for titers of zero. This shows that using SPRS antibodies can be detected with a higher sensitivity than titration assay

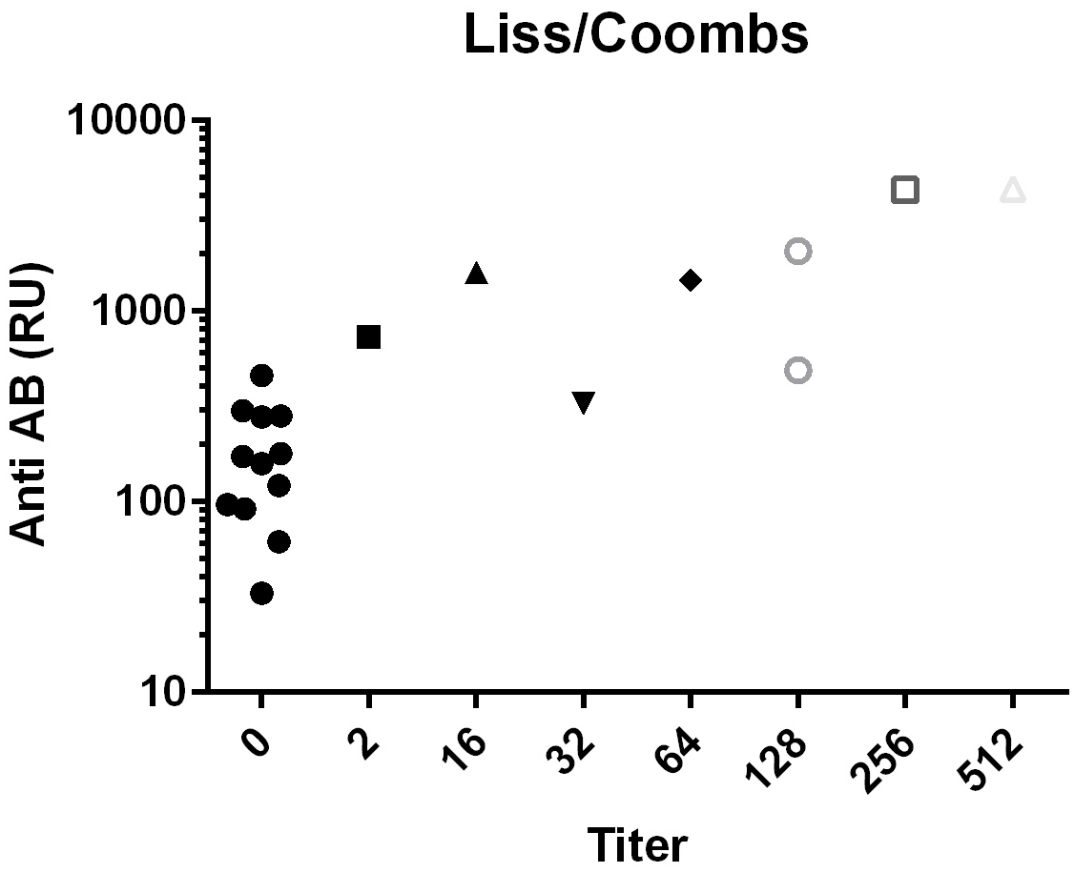

Figure 3.7: Response units as measured by SPRS were plotted against titers as measured by the DiaMed MicroTyping system using Liss/Coombs cards to evaluate resolution and sensitivity of both methods. RUs do correlate to titers (see figures 3.4, 3.5), however the RUs for a given titer vary heavily with the variation being greatest for titers of zero. This shows that using SPRS antibodies can be detected with a higher sensitivity than titration assay

Table 3.3: Association and dissociation rate constants and dissociation constant calculated from SPRS sensorgrams from two serum samples healthy controls and a monoclonal anti-A IgG antibody (clone 9A, Abcam, Cambridge, MA, USA; clone NaM87-1F6, BD Pharmingen, San Jose, CA, USA). Values were only calculated from binding curves showing sufficient curvature (see figure 3.8)

	k_a	k_d	K_D
HC1	6.78E+08	3.22E+01	4.75E-08
HC4	1.90E+09	7.99E+01	4.20E-08
anti-A IgG	2.68E+07	2.69E+00	1.00E-07

3.1.2 Establishment of avidity estimation of anti polysaccharide antibodies in serum by SPRS

As anti-A antibody titers are higher in human serum than anti-B titers and due to increased time and resource demands of kinetic measurements using SPRS all measurements were performed using only immobilized blood group A trisaccharide, thus determining affinity for anti-A antibodies only. Data analysis could only be performed on curves showing appropriate curvature as otherwise MTL dominates the binding process and mass transfer rates are calculated instead of rate constants. Seven healthy controls and a monoclonal anti-A IgG antibody were measured of which only the binding curves of two serum samples and the monoclonal antibody showed curvature and thus only those were analysed (table 3.3, figure 3.8). Since the monoclonal antibody underwent high affinity maturation its affinity should not be outreached by those of serum samples. This serves as an additional control of data quality.

Manual assessment of SPRS sensorgrams by calculating half-life decay

The accompanying software (BIAEvaluation) offers the possibility to calculate k_a, k_d and K_D based on the Langmuir adsorption model considering multiple concentrations and a blank in the process. To verify automatically calculated data it is useful to develop an additional manual method of data analysis. This approach allows for a visual judgement of each sensorgram to decide whether to disregard or consider entire measurements or parts of it, thus increasing the quality of data analysis. Moreover it is not necessary to calculate concentrations in g/l, so an additional bias introduced by regression analysis is avoided. However the biggest advantage of manually analysing kinetic parameters from sensorgrams is that all curves can be used not only those selected in the first place by the software. Thus also measurements for the purpose of quantification can be used, if the analysis conditions are comparable to those of kinetic measurements, meaning that longer association

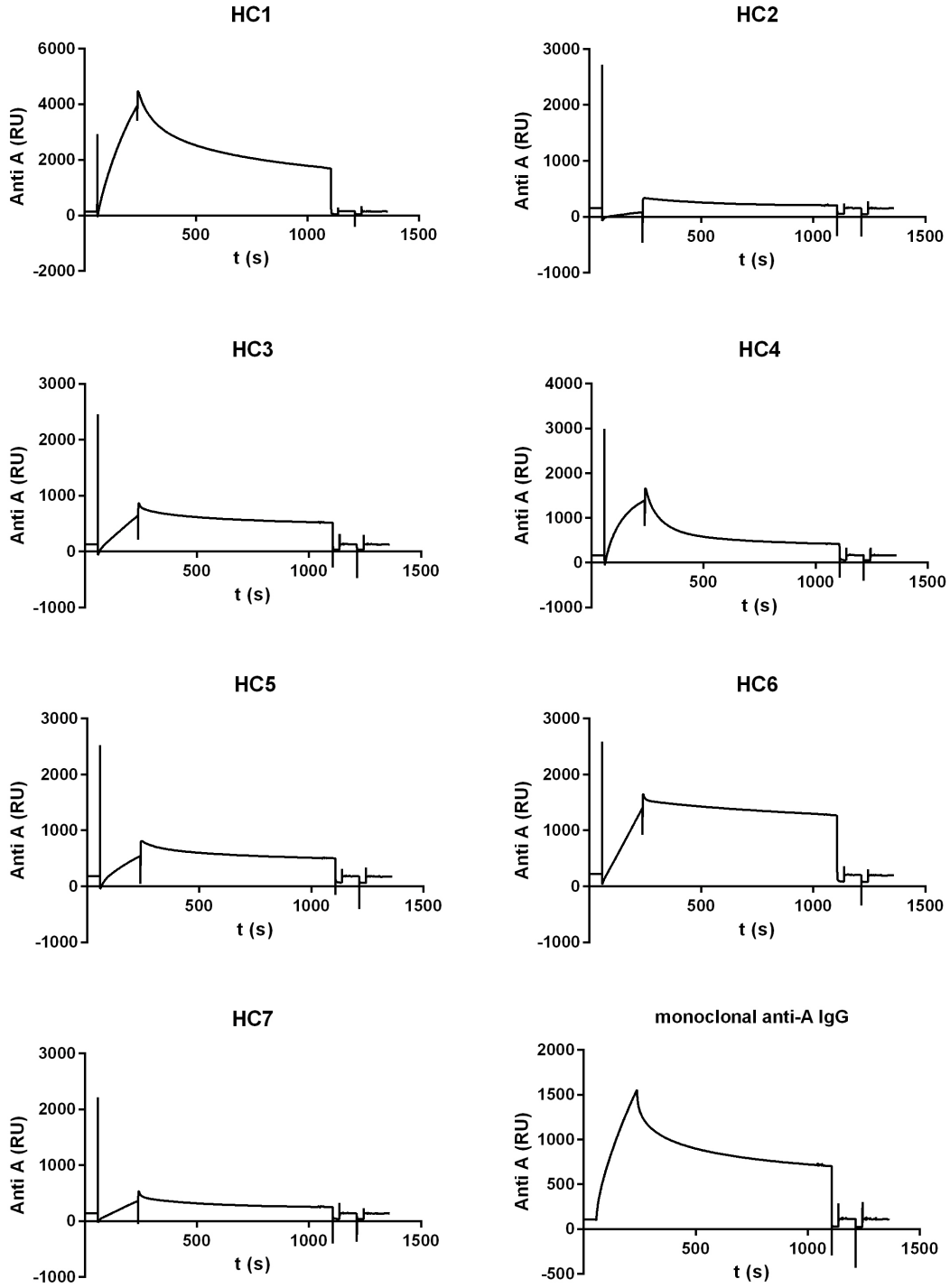

Figure 3.8: SPRS Sensorgrams derived from measurements of serum samples from seven healthy controls and a monoclonal anti-A IgG antibody (clone 9A, Abcam, Cambridge, MA, USA; clone NaM87-1F6, BD Pharmingen, San Jose, CA, USA). Injection of sample was stopped after 200 s and and a continuous flow of buffer was maintained for 800 s to record the decrease of response units to calculate K_D and $t_{1/2}$. Only sensorgrams from HC1, HC4 and monoclonal anti-A IgG were analyzed since only those showed sufficient curvature. For all other samples the contribution of MTL was too high for analysis.

and dissociation time were chosen. To compute $t_{1/2}$ the equation for exponential decay was adapted (equation 3.1) to calculate the half-life of the antigen-antibody interaction ($t_{1/2}$), which is the time until half of the complexes were dissociated. Hereby N_0 are RU at the start of decay, N(t) are RU at end the of decay, $t_{1/2}$ is half-life in seconds and Δt is the time of dissociation.

$$\mathrm{t}_{1/2} = \frac{\Delta \mathrm{t}}{\ln_2\left(\frac{\mathrm{N(t)}}{\mathrm{N}_0}\right)} \tag{3.1}$$

In practice the global maximum of the curve has to be determined first. The response units at the global maximum serve as N_0. To the time at global maximum (t) a certain amount of dissociation time (Δt) is added to compute the time at the end of dissociation (t) and N(t) is read accordingly. Δt can be chosen arbitrarily but has to be equal for all samples that are compared. This becomes imperative when kinetic parameters are calculated from quantification measurements as dissociation times are significantly lower. Theoretically the dissociation rate constant and half-life decay are not dependent on the concentration of antigen-antibody complexes (equation 1.8). However, since the manual determination of $t_{1/2}$ does not consider different concentrations of antibodies within serum samples and k_d as calculated by BIAEvaluation software does, both had to be compared. This was performed for the two serum samples and the monoclonal anti-A IgG antibody which met the criteria for data analysis. Half life decay and k_d showed a highly negative correlation as expected (figure 3.9), since $t_{1/2}$ represents how long the interaction endures, and k_d how many complexes dissociate per second (see equation 1.6). The non-parametric two tailed Spearman test for correlation does not show statistically significant correlation due to low sample size (p=0.3333), while the parametric two-tailed pearson test does show statistical significant correlation (p=0.0409). The visual correlation depicted in figure 3.9 confirms the manual determination of $t_{1/2}$ to be valid.

Moreover $t_{1/2}$ as determined using different concentrations of the same sample were compared to further prove concentration-independence, inter-assay repeatability and robustness of $t_{1/2}$. For this two concentrations (the higher concentration double) of the two serum samples from healthy patients and a monoclonal anti-A IgG antibody were analysed. All samples were used concentrated and diluted twofold. Intra- and inter-concentration standard deviation (SD) and coefficient of variation (CV) were calculated (table 3.4, figure 3.10). Both prove to be low enough to allow for determination of $t_{1/2}$ at different concentrations of antibody within serum samples. In contrast to ELISA in SPRS each sample is assessed by a separate run, thus intra-concentration SD and CV also serve as a measure of assay repeatability.

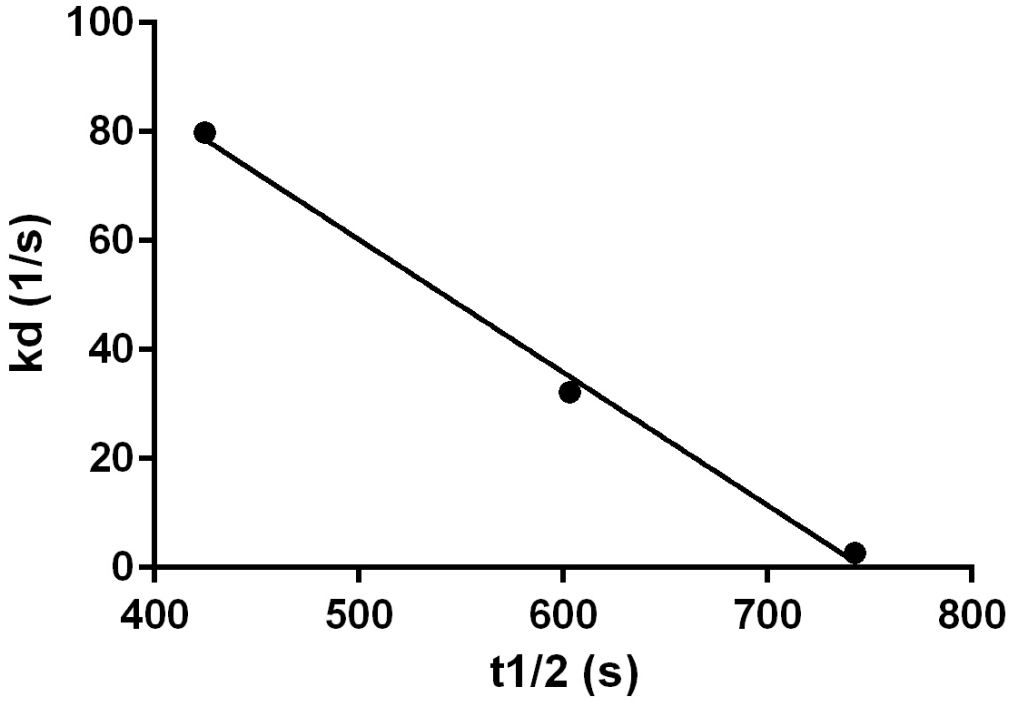

Figure 3.9: Correlation of k_d as determined by BIAEvaluation software and manually calculated $t_{1/2}$ derived from serum samples of two healthy controls and a monoclonal anti-A IgG antibody (clone 9A, Abcam, Cambridge, MA, USA; clone NaM87-1F6, BD Pharmingen, San Jose, CA, USA). k_d and $t_{1/2}$ were only calculated for samples showing sufficient curvature (see figure 3.8); high $t_{1/2}$ and low k_d represent a bond with high avidity, thus the correlation is negative. This proves the validity of the manual calculation of $t_{1/2}$.

Table 3.4: Comparison of intra- and inter-concentration CVs for $t_{1/2}$ of anti-A IgG antibody binding as examined by SPR in serum samples from two healthy controls (HC1 and HC2) and monoclonal anti-A IgG (clone 9A, Abcam, Cambridge, MA, USA; clone NaM87-1F6, BD Pharmingen, San Jose, CA, USA); three measurements of each sample were performed, twice using equal concentration and the third time the sample was diluted by half; $t_{1/2}$ was calculated for all measurements and standard devation was calculated, for the equi-concentration samples (intra.conc) and for all three concentrations (inter.conc). Both standard deviations were low for all samples, proving the robustness of the method and data analysis (calculation of t_{1_2})

	$t_{1/2}$ [s]						
Sample	Conc.1	Conc.2	SD	CV (%)	1:2	SD	CV (%)
			intra.conc.			inter.conc.	
HC1	592	593	0.35	0.06	624	15	2.44
HC2	405	430	12	2.91	438	14	3.28
anti-A IgG	709	704	2.6	0.37	814	51	6.82

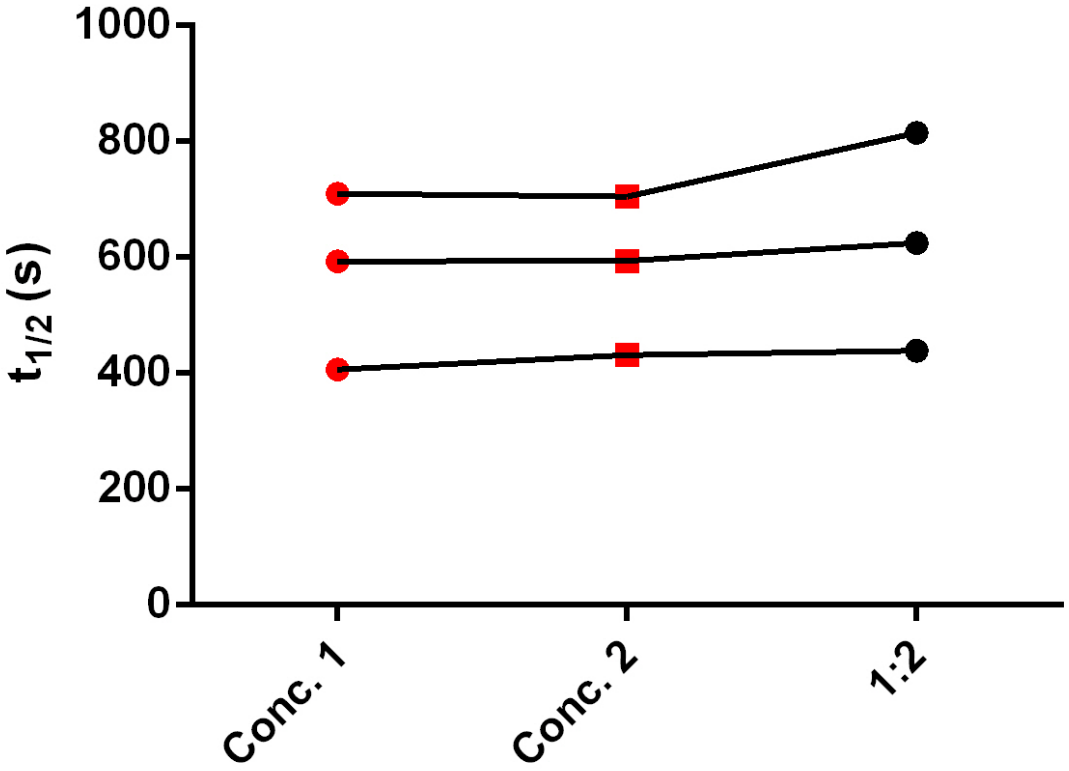

Figure 3.10: Comparison of $t_{1/2}$ at high and low concentration of anti-A antibodies (dilution factor: 2); three measurements of each sample were performed, twice using equal concentration (Conc.1, Conc.2) and the third time the sample was diluted by half (1:2); $t_{1/2}$ was calculated for all measurements. $t_{1/2}$ calculated from the same serum sample but different measurements are connected by a horizontal black line

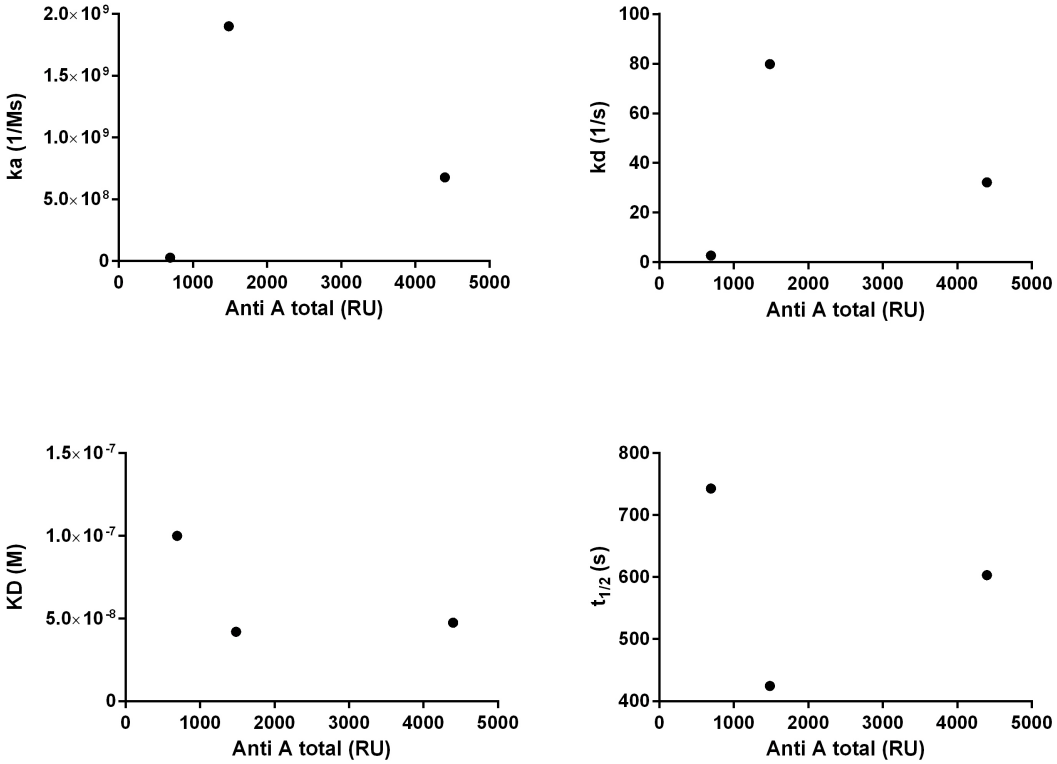

Figure 3.11: Correlation between total anti-A concentration and kinetic parameters. Association- and dissociation rate constants (k_a and k_d), calculated dissociation equilibrium constant (K_D) and half-life decay ($t_{1/2}$) were plotted against total amount of anti-A antibodies and statistically tested (Spearman) to account for concentration dependence of kinetic parameters. Neither of the four parameters show statistically significant correlation.

RU as a measure of concentration is independent from $t_{1/2}$

Since determination of avidity of antibodies as a parameter for diagnosis of antibody deficiency is meant as an addition to the measurement of their concentration it must be ensured that the method of choice differentiates between these two parameters. The concentration of total anti-A antibodies was plotted against all four kinetic parameters (figure 3.11). This showed no correlation whatsoever, for neither parameter.

Determination of $t_{1/2}$ from quantitative measurements

As routine application is the objective for the method, improving efficacy is pivotal. Thus the possibility to determine the kinetic parameter without additional measurements is always the goal. To apply the determination of $t_{1/2}$ to quantitative measurements the dissociation time Δt was lowered significantly and dissociation occurring after injection of anti-A antibody but before second injection of isotype

Table 3.5: Comparison of $t_{1/2}$ calculated from quantitative and kinetic measurements: M1, M2 and M3: measurement 1, 2 and 3; Quant: $t_{1/2}$ derived from quantitative measurements; Kinetic: $t_{1/2}$ derived from kinetic measurements; HC1, HC2: healthy control 1, 2. Standard deviation (SD) and coefficient of variation show that $t_{1/2}$ derived from quantitative measurements (lower dissociation time) is less precise than data calculated from kinetic measurements, but still meaningful, although with a higher variation.

	HC1		HC2	
	Quant.	Kinetic	Quant.	Kinetic
M1	284.0	177.8	191.2	86.8
M2	203.2	178.3	91.1	91,3
M3		159.5		87.4
Mean	240	170	140	89
SD	40	9	50	2
CV	17%	5%	36%	3%

specific antibodies (about 70 seconds) was analysed. Data calculated thusly can only be compared to those calculated from kinetic measurements if equal Δt is chosen. Three kinetic (total dissociation time: 800 seconds) and two quantitative measurements (total dissociation time: 70 seconds) for HC1 and HC2 were performed and $t_{1/2}$ was calculated for both considering only 70 seconds of dissociation for all measurements (table 3.5). SD and CV are significantly higher for quantitative measurements as to be expected, but overall $t_{1/2}$ remains meaningful.

3.1.3 Final Workflow

Figure 3.12 (*1*) shows the final workflow for SPRS measurements of blood group antibody titers and binding characteristics. Firstly a calibration curve must be calculated, so several known concentrations of the antibody of interest must be measured and resulting RU correlated to their concentration to perform regression analysis. Secondly antibodies within a sample of interest are measured using a quantification protocol (see Methods) including a second injection with secondary anti isotype antibodies. Thirdly a kinetic protocol is applied to the sample using at least two concentrations (one of them double) and a blank. At last data is exported to the BIAevaluation software to calculate k_a, k_d, K_D or raw data is exported as .txt file to calculate $t_{1/2}$ using Microsoft Excel.

3.1.4 Application

To put the isotype-specific quantification of blood group antibodies into practice, firstly the levels and binding characteristics of natural antibodies directed against

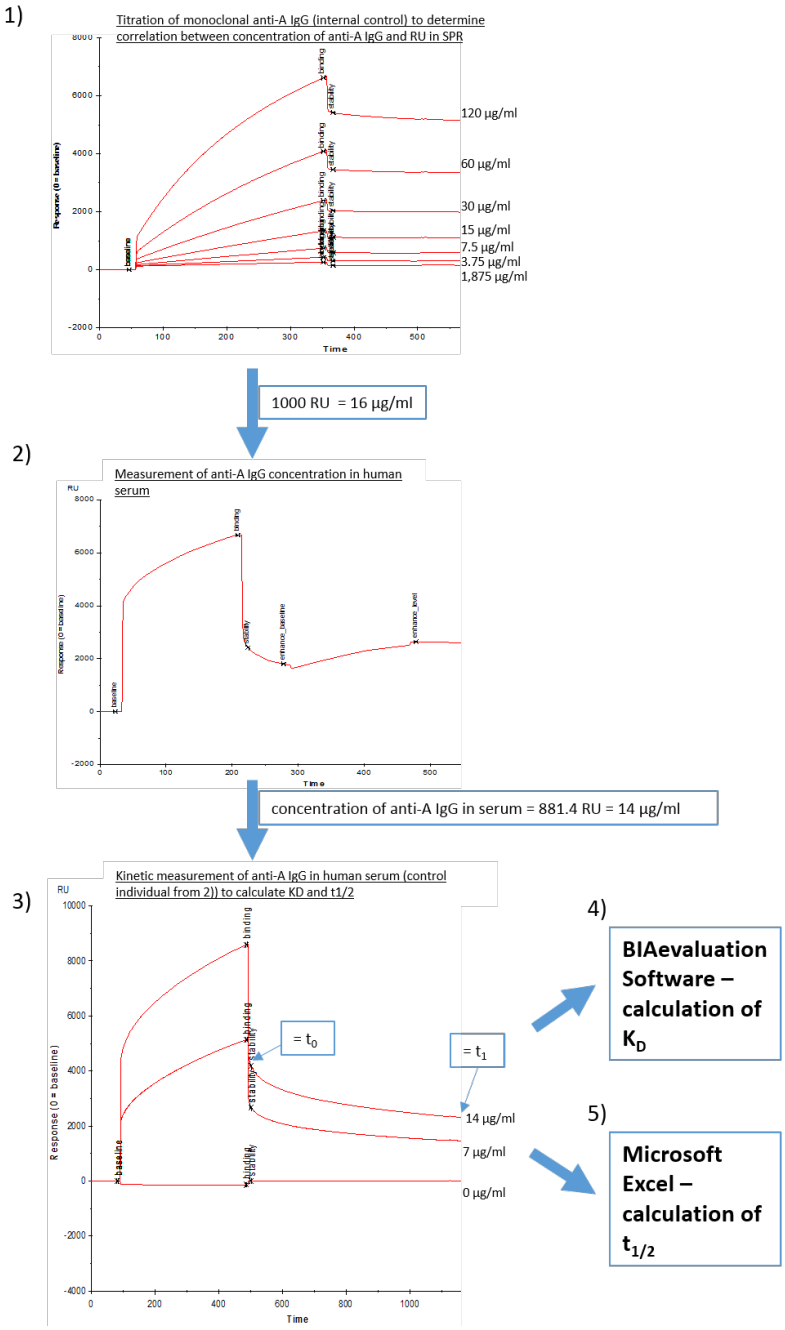

Figure 3.12: Process of quantification and avidity estimation of anti-A IgG antibodies in human serum. „Panel (1) different concentrations of monoclonal anti-A IgG (internal control) were measured to correlate response units to micrograms per millilitre, (2) anti-A IgG levels in human serum were determined utilizing a second injection of anti-IgG (Sigma), (3) different dilutions of human serum were measured without addition of second step reagent, and binding curves were recorded for a total of 1,200 s, (4) an estimate of kd, ka and KD was calculated using the BIAevaluation Software (GE Healthcare) with input of the concentrations of anti-A IgG determined in steps (2) and (3) as described above and (5) single data points were exported and $t_{1/2}$ was computed using MS Excel; t0 and t1 are start and end point of dissociation and have to remain equal for all compared values of $t_{1/2}$ "*(1)*

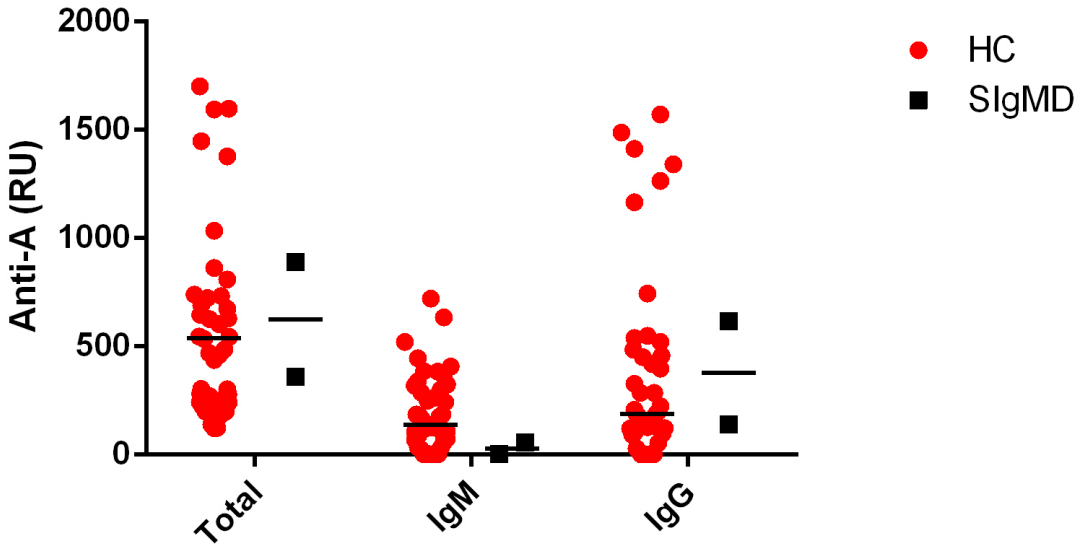

Figure 3.13: Isotype specific quantification of anti-A antibodies by SPRS. Healthy controls (HC) are plotted against patients with selective IgM deficiency (SIgMD)s. Concentration of anti-A total and IgG antibodies are within normal range, whereas anti-A IgM antibodies are not detectable, showing that the deficiency extends to Blood group antibodies, which represent natural antibodies, aswell.

carbohydrate epitopes (blood group isoagglutinins) were determined in patients with selective IgM deficiency who „displayed a defective IgM responsiveness to T-independent bacterial polysaccharide antigens such as 23-valent pneumococcal capsular polysaccharides, either after vaccination with Pneumo 23 Merieux b or following natural exposure/infection, or to tetravalent unconjugated meningococcal vaccine (Mencevax)“(*2*). No anti-A IgM antibodies were detected in both patients, while anti-A IgG antibody titers were normal when compared to healthy controls (figure 3.13) Also a possible impairment in anti-A avidity was investigated using the SPRS assay described, to account for functionality of existing isotypes of natural antibodies. No impairment was found (figure 3.14). These results were published in the course of a study that investigated anti-A/B blood group antibody response in healthy individuals and patients with Type 1 Diabetes Mellitus after vaccination with pneumococcal polysaccharide (*2*) (see Ref (*2*) in Appendix). Secondly K_D of anti-A antibodies were determined in three healthy individuals and in two patients with Diabetes Mellitus 1, a frequent autoimmune disease, before and after vaccination with PnP vaccine, due to concerns that vaccination might lead to autoantibody formation as mentioned above. Also „one healthy individual that was not included in the vaccination protocol but showed high titer for blood group anti-A antibodies was included as a control.“(*1*). As K_D remains unaltered, this serves as evidence that immunization with Pn23 „has no effect on binding characteristics of blood group

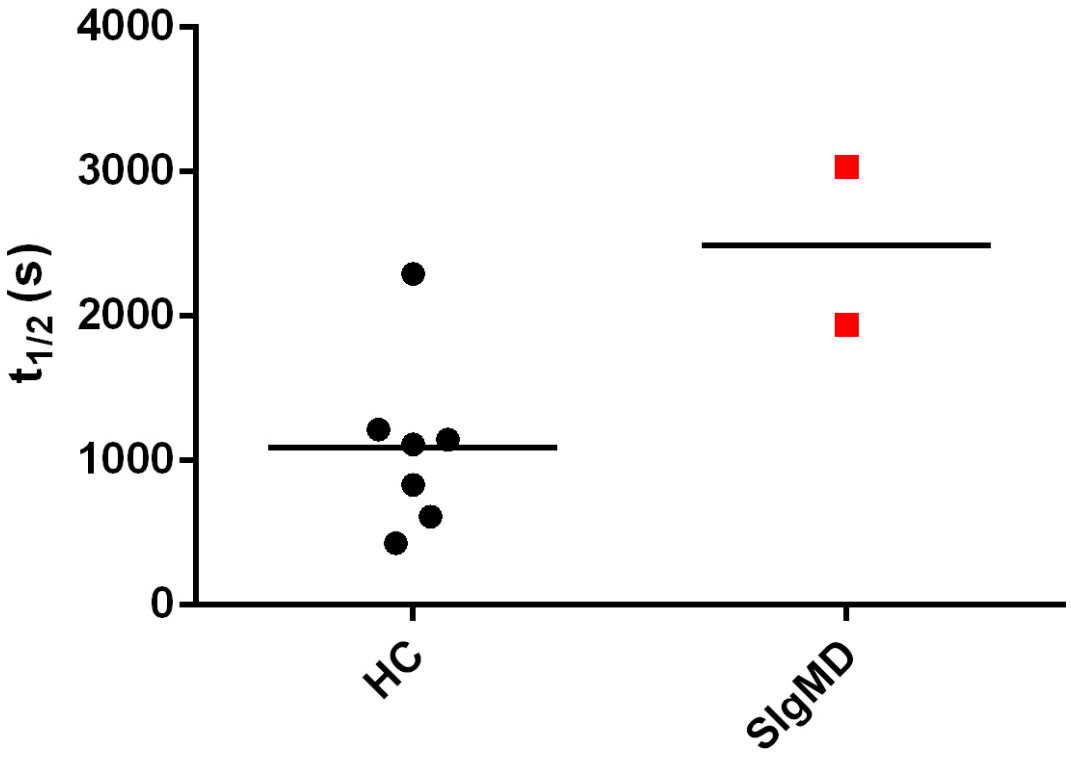

Figure 3.14: Half life decay ($t_{1/2}$) of anti BG A IgG antibodies in healthy controls (HC) and patients suffering from selective IgM deficiency (SIgMD) as determined by SPRS. No impairment of binding stability was detected for anti BG A IgG in patient compared to controls.

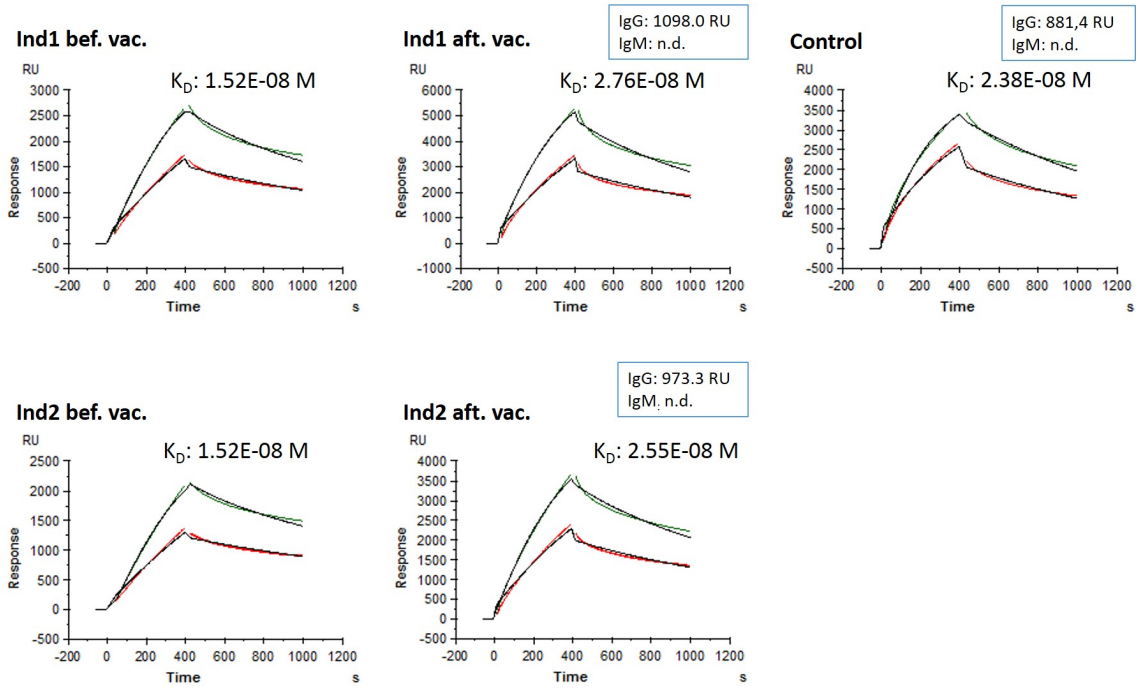

Figure 3.15: Estimated affinity constant K_D of blood group specific anti-A antibodies were analyzed „before and after pneumococcal vaccination in serum samples of three healthy individuals and two patients with type I DM selected for their initially high anti-A antibody titer (>than 1:256 or >than 700 RU). Kinetic measurements of anti-A antibodies binding to surface bound trisaccharide before and after vaccination are depicted in two representative individuals (a healthy individual, Ind1, and a DM I patient, Ind2); one healthy individual that was not included in the vaccination protocol but showed high titer for blood group anti-A antibodies was measured in parallel (Control). Green curves represent serum sample and red curves serum sample diluted by half; the black curves depict the calculated fit. n.d.: not detectable "these results were published in 2016 (*1*)

anti-A/B IgG antibodies, neither in the healthy individuals nor in the patients tested "(*1*) (figure 3.15). The results were published in 2016 (*1*).

3.2 Anti-A/B ELISA

To directly compare avidity estimated by SPRS and ELISA it was attempted to establish a sandwich ELISA coating blood group trisaccharides onto the ELISA plate. Since this antigen is small it had to be presented in a directed way. Thus a coating system was used where maleic anhydride activated plates and amine derivatives of blood group trisaccharides form a peptide bond with each other. However a signal specific for bound antibodies could not be generated. Ultimately when using PBS as dilution buffer the non-specific background was too high to differentiate it from a specific signal, or when adding 5% BSA to the dilution buffer OD were too low in general (see table 3.6). This did not change for different concentrations of

Table 3.6: Comparison of OD values derived from ELISA measurements when PBS or PBS + 5% BSA were used to dilute primary and secondary antibodies. Using PBS a specific signal is obtained for the highest concentration of standard antibody (STD), but not for the remaining concentrations. Diluting with PBS + 5 %BSA yielded no specific signal whatsoever, indicating a blockage of binding sites by BSA.

STD. (ng/ml)	PBS	PBS + 5%BSA
	OD	
1000	0.922	0.153
500	0.527	0.138
250	0.334	0.136
125	0.321	0.143
62.5	0.374	0.151
31.25	0.627	0.158
BLK	0.567	0.142
BLK	0.449	0.145

coating or secondary antibodies, when using PBS as dilution buffer (table 3.7) or different reagents for blocking (PBS + 5% BSA + 0.05 % Tween20; SuperBlock (PBS) Blocking Buffer (Thermo Scientific, Nr. 37515), Ethanolamine, SuperBlock + Ethanolamine) (table 3.8). Thus an alternate analyte had to be used, forfeiting the possibility of direct comparison between SPRS and ELISA. For this binding characteristics of anti 23 valent pneumococcal vaccine (containing capsular pneumococcal polysaccharides) IgG antibodies were examined, since determination of those antibody titers is routinely used in clinical diagnostic service e.g. as an indicator for selective polysaccharide antibody deficiency (SPAD). Including avidity of those antibodies in the diagnostic work-up could offer insight into possible antibody failure were antibody titers are unaltered but binding characteristics are impaired leading to the typical clinical phenotype of susceptibility to bacterial infections.

3.3 Anti-PNV23 IgG titration ELISA

To interpolate the binding curve the Hill equation is used (see equation 1.20). This regression model considers multiple binding sites and yields a coefficient (Hill coefficient h) as a measure of cooperativity between binding sites. This equation was originally worked out for the binding of oxygen to haemoglobin. Positive cooperativity means this affinity of binding site two for the ligand increases once ligand has bound on binding site one and for negative cooperativity the affinity decreases. So binding of one ligand molecule either facilitates or hinders binding of subsequent ligands by e.g. conformational changes within the receptor molecule resulting in positive or negative cooperativity. If no cooperativity occurs the Hill coefficient equals

Table 3.7: Comparison of 10, 5 and 1 μg/ml of trisaccharid A (Dextra Laboratories Ltd., Reading, UK) and 5, 2.5, 1.25 and 0.75 1 μg/ml of secondary antibody (anti mouse IgG) for the analysis of monoclonal goat anti mouse BG A antibodies (STD.) (abcam, HE-193) using ELISA. None of these setups led to a specific signal, but 10 μg/ml of trisaccharid A and 5 μg/ml of secondary antibody were chosen to proceed, since the absolute signal was high and the difference between standard concentrations inidicated a somewhat specific signal.

TRI.A (μg/ml)	10				5				1			
SEC. AB (μg/ml)	5	2.5	1.25	0.75	5	2.5	1.25	0.75	5	2.5	1.25	0.75
STD. (ng/ml)	OD											
1000	1.943	0.908	0.511	0.333	2.392	1.233	0.672	0.473	4.178	2.202	1.132	0.726
500	1.686	1.012	0.525	0.339	1.880	1.092	0.603	0.412	4.195	2.112	1.124	0.668
250	1.634	0.905	0.525	0.308	1.695	1.083	0.552	0.364	3.530	1.902	1.050	0.594
125	1.456	0.795	0.432	0.292	1.834	0.996	0.546	0.365	3.621	1.857	0.974	0.578
62.5	1.482	0.784	0.525	0.306	2.178	1.014	0.564	0.336	3.436	1.841	0.975	0.573
31.25	1.338	0.724	0.493	0.331	2.100	0.955	0.597	0.359	3.724	1.822	1.018	0.577
15.63	1.412	0.901	0.562	0.358	1.917	0.975	0.584	0.394	3.942	1.905	1.011	0.561
BLK	1.843	0.974	0.560	0.383	2.494	1.345	0.710	0.400	3.812	1.967	1.076	0.652

one. The microscopic equilibrium dissociation constant K_d is given as $K_d = (K_D)^h$ with h being the Hill coefficient and K_D the concentration (dilution) at $B_{max}/2$. Since polyclonal antibodies in a highly complex matrix are measured, the validity of considering the Hill coefficient had to be determined at first. Since establishment of a blood group ELISA failed, substitutes to assess the validity of the parameter had to be used instead of SPRS and ELISA validating each other. Generally the in- or exclusion of the Hill coefficient depends on the interpretation of why it deviates from one.

3.3.1 Establishment of data analysis

The One-site Hill equation was compared to three other regression models. Firstly a two-site regression model built into Graphpad Prism 6 software, which divides the binding curve into two equal parts and calculates two values for B_{max} in this way, leading to two values for K_D (K_Dhigh and K_Dlow). Secondly a simple hyperbolic model and thirdly the regression model suggested for titration curves by Eble et al (*14*) were used for regression. From those four regression models the One-site Hill equation and the two site regression model were used for further analysis due to a combination of high determination coefficents (R^2) and ease of use (figure

Table 3.8: Analysis of seven different concentrations and a blank (BLK: dilution buffer only) of monoclonal mouse anti-A IgG (STD.) using different reagents for blocking the plate after coating and to dilute reagents. As blocking reagents PBS + bovine serum albumin (5%) + Tween20 (0.05%) and SuperBlock (PBS) Blocking Buffer (Thermo Scientific, Nr. 37515) were used. Additionally these blocking reagents were tested with and without addition of ethanolamine, to deactive remaining maleic anhydride residues. PBS with and without addition of 10% fetal calf serum were compared as dilution buffer for primary and secondary antibodies. A specific signal was not obtained for any of those setups.

BLOCK	PBS+BSA+Tw20				SuperBlock			
	-		$+EtNH_2$		-		$+EtNH_2$	
DIL.BUF.	PBS	PBS + FCS (10%)	PBS	PBS + FCS (10%)	PBS	PBS + FCS (10%)	PBS	PBS + FCS (10%)
STD. (ng/ml)	OD							
1000	0.921	0.125	0.803	0.136	1.022	0.134	1.117	0.122
500	0.860	0.128	0,286	0.127	0.642	0.134	0.72	0.127
250	0.309	0.126	0.260	0.120	0.615	0.140	0.728	0.128
125	0.274	0.121	0.262	0.124	0.672	0.130	0.729	0.130
62.5	0.277	0.118	0.537	0.123	0.830	0.125	0.924	0.132
31.25	0.293	0.122	0.309	0.122	0.687	0.128	0.829	0.135
15.63	0.289	0.14	0.312	0.127	0.769	0.126	1.155	0.149
BLK	0.607	0.12	0.335	0.126	0.914	0.130	1.617	0.141

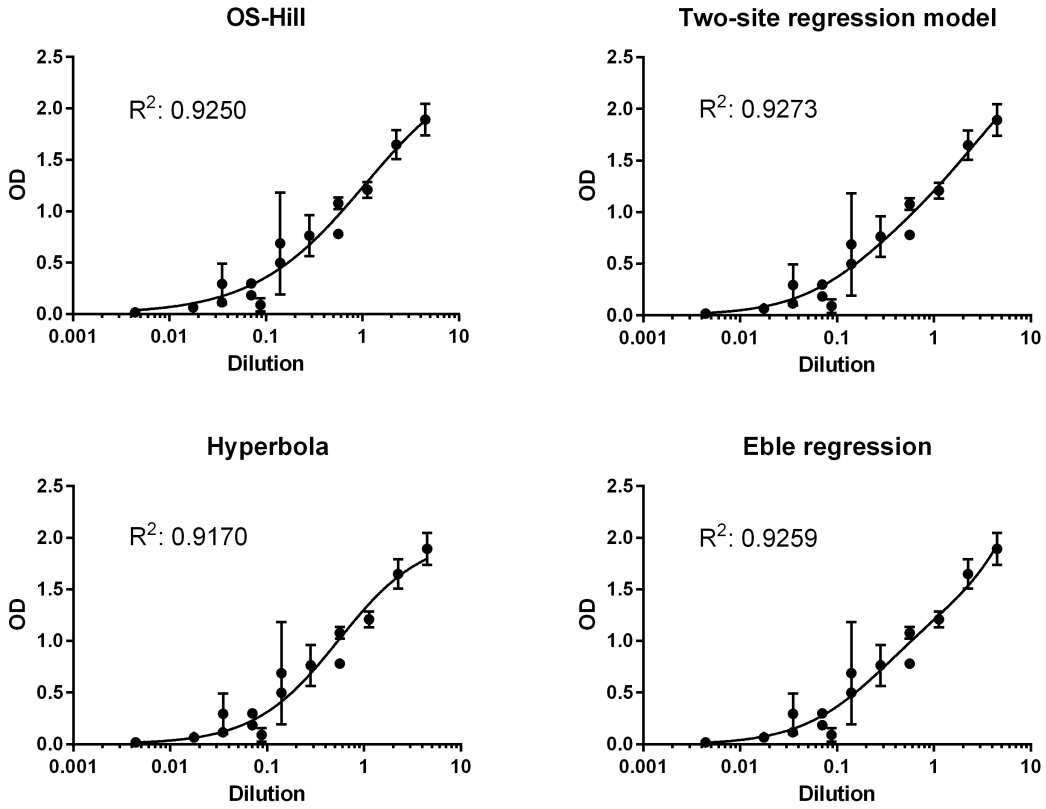

Figure 3.16: Interpolation of data points derived from anti-PnV23 IgG ELISA measurements using four different regression models; 11 different dilutions were used and duplicates measured; due to a combination of high determination coefficient and ease of use the OS-Hill and the two-site regression models were used for further analysis

3.16). 22 samples were measured and analysed using the One-site Hill equation (OS-Hill) with (K_D) and without (K_d) considering the Hill coefficient and the two-sites regression model (figure 3.17). For all values of K_d and K_D, $\frac{1}{K_d}$ and $\frac{1}{K_D}$ were calculated. Reciprocal values K_d and K_D are used for analysis and depicted but for simplification these values are still written as K_d and K_D. These data show no significant difference between the two regression models (figure 3.17). But using the two-site regression model only 55% of the data could be analysed due to four data points being generally too few. This could be circumvented by doubling up on data points, but this would decrease the throughput of the method by 50%. Thus the Hill-equation was used for further analysis. Still the question if the Hill-coefficient indicating cooperativity should be considered remained to be answered.

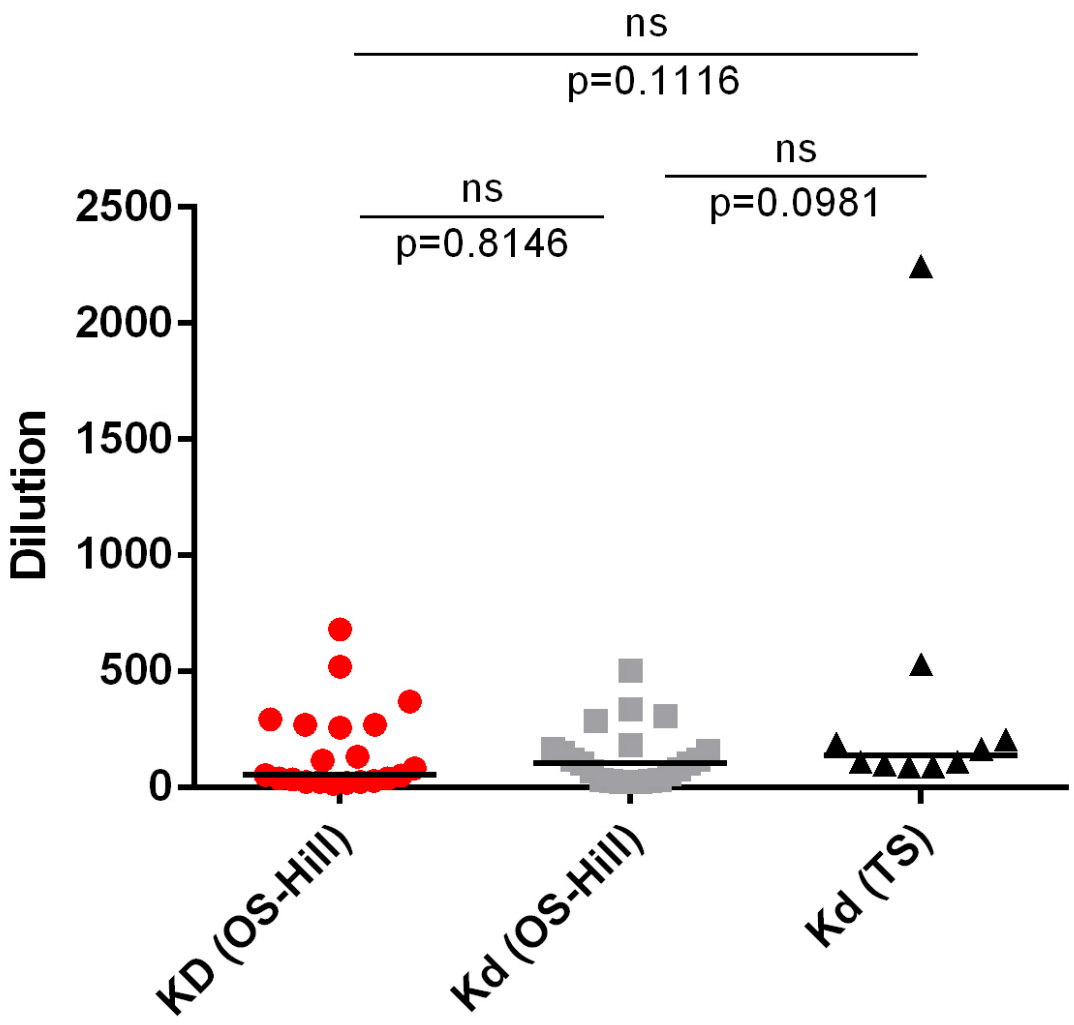

Figure 3.17: Comparison of K_D calulated using the one-site Hill equation (OS Hill) and two-site regression model (TS); for the one-site Hill equation macroscopic dissociation equilibrium constant (K_D) and microscopic dissociation equilibrium constant (K_d) are depicted; data points and median are shown. There is no significant difference between both regression models, but due the OS-Hill equation accepting fewer data points, it was used for further analysis. The question of calculating macroscopic or microscopic dissociation equilibrium constant remained to be answered. Statistical evaluation was performed using the Mann-Whitney U-Test.

3.3.2 Consideration of Hill coefficient

To evaluate if the Hill coefficient is to be considered two different dilution ranges for the same sample were analysed. A valid parameter for avidity has to remain constant for different dilution ranges because it should not be dependant on concentration. Due to the definition of K_D being the concentration or dilution at half-maximum binding, maximum binding (B_{max}) has to be calculated from the binding curve. This can only be done with satisfying precision if the saturation part of the binding curve is depicted, meaning that maximum binding is actually achieved. Thus data were divided into binding curves that reached saturation and those who did not and K_D, K_d, and titers were compared (figure 3.18). These results show that considering the Hill-coefficient generates a concentration dependence of K_D. This means while it might be valuable for defined receptor ligands or monoclonal antibodies used under standardized conditions, it cannot be considered for patient serum measurements. Figure 3.19 shows the binding curves of four different samples (Pat 1 - 4) for both dilution ranges. Pat 1 and 3 are exemplary for the difference in K_D when saturation is achieved for one dilution range (1:5, 1:40, 1:160, 1:640) but not for the second one (1:20, 1:160, 1:640, 1:2560). Pat 2 and 4 on the other hand yield an equivalent K_D at both dilution ranges, because saturation is achieved for both. This shows that a meaningful avidity parameter can only be calculated when saturation is acquired, as otherwise K_D will differ for different concentration ranges. Saturation occurred for a titer equal to or above 250, which was used as a threshold for further analysis. However the binding curve should always be evaluated, to ensure quality of data. Generally speaking K_D of binding curves that do not reach saturation tend to be estimated too low, but more data have to be collected to confirm that. In practice the binding curve reaching saturation for both dilution ranges means that the concentrations of antibodies are within the range of detection for a given concentration of coating antigen. This shows that the concentration of coating molecules has to be suitable for a certain concentration of antibodies. If the concentration of antibody is out of range for the coated antigen, the concentration of the sample must be either increased or decreased or the concentration of coated antigen has to be adjusted. Summing up the avidity of anti-PNV23 IgG antibodies within serum samples can be estimated using a titration ELISA and the Hill-equation for binding curve regression as long as said curve reaches saturation (meaning that the optical density does not increase for the two highest concentrations of the titration curve, indicating the occupation of all binding sites) and the Hill-coefficient is not considered, thus only the macroscopic dissociation equlibrium constant K_D is calculated.

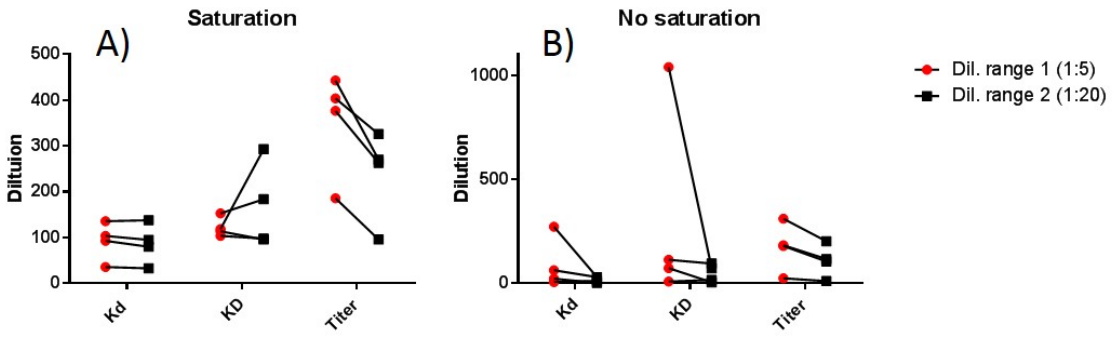

Figure 3.18: K_D, K_d and titers are compared for binding curves reaching saturation (Panel A) and those who do not (Panel B). Examples for corresponding binding curves are depicted in figure 3.14. K_D: macroscopic dissociation equilibrium constant (Hill-coefficient is not considered), K_d: microscopic dissociation equilibrium constant (Hill-coefficient is considered), titer: dilution factor at OD = 0.5; two different dilution ranges were prepared: dil.range 1: 1:5, 1:40, 1:160, 1:640 and dil.range 2: 1:20, 1:160, 1:640, 1:2560 (dil.range 1 : dil.range 2 = 1:4), leading two a difference in titer. However avidity parameters should remain unaltered for different dilution ranges, which is the case for K_D but not K_d when reaching saturation and for neither when saturation is not achieved.

3.3.3 Independence of K_D from the serum antibody concentration

K_D is primarily meant to be used as an additional parameter to antibody titers, so most importantly the independence of K_D from the titer had to be established. To achieve this pneumococcal IgG antibodies in 167 samples, who were not sorted for any criteria were measured and K_D were plotted against titers to perform statistical analysis (Spearmann-test) (figure 3.20). Those results were also sorted for saturation of binding curves and K_D was plotted against titers. This shows a strong correlation ($p>0.0001$) between avidity (K_D) and concentration (titer) if samples are not sorted, but no correlation ($p=0.1944$) if only saturated binding curves are included, making K_D dervied from those curves an independent parameter and a valuable addition for diagnosis. Moreover K_D and titers derived from the sorted samples were compared using the Mann-Whitney U-test, which yielded a p-value lower than 0.0001 proving a significant difference (figure 3.21).

3.3.4 Variation of PNV23 antigen concentration for coating

Since Bruderer et al suggested that the amount of mAbs bound to the immobilized antigen reflects mainly the total mAb concentration for plates coated at high antigen concentration, whereas its reflects primarily the mAbs affinities at low coating concentrations (*40*, *41*), different concentrations of PNV23 vaccine were immobilized.

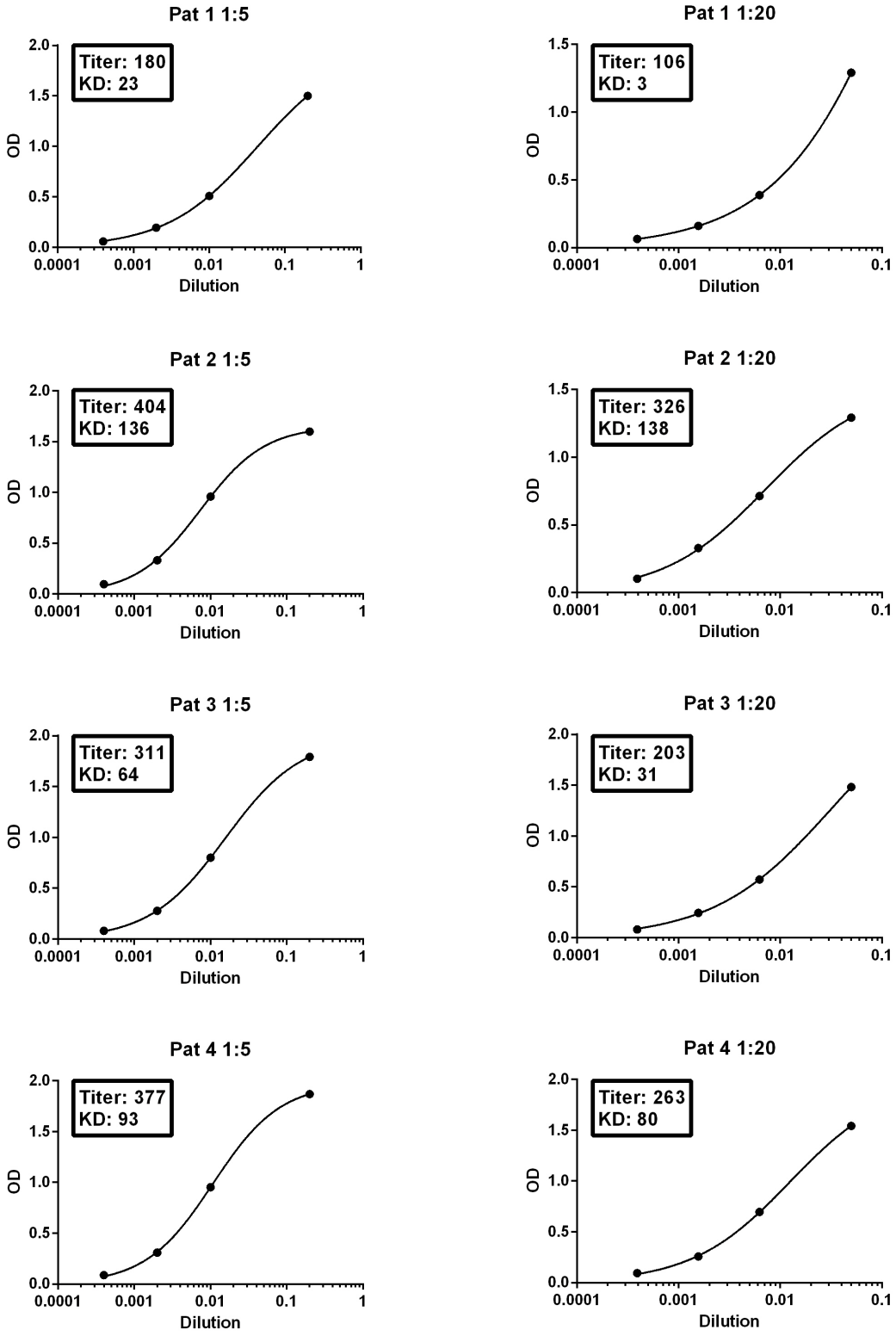

Figure 3.19: Examplary binding curves for four samples diluted differently. Binding curves of Pat 1 and 3 reached saturation at dilution range 1:5 but not at 1:20 leading to a significant difference in K_D. Pat 1 and 4 on the other hand yield binding curves that reach saturation at both dilution ranges, resulting in equivalent K_D. These curves also show that a titer of about 250 constitutes a threshold for saturation.

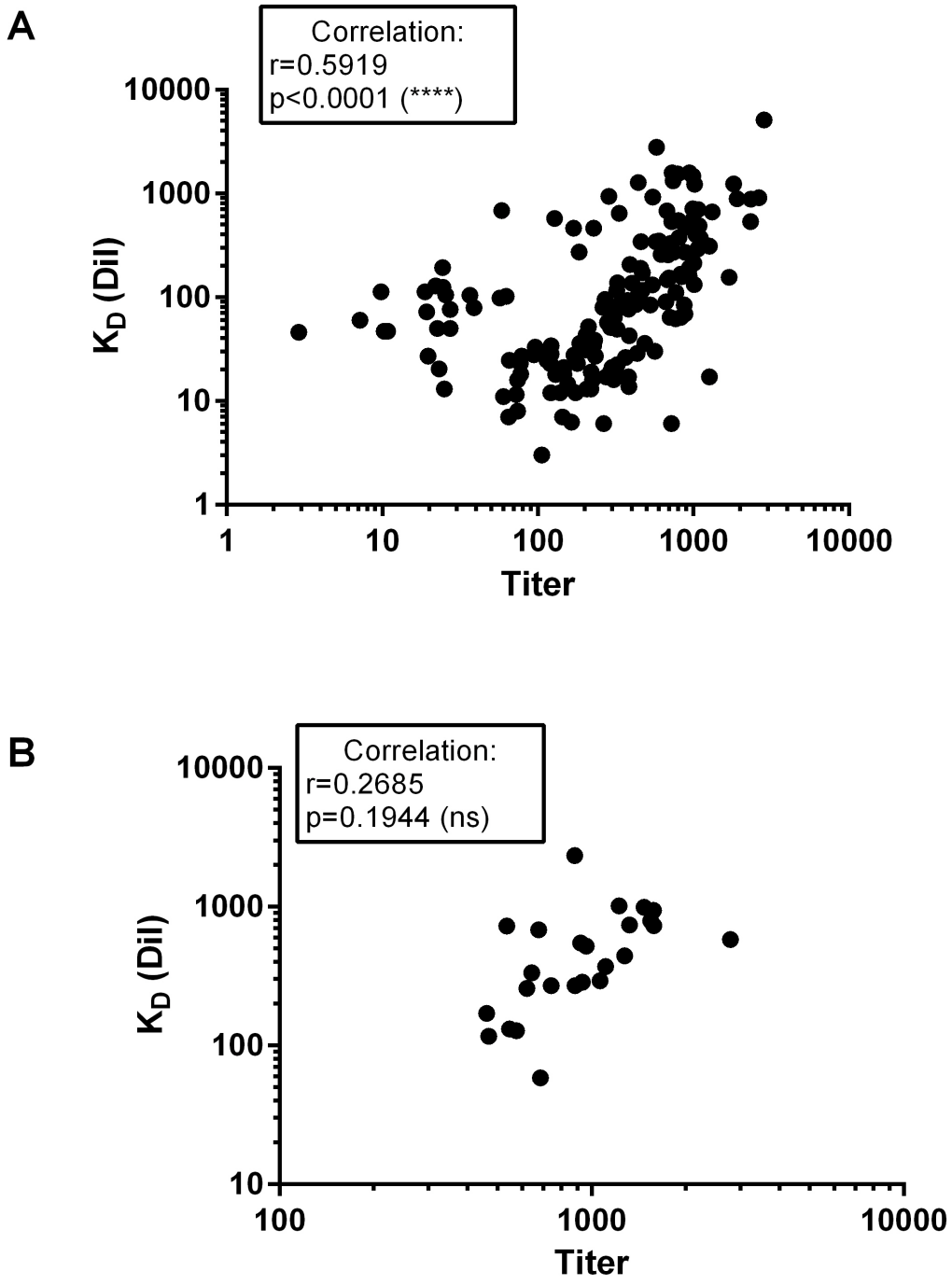

Figure 3.20: Correlation between K_D and titers for A) all samples (n=167) and B) samples sorted for saturation of binding curve (n=25). The determined avidity (K_D) correlates strongly to the concentration (titer) of the sample if binding curves not reaching saturation are included (A). If only measurements with a binding curve reaching saturation are included avidity and concentration do not correlate.

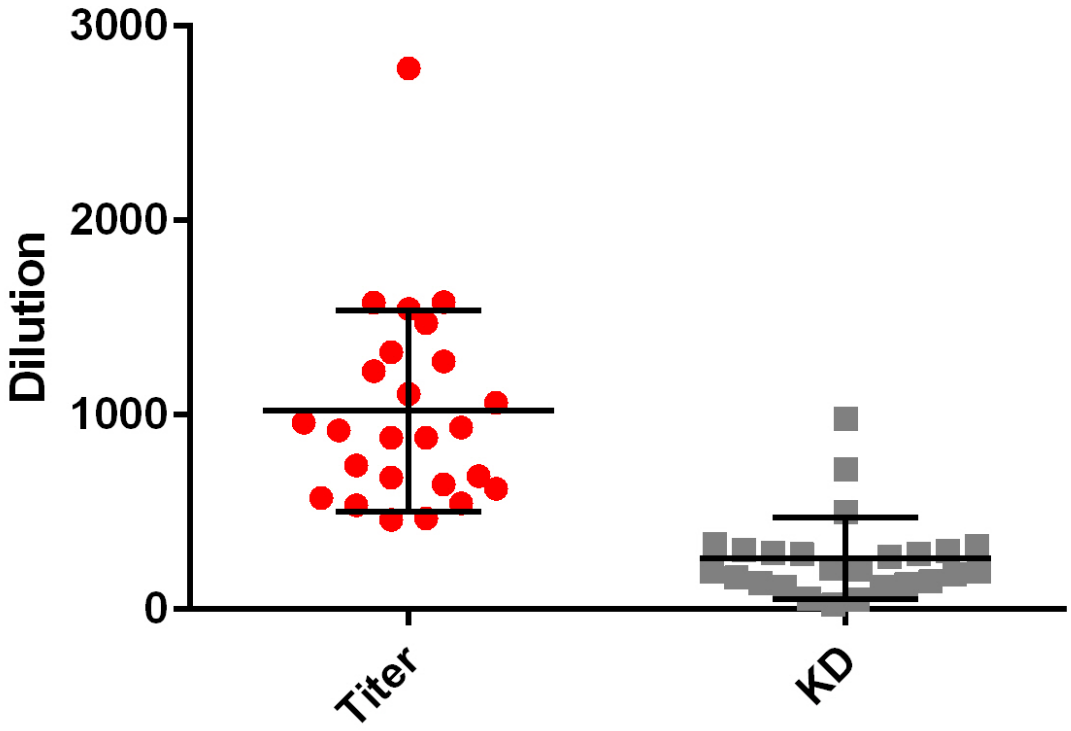

Figure 3.21: Dotplot of Titer and K_D derived from measurement of 25 serum samples; data-points, median and standard deviation are shown; K_D and titers differ significantly ($p < 0.0001$)

Table 3.9: Determination of titer and K_D of anti-PNV23 IgG using 250, 12.5, 5 and 2.5 μg/ml of capture antibody coated onto the plate. This shows that titer varies strongly, while variation of K_D is smaller. Seeing as the variable titer depends upon, concentration of capture antibody and K_D is not, these results align with theory.

Coat.conc. (μg/ml)	titer	K_D
250	1000	290
12.5	167	97
5	37	177
2.5	not calculable	

The plates were coated with 250 (the concentration used for assessment of titer), 12.5, 5 and 2.5 μg/ml antigen and one sample with a titer around 1000 was measured using all four coating concentrations (figure 3.22, table 3.9). This shows vast differences in titer for different concentrations of coated antigen, whereas K_D varies less. The minor difference in K_D with 290 for high concentration of coated antigen (250μg/ml) and 177 for low concentration (5μg/ml) indicates that the same magnitude of binding characteristic is determined for the sample at both concentrations. The binding curves (figure 3.22) also show that in this case 12.5 μg/ml is the most optimal setup, because the sigmoidal form of the curve is approached the closest and the slope is the steepest. This curve yields a K_D of 97, which is assumed to be the most precise. The difference to K_D calculated from the other concentrations of coated antigen is still acceptably low. Titers are dependent upon concentrations of coated antigen because the higher the concentration of coated antigens the lower the concentration of primary antibody (analyte) has to be to achieve an optical density of 0.5, as more binding sites are available. This is reflected in the results of this experiment (table 3.9). Thus no evidence was found that significant differences in binding properties are determined when high and low concentrations of coating antigen were used for K_D data analysis.

For this sample (positive control) 12.5 μg/ml, would be the optimal coating concentration, however considering the typical range of titers within human serum sample, considerably higher titers have to be analysed. Thus 250μg/ml is chosen as coating concentration for further analysis.

3.3.5 Repeatability

To determine the repeatability of the method replicates of a positive control serum were measured on ten different days to calculate K_D and titers from different preparations (table 3.10). The accepted range for titers, which serves as a criterium for reporting of diagnostical findings and was determined in-house specifically for this

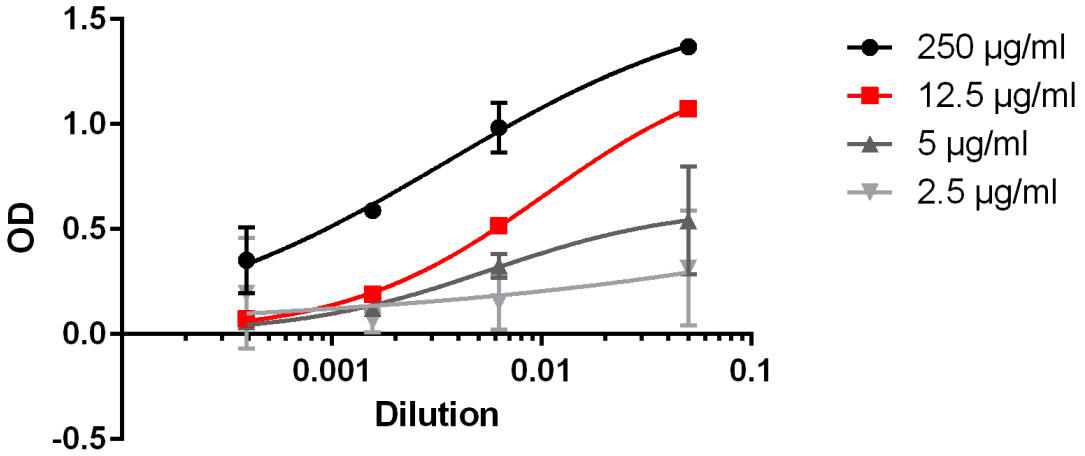

Figure 3.22: Binding curves depicting the optical density for different dilutions of anti-PNV23 IgG calculated from of a serum sample measured at different concentrations of coated antigen. 12.5 μg/ml yields the most optimal curve, since the sigmoidal form is approached the closest, meaning both the upper and lower limit of detection lie within the dilution range for the given antibody. However the optimal concentration of coated antigen depends on the concentration of antibody in the serum sample. This also shows that dilution increases for lower concentrations of coated antigen to achieve an optical density of 0.5 resulting in a lower titer.

method of determining anti-PNV23 IgG titers, lies between a titer of 295 and 440. Since the SD and CV of K_D is lower than SD and CV of titers, which still lie within the accepted range, repeatability of K_D determination is sufficient.

3.3.6 Could difference in optical density measured after different incubation periods serve as a substitute for calculation of K_D ?

To look for an alternative parameter for avidity serum samples were incubated for different durations (5 min, 15 min and 60 min) and the differences of OD were calculated. This was based on the hypothesis that antibodies with high avidity bind faster, leading to the correlation of the difference between short and long incubation with high or low antibody avidity. For all three differences in OD after different incubation times the median was around zero or below indicating that basically all binding events already occurred within the first five minutes (figure 3.23). The median for the difference between 15 and 5 min of incubation was detectable for some samples, but still significantly less than K_D.

To detect any difference the incubation duration must be lower than five minutes which is not feasible using ELISA as an analysis system. From this it follows that difference in OD after different incubation period using ELISA is no valid substitute

Table 3.10: Assessment of repeatibility of measurement of K_D using titration ELISA. R represents the replicates of K_D measurement, PC is the positive control used in determination of anti PN23 titers and K_D and SD stands for standard deviation. Values were determined on different days, while method and operator were kept constant. All values of titers are within the accepted range for output of diagnostical findings, which was determined in-house specifically for this method of determining anti-PNV23 titers. SD of K_D is lower than SD of titers and thus repeatability sufficient.

R	K_D (PC)	titer (PC)
1	101	352
2	102	325
3	109	360
4	158	358
5	121	358
6	72	367
7	82	209
8	125	366
9	129	392
10	120	321
Mean	112	341
SD	23	48
CV	21%	14%

for the calculation of avidity.

3.3.7 Shorter incubation period of serum sample tested in ELISA

This raised the question if titer and K_D can actually be determined using shorter incubation periods of time. To address this possibility several human serum samples were measured after 5, 15 and 60 minutes of incubation and K_D and titers were determined. K_D increased with longer duration of incubation, since an increase in OD results in a higher value of B_{max}, whereas the impact on titer is less pronounced, showing just a slight decrease. This could be indication for dissociation of already bound antibody (figure 3.24). No change of median was statistically significant. To ensure that binding events reach equilibrium and thus optimal K_D and titers are calculated, 60 minutes were chosen as incubation period.

3.3.8 Summary

The results of the development of determination of K_D and optimization of the analysis resulted in a specific titration ELISA assay setup. Those specificities and

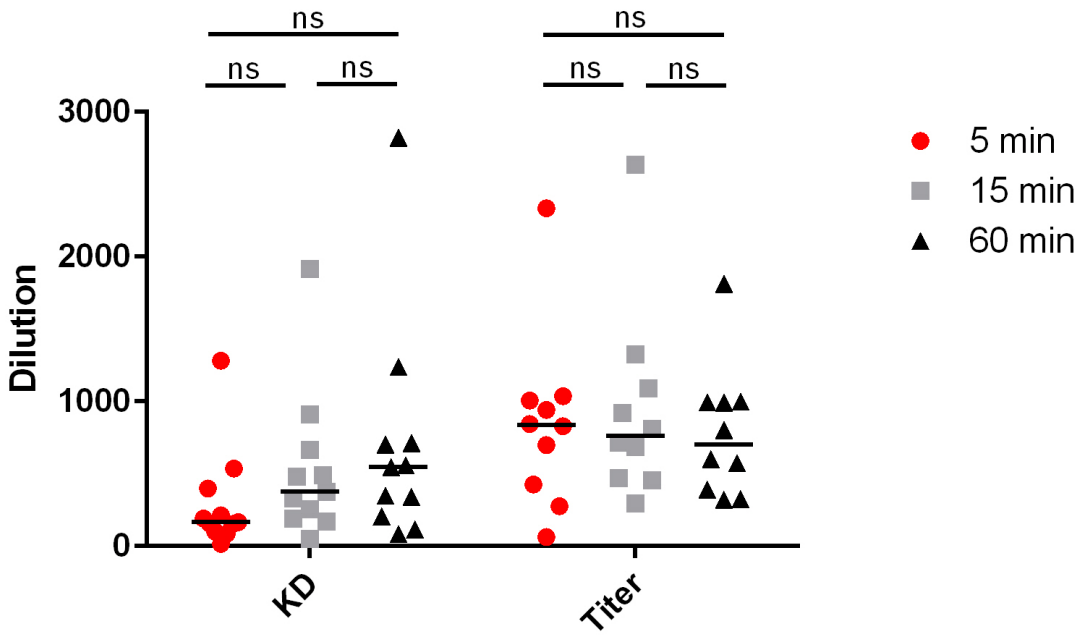

Figure 3.23: K_D versus difference in OD for anti-PNV23 IgG after different incubation period of serum sample (n=8); data points and median are shown. The median of difference in OD for all incubation periods lies around zero, indicating that all binding events already took place within the first five minutes. However shorter incubation periods are not feasible using ELISA as method of analysis making difference of OD after different incubation periods no valid subsitute for K_D. Statistical analysis was performed using the Mann-Whitney U-Test.

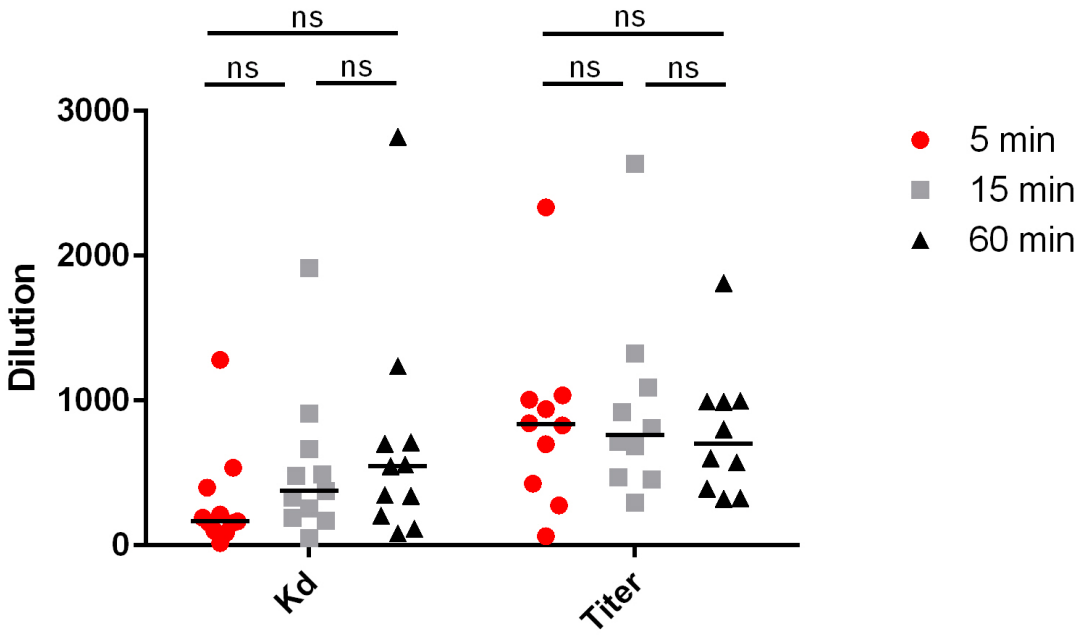

Figure 3.24: K_D and titer of anti-PNV23 IgG for different incubation periods of human serum sample (n=11); data points and median (horizontal bars) are shown. K_D increases for higher incubation periods, due to OD increasing with time, resulting in a higher B_{max}, whereas titer decreases probably due to dissociation of bound antibody with time. No change in median was statistically significant, but to ensure equilibrium of binding events and thus calculating K_D and titer under optimal conditions, 60 min was chosen as incubation period for further analysis.

Table 3.11: Summary of the development of calculating K_D from titration binding curves, validation of the analysis and the optimization of the ELISA setup for generating the necessary data.

DATA ANALYSIS	One-site Hill equation was chosen as regression model. Saturation of binding curve must be achieved to precisely estimate B_{max} and K_D as a result.
HILL-COEFFICIENT	is not considered
CONCENTRATION DEPENDENCE	does not exist, making K_D a valuable addition to titers for diagnostic purposes
COATING-CONCENTRATION	The nature of the parameter does not depend on the coating concentration used. 250μg/ml was chosen as coating concentration.
REPEATABILITY	is sufficient.
ΔOD AS SUBSTITUTE FOR K_D	not possible
INCUBATION PERIOD	60 min necessary

the properties of K_D determination using this setup are summarized in table 3.11

3.3.9 Application

Anti-PNV23 IgG antibody avidity before and after vaccination

K_D of anti-PNV23 IgG antibodies was determined in 17 individuals with intact antibody production before and six to eight weeks after vaccination with PNV23 vaccine. Those individuals were selected based on a tenfold increase in IgG titer after vaccination, indicative of a substantial IgG response to pneumococcal vaccination. The increase of K_D and titers after vaccination was statistically significant (figure 3.25). K_D increased after vaccination in different individuals to a different extent (figure 3.26). The increase in titer after vaccination was more homogenous (figure 3.27). It is to be mentioned that for precise calculation of B_{max} and consequently K_D, saturation of binding curves must be achieved, which is generally the case for titers above 200 (detection limit for serum IgG antibodies in pneumococcal polysaccharide titration ELISA is 1:20). If the titer is lower the estimate of B_{max} becomes less precise, which was the case for some of the samples before vaccination. Nonetheless due to the difference of K_D and titers before and after vaccination ws highly significant ($p < 0.0001$) (figure 3.25) this does not hinder rejection of the null hypothesis.

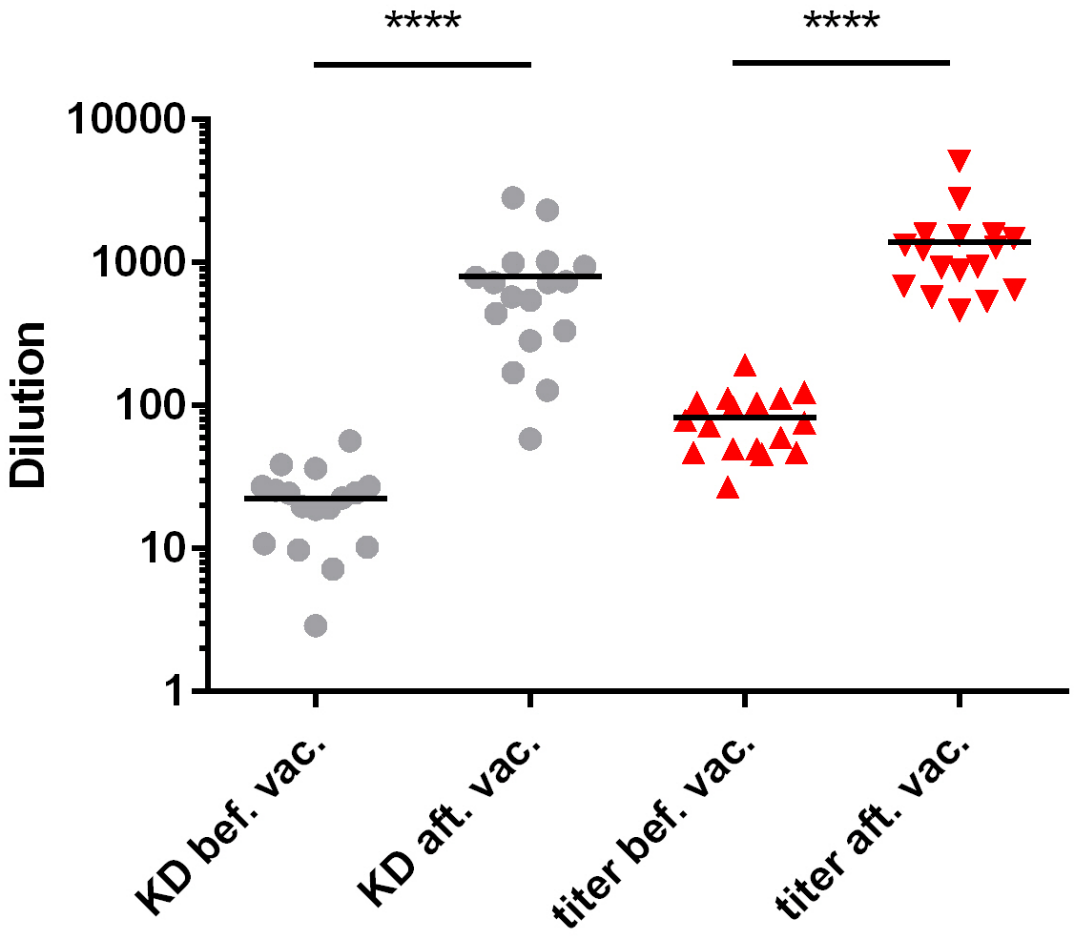

Figure 3.25: Comparison of K_D and titers for human serum samples before and after vaccination using the PNV23-vaccine. Differences before and after vaccination were statistically significant for K_D and titer. Statistical analysis was performed using the Mann-Whitney U-Test (n=17), **** = $p < 0.0001$

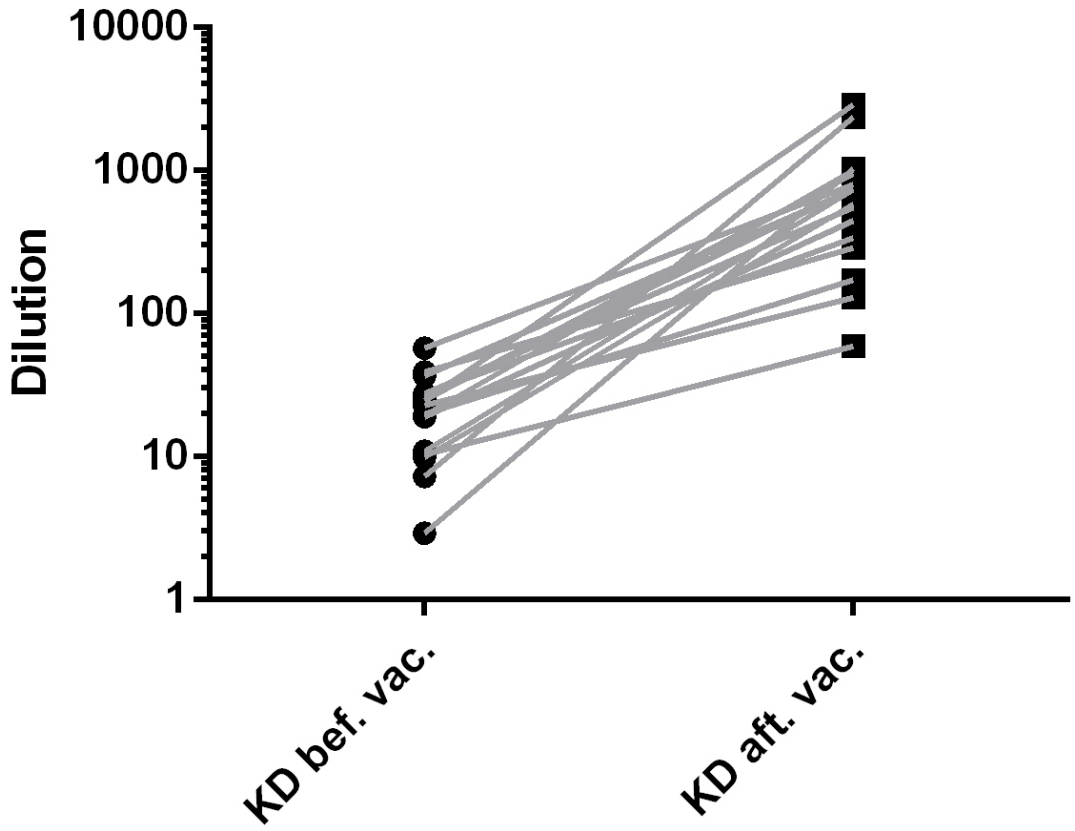

Figure 3.26: Comparison of K_D for human serum samples before and after vaccination using the PNV23-vaccine. The lines connecting the data points represents values measured in serum from the same individual before and after vaccination.

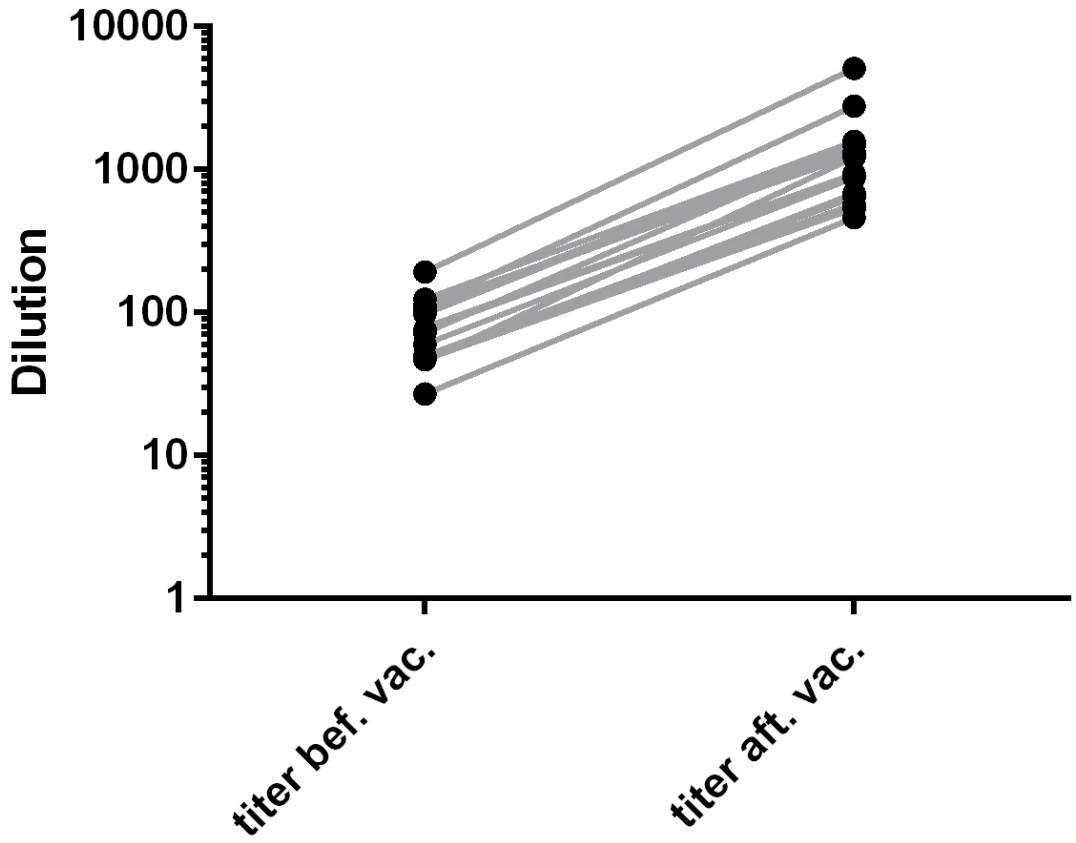

Figure 3.27: Comparison of titer for human serum samples before and after vaccination using the PNV23-vaccine. The lines connecting the data points represents values measured in serum from the same individual before and after vaccination.

Chapter 4

Conclusion and Discussion

This thesis presents two methods to determine concentration of polysaccharide antibodies in an isotype specific manner and estimate their avidity in parallel.

SPRS has been the "gold standard" for real-time detection of antigen-antibody interactions, drug discovery and drug development for approximately two decades (*5–10*, *42*). However it has not yet found its way into diagnostic routine, partly due to lack of applications and assays that can be applied to large scale analysis serum samples. Analysis of binding characteristics using SPRS is typically performed using purified monoclonal antibodies and the according software for data analysis (BIAEvaluation, GE Healthcare). Using this setup the Biacore system generates the most consistent data with the highest quality, when compared to other Biosensor-based platforms, some of them based on Biolayer Interferometry. These alternative biosensor platforms were developed to meet the growing demand of antibody-based products for various therapeutic indications, thus focusing on higher throughput (*42–44*). However implementation into diagnostic routine does not solely depend on high-throughput, but also on simplicity of sample preparation from a technological point of view. Since the continuous flow of sample over an antigen-coated surface is basically the concept of affinity chromatography, purification of antibodies is built into the system and the only issues left to deal with, are unspecific binding and MTL. Other approaches to determine physicochemical properties of antigen-antibody interactions are based on i.e. optical interference patterns (Biolayer Interferometry (*44*)) or increase of conformational stability of the receptor-ligand complex in comparison to unbound receptor and ligand (thermal shift assay (*45*)). Both lack the integrated purification step and thus are not suited for analysis of serum samples, despite having higher throughput capacities. Based on these technological considerations the SPRS-assay presented in this thesis serves as a possibility to measure binding characteristics of antibodies in serum samples. The amine labeling of the antigen constitutes a close approximation to physiological conditions in terms of antigen conformation and using serum as sample matrix provides in vivo conditions for

the antibodies. Data analysis performed using software designed to automatically calculate kinetic parameters such as the *BIAEvaluation* software (GE Healthcare) has the advantage of built-in quality control and ease of use. However calculation of those parameters is confined to analysis as intended by the developers, meaning that two separate measurements have to be performed as the intention (quantification or assessment of kinetic parameters) must be set beforehand. As an alternative the raw data can be exported and analysed manually by software such as *Microsoft Excel*. This can be used to derive kinetic parameters from measurements meant for quantification purposes using flexible dissociation durations. Since this is based on exponential decay of antigen-antibody complexes this is limited to assessing the dissociation rate. Comparison of $t_{1/2}$ with dissociation rate constants calculated by the BIAEvaluation software show little deviation, making it a valid parameter. It is still advisable to not compare data derived from kinetic and quantitative measurements, but only results calculated from curves derived from measurements using equal instrument settings (e.g. association- and dissociation-time).

Moreover the establishment of isotype specific quantification of blood group antibodies offers a sensible and reliable assay for the detection of isoagglutinins of the IgG isotype. The inferior sensitivity of determining titers of blood group antibodies by e.g. the Diamed MicroTyping system, in fact constitutes a problem in the production process of intravenous immunoglobulin preparations as some of the lots may contain substantial amounts of blood group anti-A/anti-B antibodies (*3*). In the course of this thesis a paper was published on this topic describing changes in the haematological parameters in a cohort that were likely caused by blood group antibodies within administered IVIG preparations (*3*). The presented SPRS method could possibly constitute an alternative for determination of titers of isoagglutinin concentration. Summing up SPRS is a suitable option for the determination of binding characteristics of serum antibodies but costly, which constitutes a high barrier to entry for routine use when assessing immunological parameters for clinical purposes.

ELISA on the other hand constitutes a low-budget option using devices that are commonly used in medical laboratories. Moreover a titration ELISA method offers two options within one determination, namely assessing antibody concentration and avidity. Firstly the sample of interest can be diluted within a certain range to determine their titer at absorbance of 0.5 and their avidity at half-maximum binding. K_D and titer can thus be determined from the same measurement as long as the antibody concentration is within the range of coated antigen, meaning the antibody binding curve reaches saturation. Otherwise dilution of serum (antibody) or more likely concentration of coated antigen have to be adjusted. This option offers no additional cost whatsoever but yields both titer and avidity in units of dilution. To determine both parameters in SI conformable units (g/l) a calibration curve

using analyte preparations of known concentration could be computed to quantify the analyte within the serum sample. Conducting a second experiment different concentrations of the sample yielding a separate binding curve have to be measured to read their concentration in g/l at half-maximum binding. This version requires the additional costs of a single ELISA experiment.

The difference between competitive and and non-competitive ELISA (i.e. direct or sandwich ELISA) was previously discussed in the literature (*40*). For general determination of the equilibrium constants (K_A or K_D) it was suggested that only indirect competition ELISA assays should be used. This suggestion was based on the argument that when using a non-competitive ELISA assay only an apparent equilibrium constant rather than the thermodynamically defined real equilibrium constant is determined. This is a result of factors other than affinity influencing the surface equilibrium such as steric hindrance and antigen mobility on the surface. Still relative affinity can be estimated by non-competitive ELISA assays, which has been shown to correlate albeit not coincide with the real antibody affinity in solution (*46*).

Moreover it also must be taken into account that when using indirect competition ELISA assays to determine antibody affinity to antigen, plastic surface antigen is competing with free antigen for binding sites. As pointed out by Goldberg et al (*40*) binding of antigens leads to a conformational change, which means that bound and unbound antigens competing for antibody binding sites are most likely of different conformation. Thus the affinity of the antibody likely differs for both antigens. This also constitutes a bias for the determination of *real* affinity of the antibody-analyte. Lastly while polysaccharides do form tertiary structures they are much less prone to denaturation than peptides since the energy barriers between conformations are lower (*47*), which means that the problem of denaturation due to immobilization might not exist for polysaccharides. However this is yet to be investigated. It is also to mention that in many cases, it is not necessary to determine the *real* avidity of antibodies, as relative measures suffice.

To sum up the general consensus is that a non-competitive ELISA yields a relative and semiquantitative measure of avidity. Dissociation equilibrium constants acquired using this method can be compared to each other but not to those determined by e.g. surface plasmon resonance spectroscopy. However both methods can be used to validate each other. Moreover it was suggested that the amount of mAbs bound to the immobilized antigen reflects mainly the total mAb concentration for plates coated at high antigen concentration, whereas it reflects primarily the mAb affinity at low coating concentrations (*40*, *41*). These findings could not be replicated in the presented thesis using human serum as an analyte, but it was shown that there is an optimal concentration of immobilized antigen for both determination of

titers and K_D, depending on antibody concentration within the sample. For human serum 250μg/ml work well.

The Hill-equation proved to be the model of nonlinear regression of choice when using only data points to yield high determination coefficients without frequent exclusion of samples (Figure 3.16). When using this model the Hill-coefficient serves as an indicator for data validity but should not be applied to K_D transforming it into the microscopic equilibrium dissociation constant K_d. Kd represents the ratio of dissociation to association rate constant after 60 minutes of incubation of all specific antibodies that bind to the antigen-coated surface. In the context of an ELISA experiment increased or decreased cooperativity of said antibody leads to a higher or lower probability that the second antigen-binding site binds, which in turn leads to a higher or lower probability of the antibody dissociating from the surface, resulting in more or less optical density. It is questionable that this change is detectable by spectroscopy. Thus it is unknown if - using this setup - cooperativity leads to a significant change in the avidity parameter, but it simply would be expressed within K_D. Moreover since the immobilized antigen can be thought of as semi-denaturated thus diverging from the in vivo conformation, intra-molecular signalling that leads to cooperativity might not occur at all. Label-free methods like SPR or X-ray crystallography, depicting the in-vivo system more closely, are better suited for the task of assessing cooperativity. In conclusion if unspecific binding is kept to a minimum, deviations to the Hill-coefficient from one most likely stem from inapt ratio of antibody to antigen. Data that support allostery within antibodies, either within the Fab segment changing the affinity of the antigen binding site, or from Fab to Fc region altering affinity for Fc specific molecules (e.g. Fcγ-receptor or C1q), exists. Defective allostery as a patho-mechanism or allostery as an additional consideration for intravenous immunoglobulin therapy is certainly of interest, but it cannot be investigated using the presented method (*48*).

It is sometimes advised not to use direct ELISA assays for determination of avidity, because immobilization of antigen leads to a conformational change thus altering the physiologic binding event. This can be avoided using a competitive ELISA setup because the binding event happens in solution. This is true if depicting physiological conditions for antigen and antibody is paramount, but competitive assays rely on immobilization of antigen as well to capture antibodies. Thus the affinity of antibody for both competing antigens differs. This bias must be considered when using competitive assays to determine avidity of antibodies.

It is important to note that not the same avidity constant is measured when using SPRS or ELISA. Since SPRS reads the binding event in real time while ELISA relies on establishment of an equilibrium, SPRS yields the dissociation rate constants k_a and k_d while ELISA produces the dissociation equilibrium constant K_D. As shown

above (equation 1.9) K_D can be calculated from k_a and k_d but it is important to note that the parameter that is *directly* measured is different. The methods presented in this thesis include assessment of association and dissociation rate and equilibrium constants. When evaluating biological functions of antibodies or any protein, it must be taken into account, that where equilibrium constants are equal for two different molecules, rate constants might differ. So if possible it is preferable to determine rate constants (e.g. using SPRS) and calculate the according equilibrium constants to get a full picture of the molecules'affinity. How different rate constants but equal equilibrium constants are judged, has to be the subject of further investigation.

The quality control of data derived from both SPR and ELISA measurements is ensured by manual validation by the analyst based on a set of criteria. With analytical chemistry moving towards big data and -*omics*-type analysis this shows the importance of individual competence of analysts to transform *big* into *meaningful* data.

Bibliography

(*1*) Wolfram, W., Sauerwein, K. M. T., Binder, C. J., Eibl-Musil, N., Wolf, H. M. and Fischer, M. B. (2016). Pneumococcal polysaccharide vaccination elicits IgG Anti-A/B blood group antibodies in healthy individuals and patients with type I diabetes mellitus. *Frontiers in Immunology 7*, DOI: 10.3389/fimmu.2016.00493.

(*2*) Geier, C. B., Sauerwein, K. M., Leiss-Piller, A., Zmek, I., Fischer, M. B., Eibl, M. M. and Wolf, H. M. (2018). Hypomorphic Mutations in the BCR Signalosome Lead to Selective Immunoglobulin M Deficiency and Impaired B-cell Homeostasis. *Frontiers in immunology*, DOI: 10.3389/fimmu.2018.02984.

(*3*) Cicha, A., Fischer, M. B., Wesinger, A., Haas, S., Bauer, W. M., Wolf, H. M., Sauerwein, K. M., Reininger, B., Petzelbauer, P., Pehamberger, H. and Handisurya, A. (2018). Effect of intravenous immunoglobulin administration on erythrocyte and leucocyte parameters. *Journal of the European Academy of Dermatology and Venereology*, DOI: 10.1111/jdv.14671.

(*4*) Fried, A. J., Altrich, M. L., Liu, H., Halsey, J. F. and Bonilla, F. A. (2013). Correlation of pneumococcal antibody concentration and avidity with patient clinical and immunologic characteristics. *Journal of Clinical Immunology*, DOI: 10.1007/s10875-013-9870-9.

(*5*) Krause, S., Chmiel, R., Bonifacio, E., Scholz, M., Powell, M., Furmaniak, J., Rees Smith, B., Ziegler, A. G. and Achenbach, P. (2012). IA-2 autoantibody affinity in children at risk for type 1 diabetes. *Clinical Immunology*, DOI: 10.1016/j.clim.2012.09.010.

(*6*) Trabucchi, A., Guerra, L. L., Faccinetti, N. I., Iacono, R. F., Poskus, E. and Valdez, S. N. (2012). Surface plasmon resonance reveals a different pattern of proinsulin autoantibodies concentration and affinity in diabetic patients. *PLoS ONE*, DOI: 10.1371/journal.pone.0033574.

(*7*) Lynch, H. E., Stewart, S. M., Kepler, T. B., Sempowski, G. D. and Alam, S. M. (2014). Surface plasmon resonance measurements of plasma antibody avidity during primary and secondary responses to anthrax protective antigen. *Journal of Immunological Methods*, DOI: 10.1016/j.jim.2013.11.026.

(*8*) Steinicke, F., Oltmann-Norden, I. and Wätzig, H. (2017). Long term kinetic measurements revealing precision and general performance of surface plasmon resonance biosensors. *Analytical Biochemistry*, DOI: 10.1016/j.ab.2017.05.009.

(*9*) Daga, S., Moyse, H., Briggs, D., Lowe, D., Evans, N., Jones, J., Buchli, R., McMurtrey, C., Mulder, A., Hildebrand, W., Claas, F., Higgins, R., Mitchell, D. A. and Zehnder, D. (2018). Direct quantitative measurement of the kinetics of HLA-specific antibody interactions with isolated HLA proteins. *Human Immunology*, DOI: 10.1016/j.humimm.2017.10.012.

(*10*) Klasse, P. J. (2016). How to assess the binding strength of antibodies elicited by vaccination against HIV and other viruses. *Expert Review of Vaccines*, DOI: 10.1586/14760584.2016.1128831.

(*11*) Syedbasha, M., Linnik, J., Santer, D., O'Shea, D., Barakat, K., Joyce, M., Khanna, N., Tyrrell, D. L., Houghton, M. and Egli, A. (2016). An ELISA Based Binding and Competition Method to Rapidly Determine Ligand-receptor Interactions. *Journal of Visualized Experiments*, DOI: 10.3791/53575.

(*12*) Rosenbluh, J., Kapelnikov, A., Shalev, D. E., Rusnati, M., Bugatti, A. and Loyter, A. (2006). Positively charged peptides can interact with each other, as revealed by solid phase binding assays. *Analytical Biochemistry*, DOI: 10.1016/j.ab.2006.03.002.

(*13*) Levin, A., Hayouka, Z., Helfer, M., Brack-Werner, R., Friedler, A. and Loyter, A. (2009). Peptides derived from HIV-1 integrase that bind rev stimulate viral genome integration. *PLoS ONE*, DOI: 10.1371/journal.pone.0004155.

(*14*) Eble, J. A. (2018). Titration ELISA as a Method to Determine the Dissociation Constant of Receptor Ligand Interaction. *Journal of Visualized Experiments*, DOI: 10.3791/57334.

(*15*) Pullen, G. R., Fitzgerald, M. G. and Hosking, C. S. (1986). Antibody avidity determination by ELISA using thiocyanate elution. *Journal of Immunological Methods*, DOI: 10.1016/0022-1759(86)90268-1.

(*16*) Bisswanger, H., *Enzyme Kinetics: Principles and Methods*, Second; Wiley-VCH: Weinheim, 2008.

(*17*) Tang, Y., Zeng, X. and Liang, J. (2010). Surface plasmon resonance: An introduction to a surface spectroscopy technique. *Journal of Chemical Education*, DOI: 10.1021/ed100186y.

(*18*) Sabban, S. Development of an in vitro model system for studying the interaction of Equus caballus IgE with its high- affinity FcϵRI receptor, Ph.D. Thesis, The University of Sheffield, 2011.

(*19*) Jeong, H. S., Adachi, K., Bong, K. L., Dong, G. K., Yeon, K. K., Kyoung, R. K., Hea, Y. L., Kawai, T. and Hyung, J. C. (2007). Facile and rapid direct gold surface immobilization with controlled orientation for carbohydrates. *Bioconjugate Chemistry*, DOI: 10.1021/bc700288z.

(*20*) Jonsson, U. et al. (1991). Real-time biospecific interaction analysis using surface plasmon resonance and a sensor chip technology. *BioTechniques*, DOI: 10.1016/0021-9673(92)80137-J.

(*21*) Kimura, S., Yurugi, K., Segawa, H., Kuroda, J., Sato, K., Nogawa, M., Yuasa, T., Egawa, H., Tanaka, K. and Maekawa, T. (2005). Rapid quantitation of immunoglobulin G antibodies specific for blood group antigens A and B by surface plasmon resonance. *Transfusion*, DOI: 10.1111/j.1537-2995.2005.04062.x.

(*22*) Canziani, G. A., Klakamp, S. and Myszka, D. G. (2004). Kinetic screening of antibodies from crude hybridoma samples using Biacore. *Analytical Biochemistry*, DOI: 10.1016/j.ab.2003.11.004.

(*23*) Schuck, P. and Zhao, H. (2010). The role of mass transport limitation and surface heterogeneity in the biophysical characterization of macromolecular binding processes by SPR biosensing. *Methods in molecular biology (Clifton, N.J.)*, DOI: 10.1007/978-1-60761-670-2_2.

(*24*) Morton, T. A., Myszka, D. G. and Chaiken, I. M. (1995). Interpreting complex binding kinetics from optical biosensors: A comparison of analysis by linearization, the integrated rate equation, and numerical integration. *Analytical Biochemistry*, DOI: 10.1006/abio.1995.1268.

(*25*) Björkelund, H., Gedda, L. and Andersson, K. (2011). Comparing the epidermal growth factor interaction with four different cell lines: Intriguing effects imply strong dependency of cellular context. *PLoS ONE*, DOI: 10.1371/journal.pone.0016536.

(*26*) Goutelle, S., Maurin, M., Rougier, F., Barbaut, X., Bourguignon, L., Ducher, M. and Maire, P. (2008). The Hill equation: A review of its capabilities in pharmacological modelling. *Fundamental and Clinical Pharmacology*, DOI: 10.1111/j.1472-8206.2008.00633.x.

(*27*) Ortiz, A. (2013). Derivation of Hill's equation from scale invariance. *Journal of Uncertain Systems 7*, 198–202.

(*28*) Milland, J. and Sandrin, M. S. (2006). ABO blood group and related antigens, natural antibodies and transplantation. *Tissue Antigens*, DOI: 10.1111/j.1399-0039.2006.00721.x.

(*29*) Nguyen, H. P., Seto, N. O., MacKenzie, C. R., Brade, L., Kosma, P., Brade, H. and Evans, S. V. (2003). Germline antibody recognition of distinct carbohydrate epitopes. *Nature Structural Biology*, DOI: 10.1038/nsb1014.

(*30*) Brooks, C. L., Müller-Loennies, S., Brade, L., Kosma, P., Hirama, T., MacKenzie, C. R., Brade, H. and Evans, S. V. (2008). Exploration of Specificity in Germline Monoclonal Antibody Recognition of a Range of Natural and Synthetic Epitopes. *Journal of Molecular Biology*, DOI: 10.1016/j.jmb.2008.01.018.

(*31*) Patenaude, S. I., Seto, N. O., Borisova, S. N., Szpacenko, A., Marcus, S. L., Palcic, M. M. and Evans, S. V. (2002). The structural basis for specificity in human abo(h) blood group biosynthesis. *Nature Structural Biology*, DOI: 10.1038/nsb832.

(*32*) Defrance, T., Taillardet, M. and Genestier, L. (2011). T cell-independent B cell memory. *Current Opinion in Immunology*, DOI: 10.1016/j.coi.2011.03.004.

(*33*) Finland, M. and Curnen, E. C. (1938). Agglutinins for human erythrocytes in type xiv anti-pneumococcic horse serums. *Science*, DOI: 10.1126/science.87.2262.417.

(*34*) Yuki, N. (2005). Carbohydrate mimicry: A new paradigm of autoimmune diseases. *Current Opinion in Immunology*, DOI: 10.1016/j.coi.2005.09.004.

(*35*) Yamamoto, F. (2004). Review: ABO blood group system - ABH oligosaccharide antigens, anti-A and anti-B, A and B glycosyltransferases, and ABO genes. *Immunohematology*, DOI: 10.1175/JCLI3252.1.

(*36*) Lleo, A., Invernizzi, P., Gao, B., Podda, M. and Gershwin, M. E. (2010). Definition of human autoimmunity - autoantibodies versus autoimmune disease. *Autoimmunity Reviews*, DOI: 10.1016/j.autrev.2009.12.002.

(*37*) Kubo, T., Uchida, Y., Watanabe, Y., Abe, M., Nakamura, A., Ono, M., Akira, S. and Takai, T. (2009). Augmented TLR9-induced Btk activation in PIR-B-deficient B-1 cells provokes excessive autoantibody production and autoimmunity. *The Journal of experimental medicine*, DOI: 10.1084/jem.20082392.

(*38*) Chou, M. Y., Fogelstrand, L., Hartvigsen, K., Hansen, L. F., Woelkers, D., Shaw, P. X., Choi, J., Perkmann, T., Bäckhed, F., Miller, Y. I., Hörkkö, S., Corr, M., Witztum, J. L. and Binder, C. J. (2009). Oxidation-specific epitopes are dominant targets of innate natural antibodies in mice and humans. *Journal of Clinical Investigation*, DOI: 10.1172/JCI36800.

(*39*) Chen, R. T., Pless, R. and Destefano, F. (2001). Epidemiology of autoimmune reactions induced by vaccination. *Journal of Autoimmunity*, DOI: 10.1006/jaut.2000.0491.

(*40*) Goldberg, M. E. and Djavadi-Ohaniance, L. (1993). Methods for measurement of antibody/antigen affinity based on ELISA and RIA. *Current Opinion in Immunology*, DOI: 10.1016/0952-7915(93)90018-N.

(*41*) Bruderer, U., Deusinger, M., Schürch, U. and Lang, A. B. (1992). Analyses of affinity distributions within polyclonal populations of antigen-specific antibodies. Evaluation of their accuracy in population detection using monoclonal antibodies. *Journal of Immunological Methods*, DOI: 10.1016/0022-1759(92)90114-9.

(*42*) Yang, D., Singh, A., Wu, H. and Kroe-Barrett, R. (2017). Determination of High-affinity Antibody-antigen Binding Kinetics Using Four Biosensor Platforms. *Journal of Visualized Experiments*, DOI: 10.3791/55659.

(*43*) Ecker, D. M., Jones, S. D. and Levine, H. L. (2015). The therapeutic monoclonal antibody market. *mAbs*, DOI: 10.4161/19420862.2015.989042.

(*44*) Fang, Y. (2006). Label-Free Cell-Based Assays with Optical Biosensors in Drug Discovery. *ASSAY and Drug Development Technologies*, DOI: 10.1089/adt.2006.4.583.

(*45*) Liu, W.-W., Zhu, Y. and Fang, Q. (2017). Femtomole-Scale High-Throughput Screening of Protein Ligands with Droplet-Based Thermal Shift Assay. *Analytical Chemistry*, DOI: 10.1021/acs.analchem.7b00899.

(*46*) Rath, S., Stanley, C. M. and Steward, M. W. (1988). An inhibition enzyme immunoassay for estimating relative antibody affinity and affinity heterogeneity. *Journal of Immunological Methods*, DOI: 10.1016/0022-1759(88)90204-9.

(*47*) Glaudemans, C. P., *Encyclopedia of Immunology*, Second, 1998.

(*48*) Yang, D., Kroe-Barrett, R., Singh, S., Roberts, C. J. and Laue, T. M. (2017). IgG cooperativity Is there allostery? Implications for antibody functions and therapeutic antibody development. *mAbs*, DOI: 10.1080/19420862.2017.1367074.

Appendix A

Abstracts

A.1 Abstract - english

This thesis presents two approaches to assess the avidity of antibodies against polysaccharide antigens in human serum. A special focus is directed to the applicability for diagnostic routine as the overall goal is the consideration of this parameter for the diagnosis of primary immunodeficiencies. Two methods were used to achieve this, firstly surface plasmon resonance spectroscopy (SPRS) and secondly titration ELISA. Using SPRS an assay to determine concentration in an isotype-sepcific manner and overall avidity of anti blood group A and B antibodies was established. With this technology the association rate constant ka and the dissocation rate constant kd can be determined and the association and dissociation equilibrium constants (K_A and K_D) can be calculated. Moreover a method to manually analyze sensorgrams to calculate the half-life of the antibody bound to antigen is presented. This assay offers high throughput, robustness and repeatability, but is less well suited for diagnostic routine laboratories due to high costs. To establish a method that is less costly but also reliable to determine the dissocation equilibrium constant KD a titration ELISA was developed, as equipment and reagents required for ELISA testing are readily available in diagnostic routine laboratories. For this a reliable regression model was determined and criteria for assessing the quality of analysis were established. The presented methods for assay procedure, data analysis and quality control allow for integration of antibody avidity assessment into the diagnostic routine investigation of patients with suspected antibody deficiency and can be adapted for different types of antibodies.

A.2 Abstract - german

In dieser Arbeit werden zwei Ansätze zur Abschätzung der Avidität von Antikörpern gegen Polysaccharid-Antigene in menschlichem Serum vorgestellt. Ein spezieller Fokus wird dabei auf die Anwendbarkeit in der diagnostischen Routine gelegt, da das übergeordnete Ziel die Berücksichtigung dieses Parameters bei der Diagnose von primären Immundefekten ist. Zu diesem Zweck wurden zwei Methoden verwendet, einerseits Oberflächenplasmonenresonanzspektroskopie (SPRS) und andererseits ein Titrations-ELISA System. Es wurde dabei eine Methode entwickelt, um mittels SPRS die isotyp-spezifische Konzentration von anti-A und B Antikörpern und deren Avidität zu bestimmen. Dabei können die Geschwindigkeitskonstanten k_a und k_d gemessen und die Gleichgewichtskonstanten K_A und K_D berechnet werden. Zudem wird eine Methode zur manuellen Auswertung der Sensorgramme vorgestellt, wodurch die Halbwertszeit der Antigen-Antikörper Bindung berechnet werden kann. Die Vorteile dieser Methode sind ein hoher Durchsatz, Robustheit und Wiederholbarkeit, allerdings ist sie aufgrund hoher Kosten nicht für die diagnostische Routine geeignet. Um eine günstigere aber auch verlässliche Methode zu entwickeln, um die Dissoziationsgleichgewichtskonstante K_D zu berechnen, wurde ein Titrations-ELISA System verwendet, da die Geräte und Reagenzien dazu in den meisten Routine-Laboratorien vorhanden sind. Dabei wurde ein verlässliches Regressionsmodell entwickelt und Kriterien zur Abschätzung der Datenqualität etabliert. Die vorgestellten Methoden zur Durchführung der Messung, der Datenanalyse und der Qualitätskontrolle ermöglichen die Verwendung der Aviditäts-Bestimmung zur routinemäßigen Untersuchung von Patienten mit Verdacht auf Antikörper-Defizienzen und kann für verschiedene Arten von Antikörpern adaptiert werden.

Appendix B

Publications

frontiers in Immunology

ORIGINAL RESEARCH
published: 14 November 2016
doi: 10.3389/fimmu.2016.00493

Pneumococcal Polysaccharide Vaccination Elicits IgG Anti-A/B Blood Group Antibodies in Healthy Individuals and Patients with Type I Diabetes Mellitus

Wendelin Wolfram[1†], Kai M. T. Sauerwein[2†], Christoph J. Binder[3], Nicole Eibl-Musil[4], Hermann M. Wolf[2,5†] and Michael B. Fischer[1,6†]*

[1] Clinic for Blood Group Serology and Transfusion Medicine, Medical University of Vienna, Vienna, Austria, [2] Immunology Outpatient Clinic, Vienna, Austria, [3] Department of Laboratory Medicine, Medical University of Vienna, Vienna, Austria, [4] Rudolfstiftung Hospital of the City of Vienna, Vienna, Austria, [5] Sigmund Freud Private University – Medical School, Vienna, Austria, [6] Department for Health Science and Biomedicine, Danube University Krems, Krems, Austria

Hypothesis: Blood group antibodies are natural antibodies that develop early in life in response to cross-reactive environmental antigens in the absence of antigen encounter. Even later in life structural similarities in saccharide composition between environmental antigens such as bacterial polysaccharides and blood group A/B antigens could lead to changes in serum levels, IgM/IgG isotype, and affinity maturation of blood group anti-A/B antibodies. We addressed the question whether immunization with pneumococcal polysaccharide (PnP) vaccine Pneumo 23 Vaccine "Pasteur Merieux" (Pn23) could have such an effect in patients with type I diabetes mellitus (DM I), an autoimmune disease where an aberrant immune response to microbial antigens likely plays a role.

Methods: Anti-PnP IgM and IgG responses were determined by ELISA, and the DiaMed-ID Micro Typing System was used to screen anti-A/B antibody titer before and after Pn23 immunization in 28 healthy individuals and 16 patients with DM I. In addition, surface plasmon resonance (SPR) technology using the Biacore® device and a synthetic blood group A/B trisaccharide as the antigen was applied to investigate IgM and IgG anti-A/B antibodies and to measure antibody binding dynamics.

Results: All healthy individuals and DM I patients responded with anti-PnP IgM and IgG antibody production 4–6 weeks after Pn23 immunization, while no increase in blood group anti-A/B antibody titer was observed when measured by the DiaMed-ID Micro Typing System. Interestingly, isotype-specific testing by SPR technology revealed an increase in blood group anti-A/B IgG, but not IgM, following Pn23 immunization in both patients and controls. No change in binding characteristics of blood group anti-A/B antibodies could be detected following Pn23 vaccination, supporting the assumption of an increase in IgG antibody titer with no or very little affinity maturation.

OPEN ACCESS

Edited by:
Ana María Hernández, Center of Molecular Immunology, Cuba

Reviewed by:
Jean Van Den Elsen, University of Bath, UK
Thomas Vorup-Jensen, Aarhus University, Denmark

***Correspondence:**
Michael B. Fischer
michael.fischer@donau-uni.ac.at

[†]Wendelin Wolfram and Kai M. T. Sauerwein have equally contributed as co-first authors, Hermann M. Wolf and Michael B. Fischer have equally contributed as co-last authors to this manuscript.

Specialty section:
This article was submitted to Molecular Innate Immunity, a section of the journal Frontiers in Immunology

Received: *22 July 2016*
Accepted: *25 October 2016*
Published: *14 November 2016*

Citation:
Wolfram W, Sauerwein KMT, Binder CJ, Eibl-Musil N, Wolf HM and Fischer MB (2016) Pneumococcal Polysaccharide Vaccination Elicits IgG Anti-A/B Blood Group Antibodies in Healthy Individuals and Patients with Type I Diabetes Mellitus. Front. Immunol. 7:493. doi: 10.3389/fimmu.2016.00493

Conclusion: The study provides evidence for epitope sharing between pneumococcal polysaccharides and blood group ABO antigens, which leads to a booster of blood group anti-A/B antibodies of the IgG isotype after Pn23 immunization in healthy individuals. Manifest autoimmunity such as present in DM I patients has no additional effect on the cross-reactive antibody response against pneumococcal polysaccharides and blood group antigens.

Keywords: pneumococcal polysaccharide vaccine, 23-valent pneumococcal polysaccharide vaccine, anti-blood group A/B antibodies, surface plasmon resonance, isoagglutinins, natural antibodies

INTRODUCTION

Natural antibodies are produced in the absence of overt external antigenic stimulation early in life in all healthy individuals with a functional immune system, presumably as a product of germline gene segment assembly (1). Therefore, they show low affinity to many microbial pathogens and certain cross-reactivity, even to some self-antigens (1–4). Antibodies to carbohydrate epitopes share certain characteristics with natural antibodies, e.g., the absence of extensive class switching and affinity maturation due to absent T-cell help (5). Isoagglutinins, i.e., antibodies against carbohydrate epitopes that form the AB0 antigens on red blood cells (RBCs), are considered prototypic natural antibodies that were shown to be compromised in patients with immunodeficiency (1, 4, 6). Their appearance can be explained by inapparent stimulation particularly from intestinal bacteria because antigens cross-reactive with blood group polysaccharides are widely distributed in the environment (1, 7, 8). Natural anti-ABO antibodies have long been considered to be predominantly of the IgM isotype, but antibodies of the IgG isotype are also produced, especially later in life, e.g., after alloimmunization in pregnancy or ABO-incompatible blood transfusions (1). In the case of ABO blood groups, individuals with blood group A develop an immune response to B-like antigens of microorganisms and environmental antigens like plants containing these epitopes (1, 9). B blood group individuals develop anti-A antibodies, O blood group individuals produce both anti-A and anti-B antibodies, while AB blood group subjects have neither anti-A nor anti-B because they express both antigens on their RBCs.

The human ABO blood group antigens are oligosaccharide moieties formed on precursor backbones by glycosyltransferases (4, 9, 10). Blood group O individuals have carbohydrate structures named H-antigen terminated in the sequence alpha-Fuc(1,2)Gal. The blood group A antigen is then formed from the H-antigen by an *N*-acetylgalactosaminyltransferase that uses a UDP-*N*-acetylgalactosamine (GalNAc) donor, and the blood group B antigen is formed by a galactosyltransferase that uses a UDP-galactose (Gal) donor to convert the H-antigen (4). The human A and B blood group antigens differ from each other only in the substitution of an acetamino for a hydroxyl group on the terminal saccharide residue, and this substitution can be differentially recognized by specific antibodies (1, 4, 11, 12). Interindividual variations in the titer of anti-blood group ABO antibodies exist, representing modulation of the production of these natural antibodies in response to cross-reactive environmental antigens, e.g., through immunization (1). B cells could thus recognize shared carbohydrate epitopes due to structural similarities in saccharide composition, e.g., between microbial polysaccharides (PnPs) and blood group A/B antigens, which could also have an effect on blood group anti-A/B specific antibody production after PnP-immunization. Previous findings indicate shared epitopes between blood group oligosaccharides and pneumococcal capsular polysaccharides, as antibodies cross-reacting with human erythrocytes and pneumococcal antigens have been described (7). Furthermore, it was shown that cross-reactive carbohydrate determinants (CCDs) contained in blood group antigens and microbial polysaccharides can be targeted by immunoglobulins of different isotypes, in particular by IgE, but also by IgG antibodies (13).

In addition to their role as a first line of defense against infection, natural antibodies have been shown to play an important role in the initiation of autoimmunity (2, 8, 14–16). Natural antibodies reacting with self-antigens were initially considered to represent breakdown of tolerance, thus functioning as a template for the generation of pathogenic autoantibodies produced through a process of clonal selection, somatic hypermutation, and class switching driven by antigen (14). More recently, these antibodies have been attributed an additional role in the prevention of autoimmune disease, e.g., by inhibiting activation of the adaptive immune system by molecules released from apoptotic cells that could facilitate autoimmune events (15, 16). Formation of natural antibodies with high cross-reactivity could be regulated differently in healthy individuals as compared to individuals with an autoimmune disease such as type 1 diabetes mellitus (DM I) known to present with abnormalities in antibody formation (17). In addition to high-risk HLA genes, environmental factors are thought to play an important role in the pathogenesis of DM I, such as pancreatic virus infection, T cell-mediated and autoantibody-mediated molecular mimicry, and bystander activation of autoreactive lymphocytes by proinflammatory cytokines derived from dendritic cells activated by infection-related stimuli through innate pattern recognition receptors such as TLR (18–21). A single causative infectious agent for DM I autoimmunity has not been found, pointing toward the possibility that different infectious agents are capable of non-specifically enhancing the likelihood of autoimmunity. In addition to virus infection (19, 20), bacterial infection might play a role in the development of DM I, as antibodies against mycobacterial and proinsulin epitopes (22) as well as beta cell antigens (23) show

cross-reactivity in children with new onset DM I. While human IDDM autoantigens are typically T-dependent protein antigens, microbial polysaccharides have been shown to modulate the autoimmune response leading to DM1 (24). Innate signaling *via* TLR and MyD88, pathways critical for T cell-independent (TI) immune defense (25), can reverse anergy in autoreactive B cells, suggesting that environmental factors associated with bacterial infection and inflammation may alter tolerance (26). Concerns that vaccination might lead to the development of autoimmune disease such as DM I have been raised (27), which could also relate to polysaccharide vaccines, as molecular mimicry in bacterial polysaccharide components is capable of inducing autoreactive antibodies, e.g., against some blood group antigens or neuronal gangliosides (28). In the present study, we investigated whether vaccination with Pneumo 23 Vaccine "Pasteur Merieux" (Pn23) has an effect on blood group ABO antibodies in healthy individuals and in patients with DM I. To screen for blood group anti-A/B antibodies, we used the commercially available DiaMed-ID Micro Typing System based on erythrocyte agglutination (6). To measure blood group-specific anti-A/B antibodies in healthy individuals and in patients with DM I in an isotype-specific manner, we used surface plasmon resonance (SPR) technology and synthetic A/B trisaccharides bound *via* amine-coupling to the CM5 chip (6, 11, 12). SPR using blood group-specific A/B synthetic trisaccharides is the ideal technology to investigate a potential IgM to IgG isotype shift and to investigate changes in binding characteristics of the relevant blood group anti-A/B antibodies under near to physiological conditions in real time.

MATERIALS AND METHODS

Vaccination of Healthy Individuals and Patients with Type I DM and Measurement of Anti-PnPs Antibodies

During a clinical study published previously (17), healthy individuals ($n = 39$) and patients with type I DM ($n = 20$) were immunized with the PnPs vaccine Pn23 (a 23-valent vaccine containing pneumococcal capsular polysaccharide serotypes 1, 2, 3, 4, 5, 6B, 7, 8, 9N, 9V, 10A, 11A, 12F, 14, 15B, 17F, 18C, 19A, 19F, 20, 22F, 23F, and 33F, Pasteur Merieux Connaught, Lyon, France) after informed consent was obtained (17, 29). Type I DM patients were, on average, 16 ± 7.4 years (SD) at the onset of disease, and at that time they tested positive for GAD autoantibodies. Age at initiation of the vaccination study was 31.7 ± 8.8 years (SD). For a detailed description of patients and controls, see Ref. (17). Blood samples were drawn 4–6 weeks after vaccination, the serum was immediately separated from the cellular blood component, dispensed into 500 µl aliquots, and stored until analysis in a freezer at −20°C. For this follow-up study, serum aliquots stored at −20°C were still available from 28 healthy controls and 16 DM I patients; selection of this subset of the previous study was only because no more serum was available from the other controls and DM I patients of the original study. Anti-PnPs antibodies were determined by a home-made ELISA detecting all serotypes as previously described (17, 30).

Determination of Anti-A/B Antibody Titers by the DiaMed-ID Micro Typing System

Titers of blood group anti-A and anti-B antibodies were determined by the DiaMed-ID Micro Typing System (Bio-Rad Lab. Inc., Hercules, CA, USA) used according to the manufacturer's protocol. The ID-Card 50520 (NaCl) was used to measure IgM, while the ID-Card 50531 [LISS/Coombs containing polyspecific anti-human gamma globulin (AHG) serum] was used to determine IgG in addition to IgM. The serum samples were serially twofold diluted with 0.9% saline solution starting with 500 µl serum and 500 µl saline solutions. Also, 25 µl of each dilution were pipetted into a single column of the microtube gel card, and 50 µl of DiaMed-ID-DiaCell ABO/I-II test cell suspensions A_1 or B (Bio-Rad Lab.) was added. ID-Card 50520 (NaCl) cards were incubated at room temperature for 15 min, the ID-Cards (LISS/Coombs) at 37°C, and thereafter centrifuged in a DiaMed-ID-Centrifuge 24 S for 10 min at 910 rpm. Results were read immediately after centrifugation and were subdivided into positive and negative results. The titer that led to visible agglutination of erythrocytes dispersed in the gel was selected positive. In an individual with blood group O, both anti-A and anti-B antibody titers were used for statistical analysis, while in an individual with blood group A, only anti-B antibody titers, and in an individual with blood group B, only anti-A antibody titers were used for statistical analysis; none of the study individuals had blood group AB.

Determination of Anti-A/B Antibodies by Surface Plasmon Resonance

The erythrocyte aggregation assays based on the DiaMed-ID Micro Typing System are semiquantitative assays that cannot determine in an isotype-specific way a subtle increase of anti-A/B IgG and/or IgM antibodies against blood group A/B antigens. Therefore, we used SPR to measure anti-A/B antibodies as previously described (6, 11, 12). Amine-labeled blood group A and B trisaccharides (Dextra Laboratories Ltd., Reading, UK) were immobilized on two-channel sensor chips CM5 (General Electric Health Care, Freiburg, Germany) using standard protocols (31, 32). In brief, the CM5 sensor chip surface was activated with 100 µl 0.05 mol/l *N*-hydroxy-succinimide and 0.2 mol/l *N*-ethyl-*N*′-dimethylamino-propylcarbodiimide injected into the buffer stream of HBS-EP (0.01 mol/l HEPES buffer, pH 7.4, containing 0.15 mol/l NaCl, 3 mmol/l EDTA, and 0.005% surfactant P20) as described previously (6). The buffer stream was passed through FC-1 and FC-2 of the two-channel Biacore® X instrument (GE Health Care) at a flow rate of 5 µl/min for 20 min. Subsequently, 15 µl of a blood group A/B trisaccharide amine derivative solution at a concentration of 1 mg/ml, prepared with borate (pH 8.5), was injected into the buffer stream and passed through FC-1 at a flow rate of 5 µl/min and was halted after injection of 7 µl for 2 h; FC-2 served as a blank control. Residual active ester groups on the sensor surface were then deactivated by injecting 100 µl of 1 mol/l ethanolamine–HCl (pH 8.5) into the buffer stream and passing it through FC-1 and FC-2, and by passing the buffer stream through the cell until a stable baseline was achieved. To measure anti-blood group A/B antibodies, serum was diluted by

half with the HBS-EP, and 100 µl of the diluted plasma samples were passed through FC-1 and FC-2 at a flow rate of 20 µl/min for 5-min duration. When the association phase was finished, binding of antibody was recorded and is expressed as resonance units (RU at "stability" in **Figure 1**, corresponding to RUt0 in **Figure 2**, panel 3). After each measurement, the antibodies bound to the blood group trisaccharides were removed with 50 µl of 50 mmol/l NaOH buffer at a flow rate of 60 µl/min for 50 s and the chip regenerated to reach the same baseline as prior to the measurement. The amounts of anti-A/B antibody that associated with the blood group A/B trisaccharide antigen immobilized on the sensor chip surface were obtained by subtracting the FC-2 value from the FC-1 value.

Alternatively, a four channel Biacore® T200 device (kindly provided by Florian Koelle, GE Health Care) was used, which enabled us to measure both anti-A and anti-B antibodies on one chip surface (CM5-chip) at the same time. The amount of trisaccharides and the coupling procedure remained similar to the two-channel system used previously, except the contact time was adapted to 600 s and the flow rate to 10 µl/min. Flow cell one (FC-1) and three (FC-3) were immobilized without trisaccharides and served as blank during binding analysis. FC-2 was immobilized with 1 mg/ml blood group A trisaccharide and FC-4 with 1 mg/ml blood group B trisaccharide. For binding analysis, serum was diluted by half with HBS-EP and injected in FC-2 and FC-4 for 180 s at a flow rate of 10 µl/min. The flow-path was 2–1 and 4–3. To determine IgM and IgG levels of A- and B-bound antibodies, anti-human IgG Abs [polyclonal aHIgG (γ-chain), Sigma-Aldrich, St. Louis, MO, USA] and anti-human IgM [polyclonal aHIgM (µ-chain), Sigma-Aldrich, St. Louis, MO, USA] were injected for 180 s at a flow rate of 10 µl/min directly after the serum sample. For measurement of anti-A/B antibodies RU at report point "stability" (see **Figure 1**, corresponding to RUt0 in **Figure 2**, panel 3) and for levels of IgM/IgG anti-A/B antibodies levels at report point "enhance_level" (see **Figure 1**) relative to baseline were recorded. After determination of levels of IgM and IgG anti-A/B antibodies, the chip was regenerated twice with 50 mmol NaOH for 30 s at a flow rate of 10 µl/min with a stabilization period of 5 s after the second regeneration to reach the same baseline as prior to the measurement. For kinetic measurement, an association time of 200 s and dissociation time of 800 s was chosen. Dissociation of bound anti-A/B antibodies over time as a semiquantitative correlate for the strength of antibody binding was calculated according to the following formula: % dissociation = 100 − [RU at t1 (800 s)/RU at t0 (200 s)] × 100 (see **Figure 2**, panel 3 as an example for measurement of RU at t0 and at t1). To compute an affinity constant K_D the concentration of IgG antibodies in microgram per

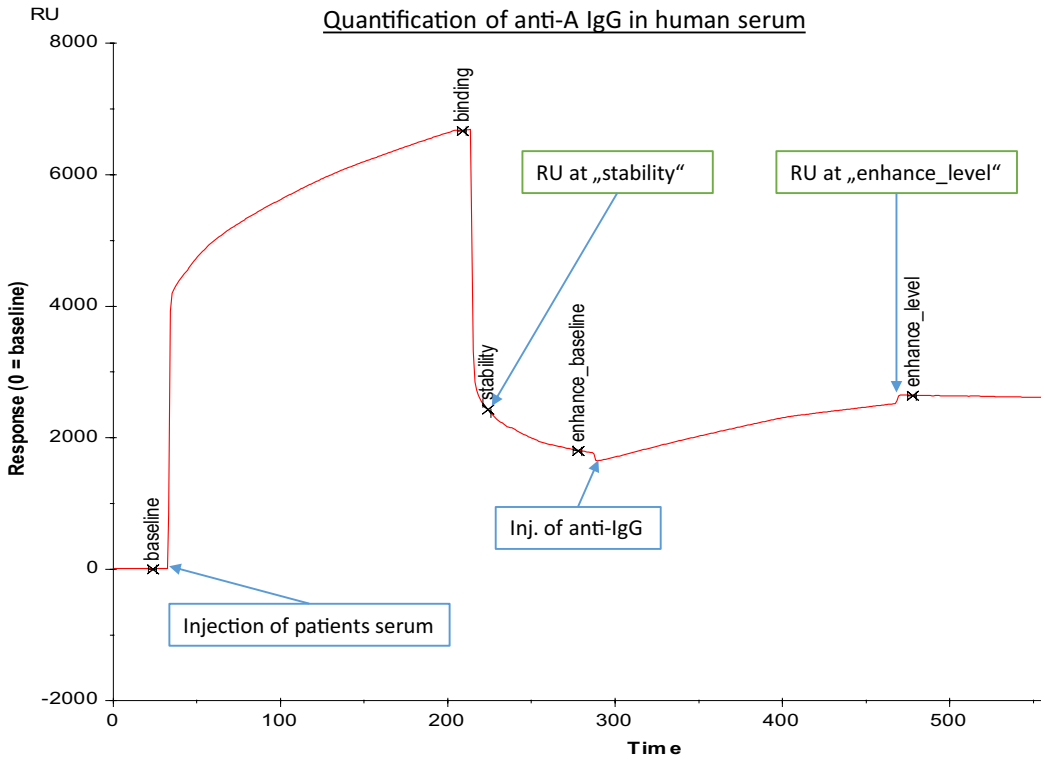

FIGURE 1 | Exemplary binding curve of quantification of anti-A IgG antibodies in human serum, as generated by BIAevaluation® software (GE Healthcare). Injection of human serum was followed by a second injection of anti-IgG; response units (RU) at "stability" were recorded to assess the concentration of anti-A blood group antibodies, while response units at "enhance_level" were representative for anti-A IgG concentration. The *x*-axis gives time in seconds, and the *y*-axis represents response units (RU).

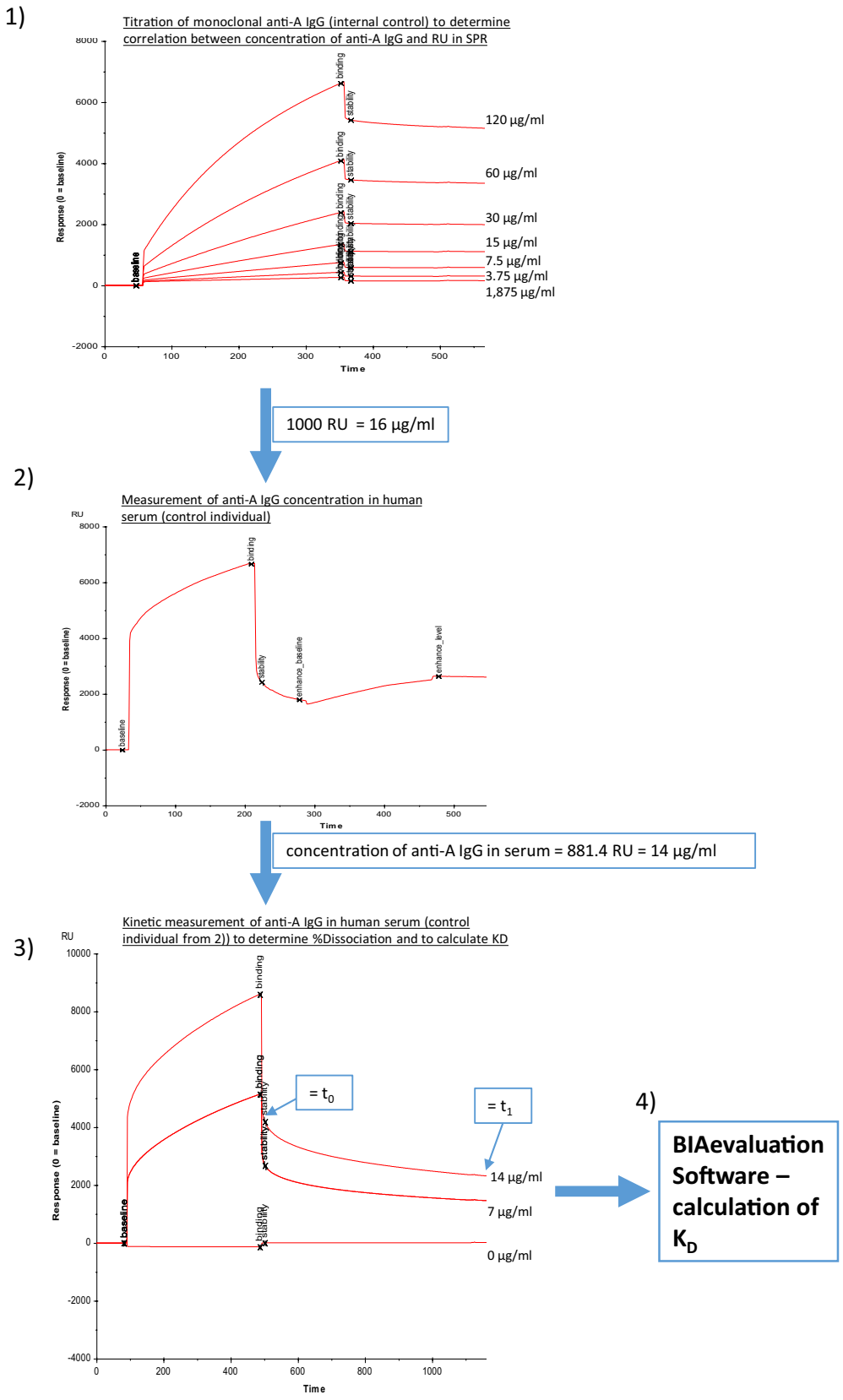

FIGURE 2 | **Determination of binding characteristics of anti-A IgG antibodies in human serum**.

(*Continued*)

FIGURE 2 | Continued

Panel (1) different concentrations of monoclonal anti-A IgG (internal control) were injected to correlate response units to micrograms per milliliter, (2) anti-A IgG levels in human serum were determined utilizing a second injection of anti-IgG (Sigma), (3) different dilutions of human serum were measured without addition of second step reagent, and binding curves were recorded for a total of 1,200 s, (4) an estimate of K_D was calculated using the BIAevaluation Software (GE Healthcare) with input of the concentrations of anti-A IgG determined in steps (2) and (3) as described in Section "Materials and Methods."

milliliter must be known, thus RUs for different concentrations of monoclonal anti-A/B IgG (clone 9A, Abcam, Cambridge, MA, USA; clone NaM87-1F6, BD Pharmingen, San Jose, CA, USA) were measured (**Figure 2**, panel 1). This enabled us to correlate an increase in response units derived from anti-A/B IgG measurements in patient serum with microgram per milliliter of anti-A/B IgG antibody by regression analysis in order to calculate the respective concentration of IgG anti-A/B (**Figure 2**, panel 2). Subsequently two dilutions of patient serum – one of them diluted 1:2 – and a blank were measured (**Figure 2**, panel 3), and the resulting binding curves were used to calculate K_D (computed as $K_D = K_{off}/K_{on}$) with the BIAevaluation® software from GE Healthcare. To fit the association/dissociation curve, a 1:1 binding model was chosen. The molecular weight of the analyte was assumed to be 150,000 Da (IgG). To assess the quality of the calculations, controls within the software were used. No external calculations were performed nor parameters added. Furthermore, as an internal control to test before each measurement was started, anti-blood group A or B IgM mAbs (anti-A murine monoclonal Abs clone MH04 and A3D3, anti-B murine monoclonal Abs clone NB1.19, NB10.5A5, and NB10.3B4, Ortho-Clinical Diagnostics, Neckargemünd, Germany), and anti-blood group A IgG mAb (clone 9A, Abcam, Cambridge, MA, USA; clone NaM87-1F6, BD Pharmingen, San Jose, CA, USA) were used to guarantee optimal chip performance and full recovery. For statistical analysis, both anti-A and anti-B antibody titers (RU) were used in an individual with blood group O, while in an individual with blood group A, only anti-B antibody titers, and in an individual with blood group B, only anti-A antibody titers were used for statistical analysis; none of the individuals in this study had blood group AB.

Statistical Analysis

Statistically significant differences between study groups were calculated using the non-parametric two-tailed Mann–Whitney *U*-test. Results are depicted using box plot diagrams, with the median represented by a cross, the interquartile range (IQR) represented by the box, and 5- and 95-percentile values represented by the whiskers.

RESULTS

Anti-PnPs Response in Healthy Individuals and in Patients with Type I DM after Pneumovax®23 Immunization

The anti-PnPs antibody response prior and 4–6 weeks after immunization with the unconjugated PnPs vaccine Pn23, a 23-valent vaccine, was determined by ELISA in an isotype-specific manner in 28 healthy individuals and 16 patients with DM I. All healthy individuals included in this study showed a significant IgM (**Figure 3A**) and IgG (**Figure 3B**) anti-PnPs antibody response following vaccination. The results confirm previous findings in patients with type I DM (17) showing a normal antibody response to unconjugated pneumococcal polysaccharide, which is likely TI, while primary antibody responses to T-cell-dependent antigens are impaired (17).

Increase in Blood Group IgG Anti-A/B Antibodies in Healthy Individuals and in Patients with Type I DM after Pneumovax®23 Immunization as Determined with the Biacore® Device

To address whether immunization with Pn23 has an effect on blood group anti-A/B antibodies in patients with DM-type I as compared to healthy individuals, we first determined antibody titers in the DiaMed-ID Micro Typing System, using the ID-Card 50520 (NaCl) as well as the ID-Card 50531 (LISS/Coombs containing poly-specific AHG serum) to determine IgG in addition to IgM anti-A/B antibodies. We could observe no difference in blood group anti-A/B antibody titer prior and post immunization with Pn23 in both, healthy individuals and patients with DM-type I when the assay used was based upon erythrocyte aggregation in physiological NaCl (direct agglutination test, **Figure 4A**) or in the presence of anti-IgG Coombs serum (indirect agglutination test, **Figure 4B**). Interestingly, in a considerable percentage of study individuals of both groups (up to approximately 25%) the A/B isoagglutinin titers were lower than 1:4 in both agglutination systems, thus confirming previous findings of a relatively low sensitivity of the agglutination system to detect low isoagglutinin titers (6). To increase sensitivity, SPR technology was applied to further analyze anti-A/B antibodies, thus allowing real-time analysis of molecular interactions between antibodies and the isolated blood group trisaccharide antigen without molecular labeling leaving the structure of both molecules intact (6, 32). With this technology, biologically relevant antibody–antigen interactions can be assessed both quantitatively and qualitatively, as the carbohydrate antigens are presented in a physiological manner (11, 12, 31). Kinetics and affinity were investigated by analyzing the time curve and level of binding and concentration of anti-A/B antibodies in the sample by measuring mass binding, which further allowed the determination of the binding forces. The comparison of the response on the active and control surface allowed for the subtraction of bulk effects associated with buffer changes and for the high serum concentration with its mass binding, thus enabling the calculation of specific binding. Using SPR analysis, we found specific anti-A/B antibody binding to the respective blood group A/B trisaccharides in all individuals tested

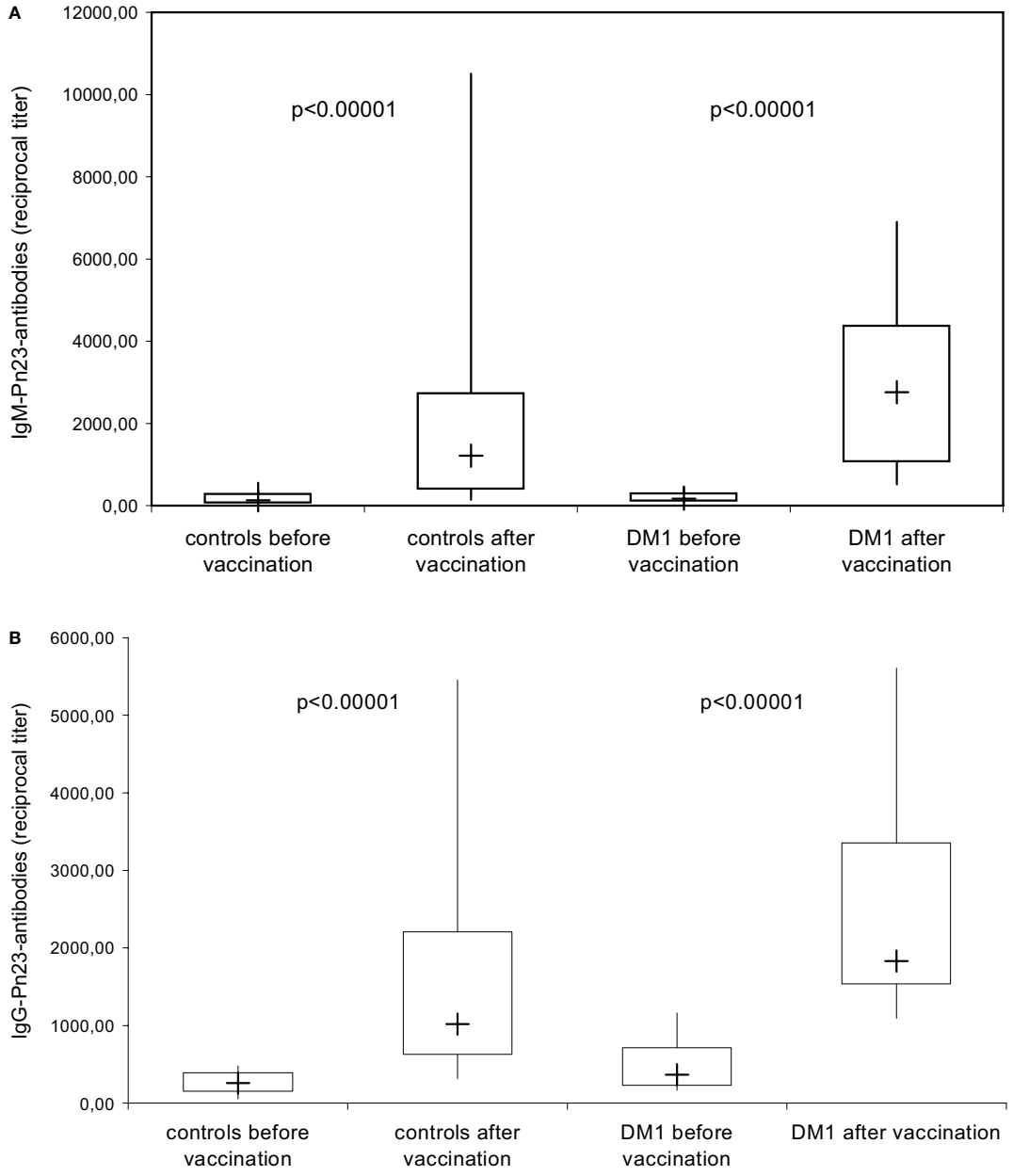

FIGURE 3 | IgM/IgG antibody response to pneumococcal polysaccharides after immunization with Pn23 vaccine. Healthy individuals (n = 28) and patients with type I DM (n = 16) were immunized with the PnPs vaccine Pneumo 23 Vaccine "Pasteur Merieux" (Pn23), and blood samples were drawn 4–6 weeks after vaccination. Antibodies against pneumococcal polysaccharides (anti-PnPs) were determined by ELISA as described in Section "Materials and Methods" and presented as IgM–Pn23-antibody response **(A)** or IgG–Pn23-antibody response **(B)**. Results are depicted using box plot diagrams, with the median represented by a cross, the interquartile range (IQR) represented by the box, and 5- and 95-percentile values represented by the whiskers; statistically significant differences between study groups were calculated using the non-parametric two-tailed Mann–Whitney U-test.

(**Figure 4C**), as has also been described previously for individuals with intact antibody responsiveness (6, 12). For all probes, a high association rate constant for the interaction and the use of a high ligand density on the sensor chip surface was found that promoted the mass transport limitation. As reference analyte with a known concentration, commercially available blood group anti-A or -B antibodies of IgM and blood group anti-A IgG were used (**Figure 2**, panel 1 shows monoclonal anti-A IgG as an example). For the example shown in **Figure 2**, panel 1, a sensor response of 1,000 RU corresponded to a shift of 0.1° in the SPR angle, which in turn correlates to approximately 16 µg/ml of anti-A IgG injected. Since the individuals selected for determination of K_D [one healthy control (Ind1) and one DM I patient (Ind2) as well as a control individual not vaccinated] contained

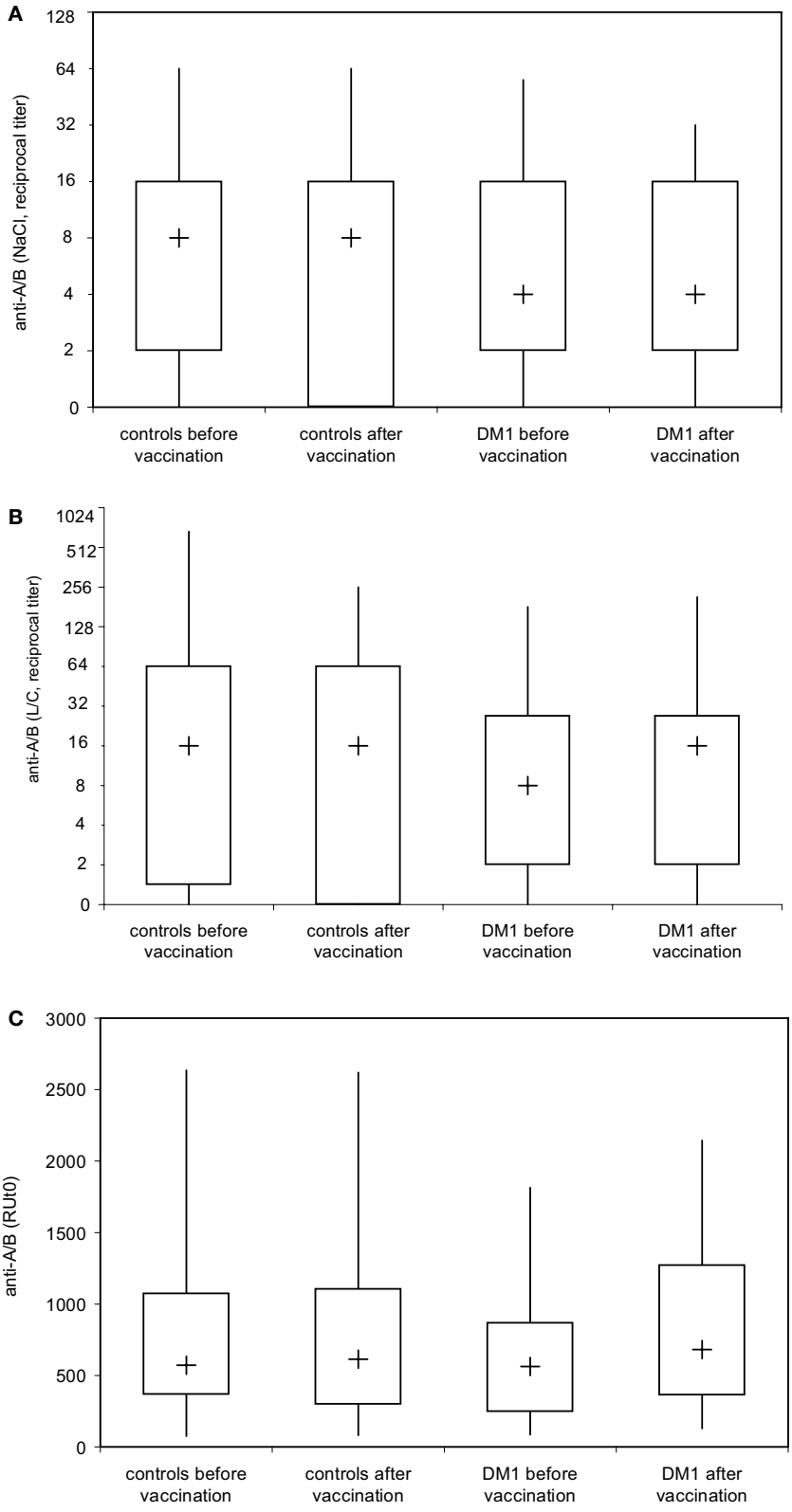

FIGURE 4 | Analysis of blood group anti-A and anti-B isoagglutinin binding to A and B trisaccharide antigen in real time by surface plasmon resonance (SPR) technology.

(*Continued*)

FIGURE 4 | Continued

Serum samples of healthy individuals ($n = 28$) and patients with type I DM ($n = 16$) were serially twofold diluted with 0.9% saline solution and blood group anti-A and/or anti-B IgM **(A)** were determined by ID-Card 50520 (NaCl), while the ID-Card 50531 (LISS/Coombs) was used to determine IgG and IgM isoagglutinins **(B)**. The titer that led to visible agglutination of erythrocytes dispersed in the gel was selected positive. Alternatively **(C)**, serum samples diluted in HES-EP buffer (1:2) were injected over either the blood group A or blood group B trisaccharide-coupled CM5 sensor chip. Binding kinetics, i.e., association and dissociation were recorded as sensorgrams in resonance units (RU) against time in FC-I and FC-II, and the amount of anti-A/B antibody that associated with the blood group A/B trisaccharide antigen immobilized on the sensor chip surface was obtained by subtracting the FC-II value from the FC-I value and is given as resonance units (RU). Results are depicted using box plot diagrams, with the median represented by a cross, the interquartile range (IQR) represented by the box, and 5- and 95-percentile values represented by the whiskers; no statistically significant differences were found between study groups as calculated using the non-parametric two-tailed Mann–Whitney *U*-test.

sufficient amounts of anti-A IgG for affinity analysis with very low to undetectable anti-A IgM, titration was only performed for IgG anti-A/B antibody. Of note, SPR technology is capable to detect anti-A/B antibodies with values of 50–180 RU in serum samples where the microtube column assay showed no erythrocyte aggregation. Even with this sensitive detection system, no change in isoagglutinin titers was found following vaccination with 23-valent PnPs, neither in healthy individuals nor in DM1 patients (**Figure 4C**).

Using the DiaMed-ID Micro Typing System in the direct and indirect agglutination assay as well as SPR technology under close to physiological conditions, both IgM- and IgG-antibodies were measured simultaneously, without discrimination between IgM and IgG response. To examine a possible booster effect of Pn23 vaccination on IgG anti-A/B antibodies only we applied isotype-specific second step antibodies to discriminate between blood group anti-A/B IgM and IgG antibodies. This system enabled us to detect an induction of blood group anti-A/B IgG (**Figure 5B**) but not IgM (**Figure 5A**) antibodies after immunization of healthy individuals with Pn23, an antibody response resembling a secondary/booster response. Interestingly, patients with type I DM showed a comparable induction of IgG isoagglutinins after immunization with Pn23 (**Figure 5B**), in agreement with their intact antibody responsiveness to pneumococcal polysaccharide, a T-independent antigen, while a significant impairment in primary antibody response to vaccination with T-cell-dependent antigens such as hepatitis A virus and diphtheria toxoid was described previously (17).

Determination of Binding Characteristics of Anti-A/B Antibodies after Pneumovax®23 Immunization

To measure whether the induction of IgG-A/B antibodies observed after Pn23 immunization was accompanied by changes in binding characteristics of the blood group anti-A antibodies, as would be the case for a T-dependent IgG-booster response, we analyzed the binding dynamics of the anti-A/B antibodies as described above (**Figure 2**). We found no substantial change in the percentage of dissociation (**Figure 6A**) or the estimate of the affinity constant (K_D, **Figure 6B**) of blood group-specific anti-A antibodies following pneumococcal vaccination, as calculated by BIAevaluation® software from GE Healthcare. For estimation of the affinity constant K_D, healthy individuals and patients with type I DM were selected that had initially high anti-A-antibody titers (>1:256 or >700 RU), associated with high anti-A IgG and low to undetectable anti-A IgM antibody levels. Only three healthy individuals and two patients with type I DM fulfilled this criterion. As shown in **Figure 6** (depicting results from one healthy individual, Ind1 and one DM I patient, Ind2), our study gives evidence that immunization with Pn23 induces an increase in IgG anti-A/B antibody titers but has no effect on binding characteristics of blood group anti-A/B IgG antibodies, neither in the healthy individuals nor in the patients tested.

DISCUSSION

Based on previous findings (7, 13) it was our hypothesis that structural similarities in saccharide composition between pneumococcal polysaccharides and blood group A/B saccharide antigens could lead to production of cross-reactive blood group anti-A/B antibodies after immunization with capsular polysaccharide vaccines, because B cells could recognize shared carbohydrate epitopes (2, 8, 10, 33, 34). In the current study, we indeed show that immunization with Pn23 vaccine is followed by induction of blood group anti-A/B antibodies of the IgG isotype in healthy individuals. Anti-A/B IgG antibodies could only be demonstrated when SPR technology using the Biacore® device was applied, while conventional technology employing erythrocyte aggregation assays using the DiaMed-ID Micro Typing System were unable to detect this side effect of Pn23 vaccination. Apparently, the increased sensitivity of SPR technology as compared to conventional erythrocyte agglutination assays as well as the near to physiological conditions of the molecular interaction between antibodies and the specific blood group trisaccharide antigen enabled us to detect the stimulation of small amounts of cross-reactive IgG antibodies (11, 12, 31, 32). A previous study described an alternative approach to measure isoagglutinins in an isotype-specific and sensitive manner by using synthetic blood group saccharides in ELISA and showed cross-reactivity between alpha-Gal and blood group B oligosaccharide (13). The increase in blood group anti-A/B IgG isotype response observed in our study provides additional evidence for a limited cross-reactivity between PnPs antigens and the carbohydrate moieties of blood group A/B trisaccharides. Whether the observed induction of IgG antibodies cross-reacting with A/B blood group antigens is of clinical relevance in healthy individuals remains to be determined but is unlikely due to the relatively small increase (approximately twofold) observed. Patients with type I DM

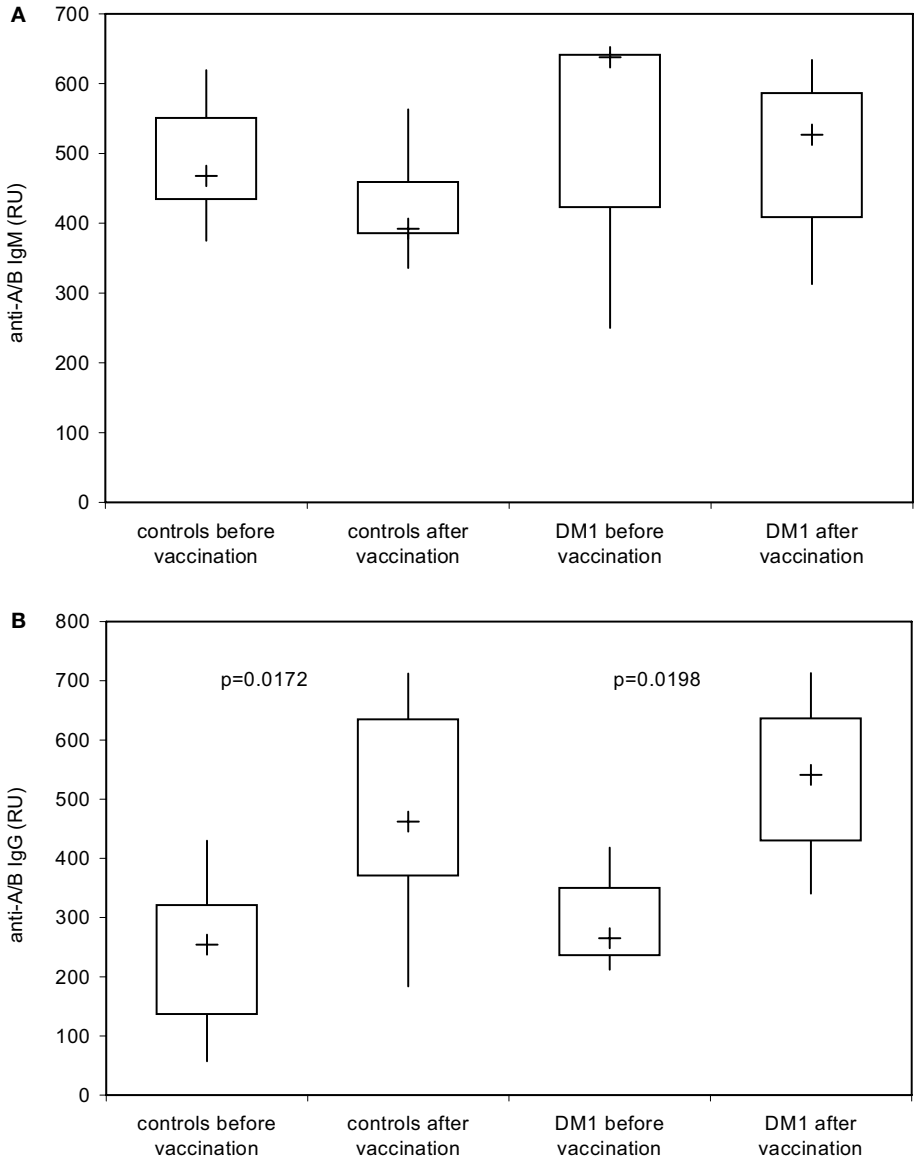

FIGURE 5 | Increase in blood group IgG anti-A/B antibodies in healthy individuals and in patients with type I DM after immunization with Pn23 vaccine as determined with the Biacore® device. To determine IgM **(A)** and IgG **(B)** anti-A/B antibodies in healthy individuals and patients with type I DM prior and post immunization with Pneumo 23 Vaccine "Pasteur Merieux" (Pn23), an anti-human IgM mAb **(A)** or anti-human IgG Abs **(B)** were applied as the second step reagents as described in Section "Materials and Methods." Results are depicted using box plot diagrams, with the median represented by a cross, the interquartile range (IQR) represented by the box, and 5- and 95-percentile values represented by the whiskers; statistically significant differences between study groups were calculated using the non-parametric two-tailed Mann–Whitney *U*-test. For the IgM antibody response, no statistically significant differences were found between study groups.

displayed a comparable cross-reactive IgG antibody response against blood group antigens following Pn23 vaccination, although these patients present an autoimmune disease with profound immunological dysregulation (17, 18). Interestingly, cross-reactive IgM antibodies were not inducible, neither in DM1 patients nor in controls. This is characteristic of a booster response effecting IgG responses only and contrary to the effect of immunization with a conventional polysaccharide antigen such as PnPs inducing both anti-PnPs IgM and IgG antibody responses following booster vaccination (**Figure 3**).

An additional benefit of the SPR-based technology employed in this study is the capability for real-time measurements of affinity of antibody–antigen interactions without the use of molecular labeling, leaving the structure of both interacting molecules intact (11, 12, 32). Calculations of K_D as performed in our study using human serum as a sample can only be an estimate for the true affinity of a given antibody since we are dealing with a variety of polyclonal antibodies of different isotypes contributing to the overall affinity of the blood group antibodies detected in the SPR analysis used. Isotype

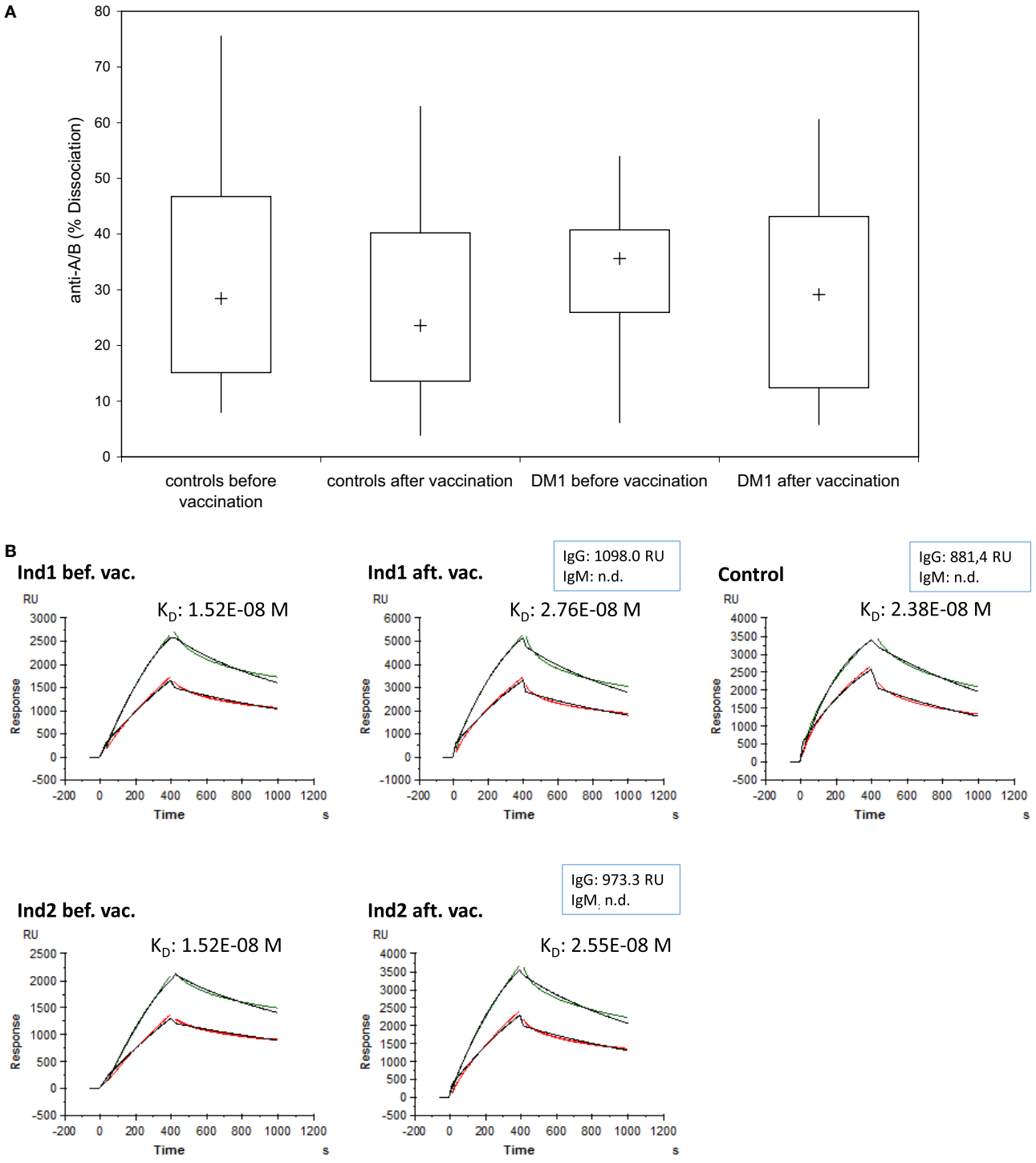

FIGURE 6 | **Binding characteristics of anti-A/B antibodies after immunization with Pn23 vaccine**. The percentage of dissociation **(A)** of blood group anti-A/B antibodies before and after immunization with Pneumo 23 Vaccine "Pasteur Merieux" (Pn23) in healthy individuals (n = 28) and in patients with type I DM (n = 16) was investigated using the Biacore device, the CM5 chip, and the synthetic blood group specific A/B trisaccharides as described in Section "Materials and Methods." Furthermore, the estimated affinity constant K_D **(B)** of blood group specific anti-A antibodies before and after pneumococcal vaccination were analyzed in serum samples of three healthy individuals and two patients with type I DM selected for their initially high anti-A antibody titer (>than 1:256 or >than 700 RU). Kinetic measurements of anti-A antibodies binding to surface bound trisaccharide before and after vaccination in two representative individuals (a healthy individual, Ind1, and a DM I patient, Ind2) who fulfilled these criteria are given; one healthy individual that was not included in the vaccination protocol but showed high titer for blood group anti-A antibodies was measured in parallel (Control). Green curves represent serum sample and red curves serum sample diluted by half; the black curves depict the calculated fit. n.d., not detectable.

bias has been limited since individuals with high blood group A IgG but low to undetectable blood group A IgM antibody were selected to estimate the binding affinity of anti-A IgG antibodies. To determine the affinity (K_D) of serum antibodies of a single specificity, isolation and immobilization of the respective immunoglobulin clone would be required, which is only possible in individuals with monoclonal gammopathy of the desired specificity. Interestingly, we did not find a marked change in binding characteristics of the cross-reactive blood group anti-A/B antibodies, indicating that a relatively small increase in IgG antibody titer occurred without additional affinity maturation. An immune response to carbohydrate antigens such as to pneumococcal capsular polysaccharide serotypes 1, 2, 3, 4, 5, 6B, 7, 8, 9N, 9V, 10A, 11A, 12F, 14, 15B, 17F, 18C, 19A, 19F, 20, 22F, 23F, and 33F is thought to be generally TI, which can limit the B cell response to the production of IgM antibodies mainly and limited amounts of IgG antibodies, and the absence of affinity maturation of the rearranged antibody genes might lead to the expression of germline sequences of antibodies with limited affinity (5, 34, 35). In previous studies, the affinity of anti-carbohydrate antibodies for their antigens was shown to be 3–5 orders lower in magnitude than affinities of anti-protein or anti-peptide antibodies for their antigens (2, 3, 8, 35). In this study, however, we found no evidence for low affinity binding of blood group A/B antibodies obtained either from healthy individuals or from patients with type I DM. When a mixture of commercially available monoclonal blood group anti-A IgM and IgG antibodies was formulated, simulating the amount and composition of naturally occurring blood group anti-A antibodies, the dissociation rate was comparable to the serum samples analyzed in **Figure 6** (data not shown). Germline antibodies recognizing carbohydrate epitopes might display significant cross-reactivity because the number of potential antigens the immune system must encounter appears to extensively outweigh the recombinational potential of the germline genes (2, 3, 34, 35). The recombinational potential of the germline genes for anti-Gal antibodies specific for blood group B substance in unimmunized individuals was shown to be limited, because anti-Gal antibodies are encoded by a group of 6–8 well-defined and structurally related germline progenitors in humans (36). Anti-Gal was shown to be the most abundant antibody in humans, constituting approximately 1% of immunoglobulins and found to be of IgG, IgM, and IgA isotype (37, 38). Cryptic antigens capable to bind anti-Gal are exposed on senescent human RBCs as well as on RBCs of patients with β-thalassemia and sickle cell anemia, but the amount of cryptic antigens expressed on RBCs was shown to be low (38). The preferential anti-Gal IgG subclass found by ELISA was IgG2 using Gal-specific synthetic saccharides, and these IgG2 antibodies showed cross-reactivity with blood group B antigen (13). ABO blood group antigens were shown to be the ideal targets to explore the concomitant effect of mutation on binding affinity and specificity of anti-carbohydrate antibodies (33). Mutant anti-carbohydrate antibodies with higher affinity achieved by single point mutations of specific residues lining the pocket on binding to the A and B blood group oligosaccharide antigens showed altered polarity, surface complementarity, and side chain aliphatic character, leading to improved binding affinity without loss of specificity (33). Furthermore, the poly-specificity in germline encoded antibodies to carbohydrate epitopes was shown to be due to greater conformational ability in their combining sites, and this flexibility helped to cope with new and changing pathogen surface structures by recognizing distinct highly conserved epitopes on bacterial polysaccharides (4, 33). Structural analysis of the affinity-matured antibody 48G7 and its germline precursor antibody showed that the germline precursor could undergo an induced fit upon binding to its cognate hapten, while the affinity-matured antibody 48G7 displayed lock and key binding. An immunological relationship between specific substances of ABO and type XIV pneumococcus gave further evidence for shared carbohydrate epitopes by showing that adsorption of the hemagglutinins in anti-type XIV horse serum with erythrocytes of each of the A/B blood groups removed the agglutinins not only of that group but also of the other groups (7). In addition to pneumococcus, other germs have been shown to cross-react with carbohydrate structures on the surface of human cells (39–43). The core oligosaccharides of low-molecular-weight LPS of pathogenic *Neisseria* spp. can mimic the carbohydrate moieties of glycosphingolipids (40). The core oligosaccharides of LPS of *Campylobacter jejuni* serotypes, which are associated with the development of Guillian–Barre' syndrome, can exhibit mimicry of gangliosides (41). Finally, the O-chain of a number of *Helicobacter pylori* strains exhibit mimicry of Lewis(x) and Lewis(y) blood group antigens, giving evidence that molecular mimicry can serve to camouflage the bacterial surface from the host (42).

In conclusion, our study provides evidence for a limited carbohydrate epitope sharing between PnPs and blood group sugar epitopes in healthy individuals as well as in patients with type I DM that could be observed after Pn23 immunization. Cross-reactive anti-polysaccharide antibody responses were comparable between patients and controls with respect to the titer and the affinity. Blood group anti-A/B antibodies are considered to be naturally occurring antibodies that occur basically in any individual with an intact immune response also in the absence of antigenic encounter. The clinical relevance of the slight increase in blood group anti-A/B IgG isotype response in healthy individuals after Pn23 immunization is certainly limited; our findings however indicate modulation of anti-A/B IgG antibodies, e.g., a booster response during life not only by encounter with the genuine antigen such as incompatible blood transfusions or alloimmunization during pregnancy but also through molecular mimicry of particular carbohydrate epitopes shared by blood group AB substances and bacterial polysaccharides such as PnPs.

ETHICS STATEMENT

The study was approved by the ethics committee of the Rudolfstiftung Hospital of the City of Vienna. Informed consent was obtained from every study participant.

AUTHOR CONTRIBUTIONS

MF and HW were the principal investigators, and they critically assessed data, performed statistical analysis, wrote the manuscript, and took primary responsibilities for the paper; WW and KS performed the experiments and analyzed the data; CB critically assessed data and was critically involved in the initial draft; NE-M conducted the clinical study and provided clinical data. All the authors critically participated in all revisions of the manuscript.

REFERENCES

1. Milland J, Sandrin MS. ABO blood group and related antigens, natural antibodies and transplantation. *Tissue Antigens* (2006) 68:459–66. doi:10.1111/j.1399-0039.2006.00721.x
2. Nguyen HP, Seto NO, MacKenzie CR, Brade L, Kosma P, Brade H, et al. Germline antibody recognition of distinct carbohydrate epitopes. *Nat Struct Biol* (2003) 10:1019–25. doi:10.1038/nsb1014
3. Brooks CL, Müller-Loennies S, Brade L, Kosma P, Hirama T, MacKenzie CR, et al. Exploration of specificity in germline monoclonal antibody recognition of a range of natural and synthetic epitopes. *J Mol Biol* (2008) 377:450–68. doi:10.1016/j.jmb.2008.01.018
4. Patenaude SI, Seto NOL, Borisova SN, Szpacenko A, Marcus SL, Palcic MM, et al. The structural basis for specificity in human ABO(H) blood group biosynthesis. *Nat Struct Biol* (2002) 9:685–90. doi:10.1038/nsb832
5. Defrance T, Taillardet M, Genestier L. T cell-independent B cell memory. *Curr Opin Immunol* (2011) 23:330–6. doi:10.1016/j.coi.2011.03.004
6. Fischer MB, Wolfram W, Binder CJ, Böhmig GA, Wahrmann M, Eibl MM, et al. Surface plasmon resonance analysis shows an IgG-isotype-specific defect in ABO blood group antibody formation in patients with common variable immunodeficiency. *Front Immunol* (2015) 6:211. doi:10.3389/fimmu.2015.00211
7. Finland M, Curnen EC. Agglutinations for human erythrocytes in type XIV anti-pneumococcic horse serum. *Science* (1938) 87:417–21. doi:10.1126/science.87.2262.417
8. Yuki N. Carbohydrate mimicry: a new paradigm of autoimmune disease. *Curr Opin Immunol* (2005) 17:577–82. doi:10.1016/j.coi.2005.09.004
9. Marcus DM. The ABO and Lewis blood-group system. Immunochemistry, genetics and relation to human disease. *N Engl J Med* (1969) 280:994–1006. doi:10.1056/NEJM196905012801806
10. Yamamoto F. ABO blood group system-ABH oligosaccharide antigens, anti-A and anti-B, A and B glycosyltransferases, and ABO genes. *Immunohematology* (2004) 20:3–22.
11. Kimura S, Yurugi K, Segawa H, Kuroda J, Sato K, Nogawa M, et al. Rapid quantification of immunoglobulin G antibodies specific for blood group antigens A and B by surface plasmon resonance. *Transfusion* (2005) 45:56–62. doi:10.1111/j.1537-2995.2005.04062.x
12. Yurugi K, Kimura S, Ashihara E, Tsuji H, Kawata A, Kamitsuji Y, et al. Rapid and accurate measurement of anti-A/B IgG antibodies in ABO-unmatched living donor liver transplantation by surface plasmon resonance. *Transfus Med* (2007) 17:97–106. doi:10.1111/j.1365-3148.2007.00737.x
13. Rispens T, Derksen NI, Commins SP, Platts-Mills TA, Aalberse RC. IgE production to α-gal is accompanied by elevated levels of specific IgG1 antibodies and low amounts of IgE to blood group B. *PLoS One* (2013) 8(2):e55566. doi:10.1371/journal.pone.0055566
14. Lleo A, Invernizzi P, Gao B, Podda M, Gershwin ME. Definition of human autoimmunity – autoantibodies versus autoimmune disease. *Autoimmun Rev* (2010) 9:A259–66. doi:10.1016/j.autrev.2009.12.002
15. Kubo T, Uchida Y, Watanabe Y, Abe M, Nakamura A, Ono M, et al. Augmented TLR9-induced Btk activation in PIR-B-deficient B-1 cells provokes excessive auto-antibody production and autoimmunity. *J Exp Med* (2009) 206:1971–82. doi:10.1084/jem.20082392
16. Chou MY, Fogelstrand L, Hartvigsen K, Hansen LF, Woelkers D, Shaw PX, et al. Oxidation-specific epitopes are dominant targets of innate natural antibodies in mice and humans. *J Clin Invest* (2009) 119:1335–49. doi:10.1172/JCI36800
17. Eibl N, Spatz M, Fischer GF, Mayr WR, Samstag A, Wolf HM, et al. Impaired primary immune response in type-1 diabetes: results from a controlled vaccination study. *Clin Immunol* (2002) 103:249–59. doi:10.1006/clim.2002.5220
18. van Belle TL, Coppieters KT, von Herrath MG. Type 1 diabetes: etiology, immunology, and therapeutic strategies. *Physiol Rev* (2011) 91:79–118. doi:10.1152/physrev.00003.2010
19. Christen U, Bender C, von Herrath MG. Infection as a cause of type 1 diabetes? *Curr Opin Rheumatol* (2012) 24:417–23. doi:10.1097/BOR.0b013e3283533719
20. Kerr JR. The role of parvovirus B19 in the pathogenesis of autoimmunity and autoimmune disease. *J Clin Pathol* (2016) 69:279–91. doi:10.1136/jclinpath-2015-203455
21. Pane JA, Coulson BS. Lessons from the mouse: potential contribution of bystander lymphocyte activation by viruses to human type 1 diabetes. *Diabetologia* (2015) 58:1149–59. doi:10.1007/s00125-015-3562-3
22. Masala S, Cossu D, Piccinini S, Rapini N, Mameli G, Manca Bitti ML, et al. Proinsulin and MAP3865c homologous epitopes are a target of antibody response in new-onset type 1 diabetes children from continental Italy. *Pediatr Diabetes* (2015) 16:189–95. doi:10.1111/pedi.12269
23. Masala S, Paccagnini D, Cossu D, Brezar V, Pacifico A, Ahmed N, et al. Antibodies recognizing *Mycobacterium avium* paratuberculosis epitopes cross-react with the beta-cell antigen ZnT8 in Sardinian type 1 diabetic patients. *PLoS One* (2011) 6(10):e26931. doi:10.1371/journal.pone.0026931
24. Williams JM, Bonami RH, Hulbert C, Thomas JW. Reversing tolerance in isotype switch–competent anti-insulin B lymphocytes. *J Immunol* (2015) 195:853–64. doi:10.4049/jimmunol.1403114
25. Maglione PJ, Simchoni N, Black S, Radigan L, Overbey JR, Bagiella E, et al. IRAK-4 and MyD88 deficiencies impair IgM responses against T-independent bacterial antigens. *Blood* (2014) 124:3561–71. doi:10.1182/blood-2014-07-587824
26. Avalos AM, Busconi L, Marshak-Rothstein A. Regulation of autoreactive B cell responses to endogenous TLR ligands. *Autoimmunity* (2010) 43:76–83. doi:10.3109/08916930903374618
27. Chen RT, Pless R, DeStefano F. Epidemiology of autoimmune reactions induced by vaccination. *J Autoimmun* (2001) 16:309–18. doi:10.1006/jaut.2000.0491
28. Moran AP. The role of endotoxin in infection: *Helicobacter pylori* and *Campylobacter jejuni*. *Subcell Biochem* (2010) 53:209–40. doi:10.1007/978-90-481-9078-2_10
29. Bogaert D, Hermans PWM, Adrian PV, Rümke HC, deGroot R. Pneumococcal vaccines: an update on current strategies. *Vaccine* (2004) 22:2209–20. doi:10.1016/j.vaccine.2003.11.038
30. Biagini RE, Schlottmann SA, Sammons DL, Smith JP, Snawder JC, Striley CAF, et al. Method for simultaneous measurement of antibodies to 23 pneumococcal capsular polysaccharides. *Clin Diagn Lab Immunol* (2003) 10:744–50. doi:10.1128/CDLI.10.5.744-750.2003
31. Canziani GA, Klakamp S, Myszka DG. Kinetic screening of antibodies from crude hybridoma sample using Biacore. *Anal Biochem* (2003) 325:301–7. doi:10.1016/j.ab.2003.11.004
32. Seo HJ, Adachi K, Lee BK, Kang DG, Kim YK, Kim KR, et al. Facile and rapid direct gold surface immobilization with controlled orientation for carbohydrates. *Bioconjug Chem* (2007) 18:2197–201. doi:10.1021/bc700288z
33. Thomas R, Patenaude SI, MacKenzie CR, To R, Hirama T, Young NM, et al. Structure of an anti-blood group A Fv and improvement of its binding affinity without loss of specificity. *J Biol Chem* (2002) 277:2059–64. doi:10.1074/jbc.M104364200
34. Wedemayer GJ, Patten PA, Wang LH, Schultz PG, Stevens RC. Structural insights into the evolution of an antibody combining site. *Science* (1997) 276:1665–9. doi:10.1126/science.276.5319.1665
35. Manimala JC, Roach TA, Li Z, Gildersleeve JC. High-throughput carbohydrate microarray profiling of 27 antibodies demonstrates widespread specificity problems. *Glycobiology* (2007) 17:17–23. doi:10.1093/glycob/cwm047

36. Wang L, Radic MZ, Galili U. Human anti-Gal heavy chain genes. *J Immunol* (1995) 155:1276–85.
37. Bello-Gil D, Manez R. Exploiting natural anti-carbohydrate antibodies for therapeutic purposes. *Biochemistry (Mosc)* (2015) 80:836–45. doi:10.1134/S0006297915070044
38. Galili U. Anti-Gal: an abundant human natural antibody of multiple pathogeneses and clinical benefits. *Immunology* (2013) 140:1–11. doi:10.1111/imm.12110
39. Gerstenbruch S, Brooks CL, Kosma P, Brade L, MacKenzie CR, Evans SV, et al. Analysis of cross-reactive and specific anti-carbohydrate antibodies against lipopolysaccharide from *Chlamydophila psittaci*. *Glycobiology* (2010) 20:461–72. doi:10.1093/glycob/cwp198
40. Moran AP, Prendergast MM, Appelmelk BJ. Molecular mimicry of host structures by bacterial lipopolysaccharides and its contribution to disease. *FEMS Immunol Med Microbiol* (1996) 16:105–15. doi:10.1111/j.1574-695X.1996.tb00127.x
41. Caudie C, Pinon AQ, Taravel D, Sivadon-Tardy V, Orlikowski D, Rozenberg F, et al. Preceding infections and anti-ganglioside antibody profiles assessed by a dot immunoassay in 306 French Guillain-Barre' syndrome patients. *J Neurol* (2011) 258:1958–64. doi:10.1007/s00415-011-6042-9
42. Moran AP. Relevance of fucosylation and Lewis antigen expression in the bacterial gastroduodenal pathogen *Helicobacter pylori*. *Carbohydr Res* (2008) 343:1952–65. doi:10.1016/j.carres.2007.12.012
43. Van Roon AM, Pannu NS, de Vrind JPM, van der Marel GA, van Boom JH, Hokke CH, et al. Structure of an anti-Lewis X Fab fragment in complex with its Lewis X antigen. *Structure* (2004) 12:1227–36. doi:10.1016/j.str.2004.05.008

Conflict of Interest Statement: The authors declare that the research was conducted in the absence of any commercial or financial relationships that could be construed as a potential conflict of interest.

frontiers in Immunology

ORIGINAL RESEARCH
published: 18 December 2018
doi: 10.3389/fimmu.2018.02984

Hypomorphic Mutations in the BCR Signalosome Lead to Selective Immunoglobulin M Deficiency and Impaired B-cell Homeostasis

*Christoph B. Geier[1], Kai M. T. Sauerwein[1], Alexander Leiss-Piller[1], Isabella Zmek[1], Michael B. Fischer[2,3], Martha M. Eibl[1,4] and Hermann M. Wolf[1,5]**

[1] Immunology Outpatient Clinic, Vienna, Austria, [2] Clinic for Blood Group Serology and Transfusion Medicine, Medical University of Vienna, Vienna, Austria, [3] Department for Health Science and Biomedicine, Danube University Krems, Krems, Austria, [4] Biomedizinische Forschungs GmbH, Vienna, Austria, [5] Medical School, Sigmund Freud Private University, Vienna, Austria

OPEN ACCESS

Edited by:
Wanli Liu,
Tsinghua University, China

Reviewed by:
Lee Ann Garrett-Sinha,
University at Buffalo, United States
Kishore Alugupalli,
Thomas Jefferson University, United States

***Correspondence:**
Hermann M. Wolf
hermann.wolf@itk.at

Specialty section:
This article was submitted to B Cell Biology, a section of the journal Frontiers in Immunology

Received: *01 August 2018*
Accepted: *04 December 2018*
Published: *18 December 2018*

Citation:
Geier CB, Sauerwein KMT, Leiss-Piller A, Zmek I, Fischer MB, Eibl MM and Wolf HM (2018) Hypomorphic Mutations in the BCR Signalosome Lead to Selective Immunoglobulin M Deficiency and Impaired B-cell Homeostasis. Front. Immunol. 9:2984. doi: 10.3389/fimmu.2018.02984

B cell activation via the B cell receptor (BCR) signalosome involves participation of signaling molecules such as BTK and BLNK. Genetic defects in these molecules are known to impair B cell differentiation and subsequently lead to agammaglobulinemia. Here we identified novel mutations in BTK and BLNK in two unrelated patients that perturb the intrinsic B-cell receptor signaling pathway and lead to selective IgM deficiency, whereas production of other immunoglobulin isotypes and IgG antibody response remain intact. Currently it is unknown how BCR signaling strength affects mature B cell development in humans. Both patients show reduced levels of BCR signalosome phosphorylation as well as impaired BCR-dependent Ca^{2+} influx, which was accompanied by a marked decrease in $IgD^{+}IgM^{+}CD27^{+}$ MZ-like B-cells. We further describe reduced expression of essential B cell differentiation factors such as BAFF-R and T-Bet in the patients' B-cells, which might contribute to the observed deficiency of MZ-like B cells. MZ-like B cells are known to produce natural IgM antibodies that play an essential role in immune homeostasis. By using surface plasmon resonance (SPR) technology and a synthetic blood group A trisaccharide as antigen we were able to show that both patients lack the presence of anti-blood group A IgM considered to be prototypical natural antibodies whereas IgG levels were normal. Antibody binding dynamics and binding affinity of anti-blood group A IgG were comparable between patients and healthy controls. These results indicate that human IgM deficiency can be associated with signaling defects in the BCR signalosome, defective production of natural IgM antibodies in the blood group A/B/0 system and abnormalities in B cell development.

Keywords: primary immunodeficiency, B-cell defects, selective IgM deficiency, BTK, BLNK, marginal-zone B cells, natural antibodies

INTRODUCTION

The B cell receptor (BCR) induces B-cell activation and differentiation following antigen exposure. Membrane bound immunoglobulins and the non-covalently bound CD79a/b (Iga/b) form the BCR complex (1). After ligand dependent BCR aggregation tyrosine residues in the cytoplasmic ITAM portion of CD79a and CD79b are phosphorylated by spleen tyrosine kinase (Syk). This phosphorylation recruits the BCR signalosome to amplify the activation, including the kinases Syk, Lyn, and Bruton tyrosine kinase (Btk), the guanine exchange factor Vav, and the adaptor proteins Grb2 and B-cell linker (BLNK) (2).

B lymphocyte homeostasis depends on tonic and induced BCR signaling. BCR signaling strength is a major driver of the developmental fate to facilitate the production and maintenance of immunocompetent pools of mature follicular (Fo) BI and FoBII cells and marginal zone (MZ) B cells while remaining self-tolerant (3). A recent study by Tsiantoulas et al. identified secreted IgM as a major regulator for BCR-signaling strength and proper B cell development in mice by acting as a negative regulator of BCR signaling (4). Immunoglobulin M plays a crucial role in the adaptive immune system, as it appears early in the course of an infection and bridges the gap between innate immunity and production of high affinity IgG (5). Beside its well-documented protective role against invasive pathogens, natural IgM plays a crucial role in immune homeostasis and immune development (5–8). A significant proportion of serum IgM consists of naturally occurring IgM, which is produced independently of exposure to foreign antigens and without the need for T helper cells. While it is clear from studies in mice that natural IgM is produced by B1 cells at birth, in humans the cellular origin of natural IgM still remains controversial. An orthologous human B-1 cell population has not been clearly identified, and the existence and phenotype of a human B cell subset responsible for production of natural IgM still remains debated (9–13).

Isolated deficiency of IgM was first described in 1967 by Hobbs and colleagues in two children with low to absent levels of serum IgM and fatal meningococcal meningitis (14). Selective Immunoglobulin M deficiency (sIgMD) is characterized by isolated low to absent levels of serum IgM and defective IgM antibody response following vaccination, infection or natural exposure, while the number of peripheral blood B lymphocytes, immunoglobulin isotype class switch, and serum levels of other immunoglobulins and IgG antibody responses are intact in the majority of patients (15–17). The clinical manifestation of sIgMD comprises a heterogenous spectrum ranging from bacterial infections in the majority of patients to atopic or autoimmune disease manifestation in otherwise asymptomatic patients (14–16). Complete selective IgM deficiency is considered a rare primary immunodeficiency with a reported prevalence of 0.03% in a community-based study (18). However, the prevalence of patients with decreased to borderline-detectable IgM is estimated to be higher, up to 2.1% in selected cohorts (19–21).

In this study we sought to identify the molecular pathomechanism leading to selective IgM deficiency. We wanted to further clarify the role partial BCR signaling defects might have in B cell development and homeostasis. Murine models on how BCR signaling strength influences MZ and FO B cell development are contradictory and data in humans are scarce (22, 23). We identified novel hypomorphic BTK and BLNK mutations that dampen BCR signaling strength in two unrelated male patients with sIgMD. We demonstrated that in these patients reduced BCR signaling is associated with impaired formation of natural IgM antibodies of the blood group AB0 system and abnormalities in MZ B-cell development, possibly due to altered expression of essential MZ-B cell differentiation factors BAFF-R and T-bet.

MATERIALS AND METHODS

Determination of Serum Immunoglobulins and Antibodies

Serum concentrations of immunoglobulins and IgG subclasses were determined by standard laser nephelometry on a Siemens nephelometric analyzer (Siemens Healthcare; Germany) using reagents purchased from Siemens-Behring Division. IgG and IgM antibodies against bacterial and viral antigens were determined using commercially available enzyme-linked immunosorbent assay (ELISA) kits [IgG antibodies against tetanus and diphtheria toxoid, tick borne encephalitis (TBE) virus, Haemophilus influenza type b (Hib)] or an in-house produced isotype-specific ELISA (IgG and IgM antibodies against 23-valent pneumococcal capsular polysaccharide) as previously described (24).

DNA Isolation and Targeted Resequencing

Genomic DNA was prepared from peripheral blood by spin column purification (QIAamp DNA Blood Mini Kit; QIAGEN, Germany). Targeted resequencing of 222 primary immunodeficiency genes listed in the 2011 IUIS expert committee report and candidate genes was performed for the two index patients. (**Table S1**) Nextera Custom Enrichment kit was used according to standard protocols (Illumina, USA). Targeted DNA library was quantified and validated using Illumina Eco Realtime (Illumina; USA) and Agilent Bioanalyzer (Agilent Technologies; USA). The library was sequenced in a multiplex pool on a single (151 bp paired-end reads) Miseq flowcell (Illumina, USA). Data analysis was performed using CLC Genomic Workbench (QIAGEN, Germany).

cDNA Preparation and Gene Expression of IgM Splice Forms

Total RNA was isolated using RNeasy Mini Kit (Qiagen, Netherlands) and Oligo dT primed cDNA library was prepared using SuperScript IV First-Strand Synthesis System (Thermo Fisher Scientific, USA) from an EBV-transformed lymphoblastoid cell line (EBV-LCL) from patients and healthy controls. Alternative spliced transcript PCR was performed to visualize different forms of IgM (precursor, secreted, and membrane) using Phire Hot Start II DNA Polymerase (Thermo Fisher Scientific; USA). Amplicons were visualized using standard LE-Agarose electrophoresis (Biozym, Germany).

Amplification-Refractory Mutation System (ARMS)

The coding sequence of BLNK (cDNA) and BTK (gDNA) was amplified using Phire Hot Start II DNA Polymerase (Thermo Fisher Scientific; USA). Allele-specific PCR was used to characterize BLNK Pro110Ala and Ala158Ser alleles. Each allele (wild type and mutant form) was amplified separately with an allele-specific primer in combination with a general primer using Maxima Hot Start Taq DNA Polymerase (Thermo Fisher Scientific, USA). All the resulting amplicons were purified and custom Sanger sequenced (Eurofins Genomic; Germany). Results were aligned to BLNK NM_013314.3 and BTK NG_009616.1 sequences as reference using CLC GenomicWorkbench (QIAGEN, Germany).

Western Blot and SDS Page

Epstein-Barr-virus transformed lymphoblastoid cell line of patient A, patient B and a healthy control were lysed for 30 min in ice-cold RIPA lysis buffer system (Santa Cruz Biotechnology, USA), and insoluble material was removed by centrifugation (16,000 × g, 10 min, 4°C). Twenty Microgram of protein were resolved in either 8%SDS-polyacrylamide gel electrophoresis (SDS-PAGE) or in 4% Native-polyacrylamide gel electrophoresis. Samples were subsequently electro transferred onto a polyvinylidene difluoride membrane (Immobilon-P; Millipore), and immunoblotted with anti-IgM antibody (2C12-3) (Santa Cruz Biotechnology Inc; USA). Detection was performed using the SuperSignal West Pico ECL detection system (Thermo Scientific; USA).

Biacore® Surface Plasmone Resonance (SPR)

A Biacore® T200 device (kindly provided by Florian Koelle, GE Health Care) was used to determine the concentration and affinity of blood-group A antibodies. For this a contact time of 600 s and a flow rate of 10 μl/min was chosen. Flow cell one (FC-1) was immobilized without trisaccharides and served as blank during binding analysis. FC-2 was immobilized with 1 mg/ml blood group A or B trisaccharide amine derivative (Dextra Laboratories Ltd., Reading, UK).

For binding analysis, serum was diluted by half with HBS-EP and injected in FC-2 for 180 s at a flow rate of 10 μl/min. The flow-path was 2–1. To determine IgM and IgG levels of blood group A- or B-bound antibodies, anti-human IgG Abs [polyclonal aHIgG (γ-chain), Sigma-Aldrich, USA] and anti-human IgM [polyclonal aHIgM (μ-chain), Sigma-Aldrich, USA] were injected for 180 s at a flow rate of 10 μl/min directly after the serum sample. The difference in resonance units (ΔRU) between report point "stability" and "baseline" was indicative for the amount of bound antibody, ΔRU between "enhance_baseline" and "enhance_level" represents the isotype-specific portion of bound antibodies. The chip was regenerated twice with 50 mmol NaOH for 30 s at a flow rate of 10 μl/min with a stabilization period of 5 s after the second regeneration to reach the same baseline as prior to the measurement.

For kinetic measurement, an association time of 200 s and dissociation time of 800 s was chosen. To analyze the curve exponential decay was assumed and the half-life (t1/2) and the dissociation constant kd of the antigen-antibody complex were calculated according to equation 1 and 2.

$$t(1/2) = ((t1)/(\ln 2(N(t)/(N(0)))$$

Equation 1 Half-life of antigen-antibody complex

$$(N0 - N(t))/\Delta t^{*}N0 = -kd$$

Equation 2 Dissociation constant kd of antigen-antibody complex

t0: time (s) at start of decay, t1: time (s) at end of decay, N0: RU at start of decay, N(t): RU at end of decay, t1/2: half-life (s), Δt: time of dissociation, kd: dissociation constant

The amount of anti-A or anti-B antibody that associated with the corresponding blood group A or B trisaccharide immobilized on the sensor chip surface was obtained by subtracting the FC-II value (RU) from the FC-I value (RU).

Flow Cytometry

Flow cytometry was performed as previously described (25). Peripheral venous blood was collected in EDTA containing tubes from patients with selective IgM deficiency and 14 healthy blood donors that served as controls. B cell subsets were characterized as follows; Naïve ($CD19^{+}IgD^{+}CD27^{-}$), Transitional($CD19^{+}CD27^{-}CD24^{high}CD38^{high}$), Follicular ($CD19^{+}CD27^{-}CD24^{dim}CD38^{dim}$), MZ ($CD19^{+}CD27^{+}IgD^{+}IgM^{+}$), Class Switched ($CD19^{+}CD27^{+}IgD^{-}IgM^{-}$), IgM-only ($CD19^{+}IgD^{-}IgM^{+}$), CD21low ($CD19^{+}IgM^{+}CD21^{low}CD38^{low}$), and Plasmablasts ($CD19^{+}CD27^{++}CD38^{++}$). All values are expressed as percent of total peripheral $CD19^{+}$ B cells. Supporting Information **Table S2** shows the monoclonal fluorophore-conjugated antibodies used. Dead cells were excluded and at least 100,000 events within the "lymphogate" were acquired. Cells were acquired with a FACSVerse (Becton Dickinson; USA) using standard protocols and analyzed using FACSuite software (Becton Dickinson; USA).

Analysis of B-cell Function

Human peripheral blood mononuclear cells (PBMCs) and LCL-EBV cell lines were isolated and generated as previously described (25). PBMC or LCL- EBV cells were transferred in 24-well flat-bottomed plates and were cultured in complete RPMI medium supplemented with 10% fetal bovine serum. 1×10^{6} cells per well were stimulated for 4 days at 37°C and 5% CO2 using 20 μg/mL goat $F_{(ab')}2$ anti–human IgM and IgD, each (Sigma-Aldrich, USA). Intracellular staining and Calcium influx was performed as previously described (26, 27). B cells were identified by $CD19^{+}$ and upregulation of activation marker was calculated by subtracting the geometric mean fluorescence intensity of unstimulated B-cells from the geometric mean of fluorescence intensity of activated B-cells. Supporting Information **Table S2** shows the monoclonal fluorophore-conjugated antibodies used.

Statistical Analysis

Statistical comparisons between experiments performed in cells from healthy controls and repeat experiments with cells from the two patients were performed by calculating the Mann Whitney *U*-test using Prism Graphpad 4.0 software. Statistically significant differences obtained in intergroup comparisons were confirmed by Kruskal–Wallis one-way analysis of variance using Prism Graphpad 4.0 software. Values of $p < 0.05$ were considered as significant, (ns statistically not significant, $^{*}p \leq 0.05$, $^{**}p \leq 0.01$.

ETHICS STATEMENT

The study was conducted in accordance with the Declaration of Helsinki and fulfills the guidelines of the Austrian Agency of Research Integrity (OeAWI). Patients gave their informed consent that anonymized data collected as part of the routine medical attendance (immunological analysis, flow cytometry analysis, and genetic mutation analysis) could be included in a scientific publication. All patient information in this study is anonymized and de-identified prior to analysis, and only anonymized and de-identified patient information is contained in this study. Samples used for genetic and molecular non-clinical analyses in this study were derived from leftover material obtained as part of the routine medical attendance the patients received. No extra intervention was carried out. With respect to the genetic and molecular non-clinical analyses this study was approved by the Ethics Committee of the Immunology Outpatient Clinic as a study using the residual specimens biobank of the Immunology Outpatient Clinic. According to the Ethics Committee of the City of Vienna and the legal regulations to be applied (§15a Abs. 3a Wiener Krankenanstaltengesetz) no additional ethics committee evaluation is required for a non-interventional study using data collected as part of the routine medical care the patients received.

PATIENT CHARACTERISTICS

Patient A was a 15-year old male referred for immunological investigation because of IgM deficiency, subtle hypogammaglobulinemia, recurrent stomatitis aphthosa and recurrent respiratory tract infections such as sinusitis and bronchitis (**Table 1**). He suffered from pneumonia at the age of 6, but otherwise had an uneventful medical history. He was the child of healthy unrelated parents of Austrian origin, a healthy brother was 10 years old. Upon initiation of antibiotic prophylaxis with amoxicillin (50% therapeutic dose daily) and pneumococcal vaccination susceptibility to respiratory infections normalized.

Patient B was a 37-year old male of Turkish descent referred for immunological investigation by the treating nephrologists because of IgM deficiency. Asymptomatic renal insufficiency was detected at the age of 28 years when a cirrhosis of the left kidney and mild hydronephrosis of the right kidney were found. Serum creatinine was 3.2 mg/dl (normal range 0.6–1.2 mg/dl), proteinuria was 2.5 g/d. He reported no increased susceptibility to infections, and his chronic renal insufficiency caused only mild clinical symptoms (development of fatigue and tachycardia upon physical strain).

TABLE 1 | Immunological Phenotype of two patients with sIgMD.

	Patient A	Patient B	Normal range
SERUM IMMUNOGLOBULIN LEVELS [mg/dl]			
IgG	745	903	790–1,700
IgA	92	791	76–450
IgM	39	27	90–350
SERUM IGG SUBCLASS LEVELS [mg/dl]			
IgG1	501	460	500–880
IgG2	158	302	150–600
IgG3	43	75	20–100
IgG4	<6	50	8–120
LYMPHOCYTE SUBPOPULATIONS (PERCENTAGE OF LYMPHOCYTES AND ABSOLUTE NUMBERS IN PARENTHESIS)			
$CD3^+$	68 (919)	80 (2,784)	53–85 (694–2,976)
$CD4^+$	40 (541)	48 (1,670)	31–66 (386–2,022)
$CD8^+$	28 (379)	28 (974)	21–43 (297–1,011)
$CD19^+$	13 (176)	14 (487)	7–23 (71–549)
$CD56^+$	17 (230)	10 (348)	6–29 (98–680)

RESULTS

Novel Hypomorphic BTK and BLNK Mutations in Two Unrelated Patients With Selective IgM-Deficiency

The mRNAs encoding the membrane-bound and secreted immunoglobulin heavy chains are produced from identical primary transcripts, which are differently processed at their 3′ ends. Regulation of membrane-bound vs. secreted forms of the immunoglobulin heavy chains depends on the competition of 2 mutual cleavage polyadenylation sites (pAs/pAm) (28). In mice targeted deletion of the mu heavy chain cleavage polyadenylation site pAs leads to deficiency of secreted IgM with intact expression of surface IgM and normal secretion of other immunoglobulin isotypes (29). Therefore, we sequenced mu heavy chain gene including the polyadenylation sites in both patients with sIgMD and found no alterations (data not shown). Both patients' B cells were able to express precursor, secreted and membrane IgM mRNA (**Figure 1A**). Furthermore protein expression of monomeric and native pentameric IgM (**Figure 1B**) and surface expression of IgM on the B cell membrane (data not shown) was comparable to healthy controls.

To elucidate the genetic basis of the patients' selective IgM deficiency we used a targeted resequencing approach to sequence potential candidate genes. In both patients, we identified defects within the intrinsic B-cell receptor signaling pathway. Patient A harbored a c615G > T missense mutation in exon 8 in the tyrosine kinase BTK. The G > T transition resulted in a glutamic acid to aspartic acid substitution at position 205 within the highly conserved proline-rich (PRR) region located at the C-terminus

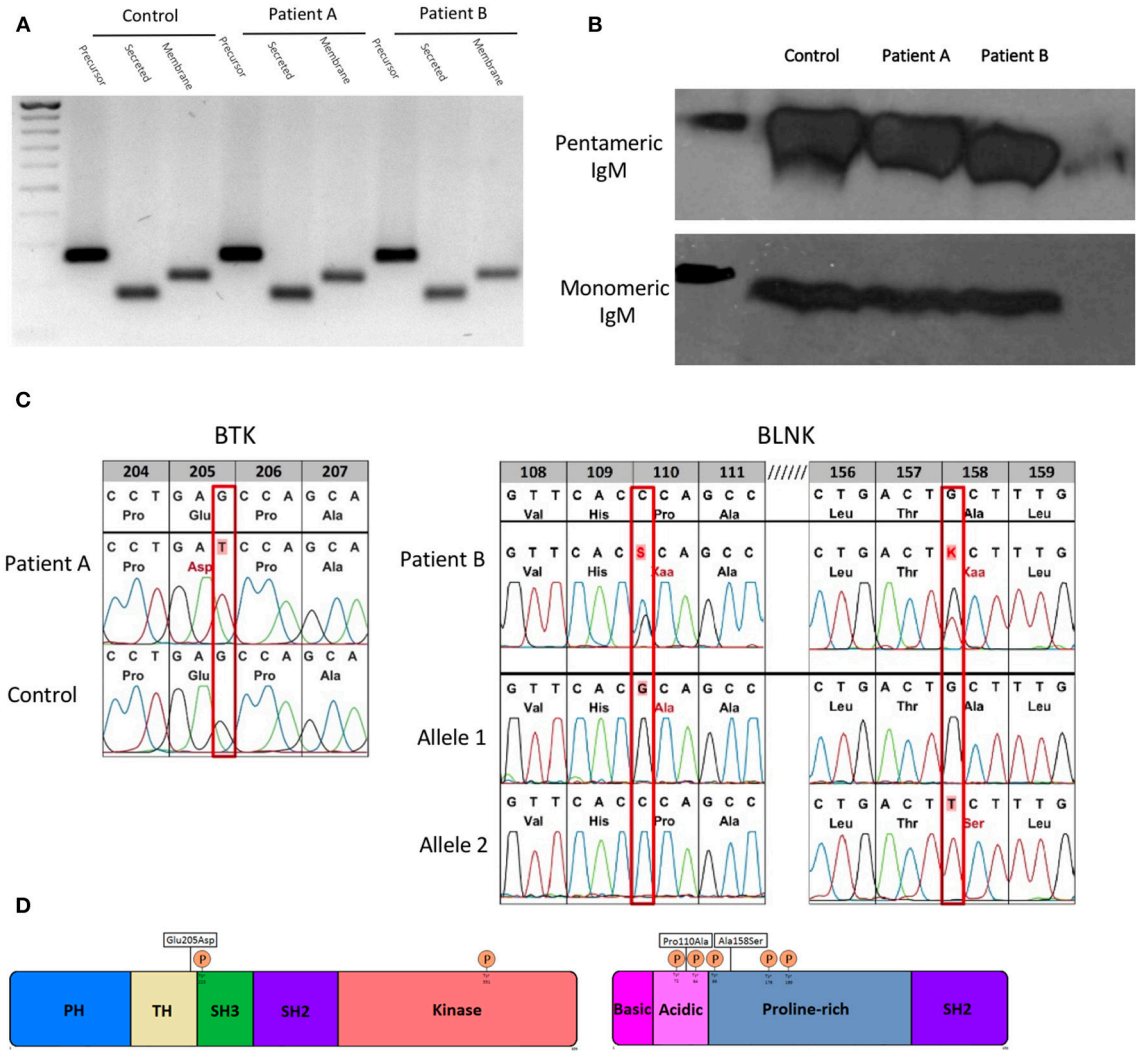

FIGURE 1 | Molecular characterization of novel hypomorphic BTK/BLNK mutations. **(A)** Gene expression of precursor, secreted and membrane IgM of patients and control EBV-LCL quantified by semi-quantitative cDNA-PCR. **(B)** Protein expression of monomeric and pentameric IgM of patients and control EBV-LCLs by SDS-PAGE or native-PAGE and detected by western blot. **(C)** BTK/BLNK Mutation analysis of genomic DNA from peripheral blood. Patient A is hemizygote for a c615G>T in BTK. Patient B is compound heterozygous in BLNK for c328C>G, c472G>T. Healthy controls served as wild type control. **(D)** Schematic depiction of mutation sites and phosphorylation sites in BTK and BLNK.

of the TEC homology (TH) domain (**Figures 1C,D**). Proline rich regions are involved in protein-protein interactions, including interactions with G proteins and intramolecular association with the SH3 domain (2). Mutations within the proline rich regions have been shown to abolish SH3 domain binding and result in functional impairment of BTK, pointing toward a potential biologic relevance of the BTK mutation found in patient A (30).

Patient B harbored a biallelic mutation in BLNK, which was subsequent identified to be compound heterozygous by amplification-refractory mutation system (ARMS). Both mutations (c328C > G, pPro110Ala/c472G > T, pAla158Ser) are located within a functionally relevant region of the N terminus domain of BLNK (**Figures 1C,D**), in close proximity to highly conserved tyrosine residues which serve as a scaffold to assemble downstream targets like VAV, NCK, BTK, and PLCγ2 (31). Restriction fragment length polymorphism (RFLP) analysis of DNA of 200 unrelated individuals did not reveal BTK or BLNK mutations identical to that seen in our sIgMD patients (data not shown).

Novel Hypomorphic BLNK and BTK Mutations Result in Impaired B-cell Receptor Signaling

Mutations within the BCR signalosome such as BTK or BLNK usually result in absent protein expression, a severe block of BCR signaling and an arrest at the pre-B cell stage, subsequently leading to agammaglobulinemia (32). Our patients had normal

numbers of peripheral blood B cells and no agammaglobulinemia (**Table 1**).

BTK and BLNK protein expression was not altered in both patients compared to healthy controls, when quantified by flow cytometry (**Figure 2A**). To assess whether novel BTK and BLNK mutations described are associated with B-cell signaling impairment we stimulated the patients' EBV transformed B-cells with αIgM and αIgD antibodies and analyzed phosphorylation of BTK and BLNK by flow-cytometry. Autophosphorylation of BTK at position Y223, located within the Src-homology 3 domain, was diminished in patient A as compared to healthy controls, suggesting a reduced SH3-mediated downstream signaling (**Figure 2B**, left panel).

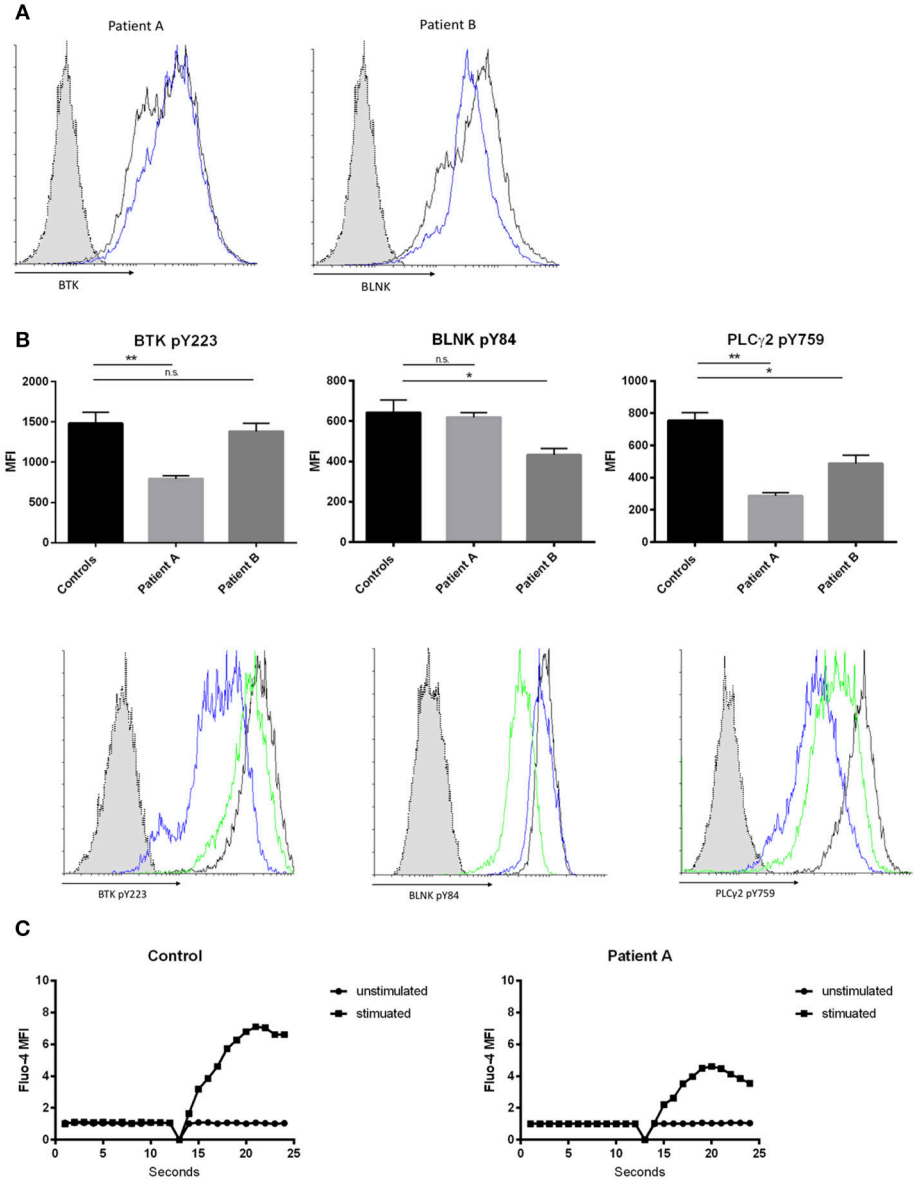

FIGURE 2 | Effects of hypomorphic BTK/BLNK mutations on BCR signaling. **(A)** Representative FACS histograms depicting BTK (left) and BLNK (right) expression of αIgM/αIgD -stimulated EBV-LCLs. Blue histograms represent patients, black histograms represent healthy control and dotted gray histograms represent isotype control. **(B)** Bar graphs and representative flow cytometry plots showing the expression of pBtk, pBLNK, and pPLCγ2 in αIgM/αIgD -stimulated EBV-LCLs. Blue histograms represent patient A, green histograms represent patient B, black histograms represent healthy control, and dotted gray histograms represent isotype control. Results in bar graphs are expressed as mean fluorescence intensity (MFI, mean ± SD) of stimulated $CD20^+$ EBV-LCLs after subtraction of expression of unstimulated $CD20^+$ EBV-LCLs (no significant difference was found in basal expression between controls and patients, data not shown). $CD20^+$ EBV-LCLs were stimulated with αIgM and αIgD antibodies. Bars represent the mean and standard deviation of five healthy controls and three repeat experiments using cells from the two patients. (*ns* = statistically not significant, $^*p \leq 0.05$, $^{**}p \leq 0.01$, Mann Whitney *U*-test) **(C)** Kinetics plot showing calcium influx of Fluo-4 loaded peripheral $CD19^+$ B cells from patient A and healthy control following activation with αIgM and αIgD antibodies.

Patient B did present with a reduction in BLNK phosphorylation at position Y84 compared to healthy controls examined in parallel. BLNK is a substrate for SYK, which phosphorylates Y84, and phosphorylated BLNK provides docking sites for various molecules including activated BTK and PLC gamma 2 (**Figure 2B**, middle panel). Activated BTK brought in proximity of PLC gamma 2 by BLNK leads to phosphorylation and activation of PLC gamma 2. Thus, we hypothesized that the hypomorphic mutations observed in BTK as well as in BLNK might impact PLC gamma 2 activation (33, 34). Phosphorylation of PLC gamma 2 at position Y759 was diminished in both patients' B cells stimulated via the BCR as compared to healthy controls examined in parallel (**Figure 2B**, right panel).

Intact BTK and BLNK activity is essential for normal BCR-dependent Ca^{2+} signaling in human B cells (33, 35). Therefore, we investigated whether the hypomorphic BTK mutation found in patient 1 results in impaired calcium flux through store operated calcium channels. Primary B-cell were loaded with Fluo-4 and activated with αIgM and αIgD. Patient A demonstrated a decreased influx of intracellular calcium, indicating abnormal function of store-operated calcium entry in this patient with selective IgM deficiency (**Figure 2C**).

Impairment of BCR Signaling Is Associated With Skewed B-cell Homeostasis in Patients With Selective IgM Deficiency

BCR signaling strength is the major determinant of the developmental fate of mature B cells. However, the precise effect of BCR-signaling on the shaping of B cell homeostasis is not yet fully clarified. Recent studies in mice report that strong BCR signaling favors MZ B cell development while other studies report increased FO B cells (4). We were interested how impaired BCR signaling might affect B cell development in our patients with selective IgM deficiency. We found a significant decrease in the numbers of MZ B cells while follicular and naïve B cells were present in normal to increased levels (**Figure 3A**). Peripheral blood numbers of transitional stage B cells, class switched memory B cells, IgM only memory B cells and plasmablasts did not differ between healthy controls and patients. We further quantified levels of CD21low B cells, as previous reports in patients with common variable immunodeficiency (CVID) associated increased CD21low B cells with defects in calcium- dependent BCR-activation (36). However, we did not find alterations in the levels of CD21low B cells in our sIgMD patients (**Figure 3A**).

Recent evidence suggests that BCR/BTK signaling positively autoregulates crosstalk with BAFF-R, which is a fundamental developmental factor for survival and differentiation of MZ B cells (3). We therefore quantified levels of BAFF-R expression following BCR activation in peripheral B-cells of patient A and EBV-LCLs of both patients. BAFF-R expression in peripheral B-cells of patient A and EBV-LCLs of both patients were significantly reduced following BCR activation (**Figures 3B,C**). In addition to BCR/BAFF-R interaction, Notch signaling pathway is essential in the generation of MZ B cells. As Notch expression is independent of BCR signaling strength, we hypnotized that NOTCH2 expression is unaffected on patients' B cells. We found a slight increase in NOTCH2 expression on both patients' EBV-LCL after BCR activation, which might resemble an insufficient compensatory mechanism (**Figure 3C**). Low TACI expression has been described as a reason for the impaired T cell independent antigen response in XID mice (37). We therefore quantified the expression of TACI in BCR-activated EBV-transformed LCL, however there was no significant difference in TACI expression between patients and healthy controls (**Figure 3C**). We further quantified levels of T-bet in peripheral B-cells of patient A, as MZ B cells migrate in a T-bet dependent manner (38). We could observe a marked reduction in T-bet expression of patient A's peripheral B-cells (**Figure 3B**).

Intact IgG Antibody Response in Patients With Selective IgM Deficiency

Furthermore, we were interested whether impaired BCR signaling and disturbed B-cell homeostasis alters T-cell dependent and T-cell independent antibody responses in patients with selective IgM deficiency.

T- dependent IgG antibody responses to protein antigens such as tick-borne encephalitis virus (TBEV), VZV, HAV, and tetanus toxoid were normal in both patients, as were IgG antibody titers against the capsular polysaccharide of Hib (**Table 2**; patient A received four childhood vaccinations with conjugated Hib vaccine, patient B's Hib-IgG were produced after natural exposure/infection). Both patients responded with normal levels of T-independent IgG titer when challenged with 23-valent unconjugated pneumococcal vaccine (patient A) or after natural exposure/infection (patient B) (**Figure 4A**, right panel). In contrast, both patients displayed a defective IgM responsiveness to T-independent bacterial polysaccharide antigens such as 23-valent pneumococcal capsular polysaccharides, either after vaccination with Pneumo 23 "Merieux" (patient A) or following natural exposure/infection (patient B) (**Figure 4A**, left panel), or tetravalent unconjugated meningococcal vaccine (Mencevax, patient A, data not shown).

In addition, we investigated how impaired BCR signaling in selective IgM deficient patients perturbs formation of natural antibodies. Blood group A/B antibodies are directed against carbohydrate epitopes that form the AB0 antigens on red blood cells (RBCs) and are considered prototypic natural antibodies (39, 40). We applied surface plasmon resonance (SPR) technology and synthetic blood group A trisaccharide as the antigen to investigate titers of IgM and IgG anti-A antibodies and real-time analysis of molecular binding dynamics. IgM anti-A antibodies were undetectable in both sIgMD patients. In contrast, IgG Anti-A antibodies were detectable in normal titers in patients compared to healthy controls (**Figure 4B**). Results were comparable when IgM and IgG titers of anti-blood group B antibodies were analyzed (data not shown).

To measure whether binding characteristics of anti-blood group A-IgG antibodies are altered in our patients, we analyzed the binding dynamics of IgG anti-A antibodies. We found no

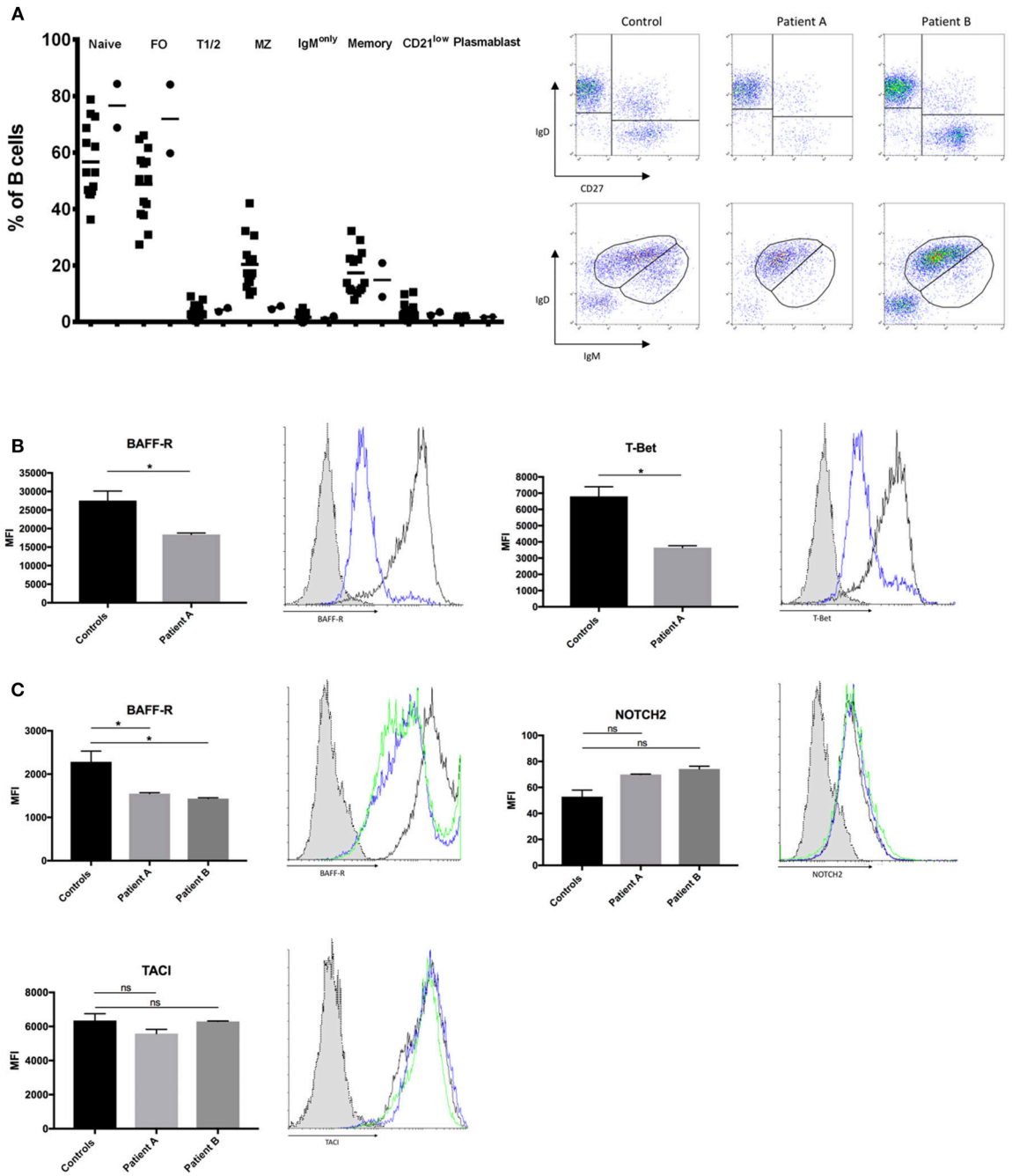

FIGURE 3 | Altered B-cell compartment in sIgMD with impaired BCR signaling. **(A)** Bar graphs and representative flow cytometry plots showing percent of total CD19$^+$B cells of Naïve (CD19$^+$IgD$^+$CD27$^-$) Transitional T1/2 (CD19$^+$CD27$^-$CD24^{high}CD38^{high}) Follicular FO (CD19$^+$CD27$^-$CD24^{dim}CD38^{dim}) MZ (CD19$^+$CD27$^+$IgD$^+$IgM$^+$), Class Switched Memory (CD19$^+$CD27$^+$IgD$^-$IgM$^-$) IgM only (CD19$^+$IgD$^-$IgM$^+$), CD21low (CD19$^+$IgM$^+$CD21^{low}CD38^{low}), and. Patients are depicted as filled circles (•) and healthy controls ($n = 14$) as filled squares (■), horizontal bars represent the mean. **(B,C)** Bar graphs and representative flow cytometry plots showing the expression of BAFF-R, T-Bet, NOTCH2, and TACI. Blue histograms represent patient A, green histograms represent patient B, black histograms represent healthy control and dotted gray histograms represent isotype control. Results are expressed as mean fluorescence intensity (MFI, mean ± SD) on stimulated peripheral CD19$^+$ B-cells or stimulated CD20$^+$ EBV-LCLs after subtracting expression of unstimulated CD19$^+$ B-cells or stimulated CD20$^+$ EBV-LCLs (no significant difference was found in basal expression between controls and patients, data not shown). Peripheral CD19$^+$ B-cells **(B)** and CD20$^+$ EBV-LCLs **(C)** were stimulated with αIgM and αIgD antibodies. Bars represent the mean and standard deviation of three experiments. *ns*, statistically not significant; *$p \leq 0.05$, Mann Whitney *U*-test.

TABLE 2 | IgG antibody response to protein and polysaccharide antigens.

Vaccine antigen	Antibody isotype	Patient A	Patient B	Normal range
Tetanus toxoid	IgG (ELISA, IU/ml)	2.60	n.a.	>0.4
HAV	IgG (ELISA, IU/L)	3,971	6,743	>100
TBEV	IgG (ELISA, U/ml)	2,024	n.a.	>310
VZV	IgG (ELISA, VE)	22.2	29.7	>11
Hib	IgG (ELISA, ug/ml)	6.08	2.69	>1

significant change in binding stability (halftime of antibody-antigen complex, **Figure 4C** left panel) and estimated affinity constant (K_d, **Figure 4C** right panel).

DISCUSSION

The identification of BTK as the cause of X-linked agammaglobulinaemia (XLA) in 1993 provided the first description of a monogenetic gene defect causative of inherited B cell deficient agammaglobulinemia (41). Since then a pleiotropic spectrum of mutations within the BCR and BCR signalosome have been described. The majority of mutations described lead to a severe block in B-cell development, while reports of milder phenotypes are scarce (42). Hypomorphic mutations usually result in low numbers of circulating B cells, low residual levels of immunoglobulins and variable defects in IgG antibody formation (43–46). Lim LM and colleagues reported two siblings with selective IgM deficiency and a missense mutation in BTK leading to a severe reduction in circulating B cells similar to previous published hypomorphic BTK mutations (42, 47). Our findings confirm and extend previous publications by reporting novel mutations in BTK and BLNK in two unrelated sIgMD patients, associated with moderately impaired BTK and BLNK function and impaired BCR signaling, indicating a functional relevance compatible with a hypomorphic nature of these mutations. The novel BTK E206D mutation in patient A is located within the TH-domain. The TH-domain consists of two distinct motifs, an N-terminal Btk motif adjacent to the PH domain and a highly conserved proline rich region (PRR) located at the C-terminus (48). The N-terminal Btk motif is involved in Zn^{2+} binding and mutations in these residues result in altered protein folding and stability and thereby cause XLA (49, 50). The PRR motif occurs twice in BTK at residues 186–192 and 200–206. The PRR-TH regions of BTK mediates specific interactions with SH3-containing proteins and thereby is essential for intermolecular or intramolecular interactions and critical for biological signal transduction (30). Mutations that lead to instability and loss of BTK protein resulted in severe XLA whereas detection of reduced levels of protein is associated with decreased clinical severity (51). BTK levels in patient A harboring the E206D mutation were not altered when quantified by flow cytometry. We hypothesize that rather than destabilizing the BTK protein, E206D impairs BCR signalosome function.

To date, 6 patients with mutations in the scaffold protein BLNK have been described (52–55). These patients lack expression of BLNK as they harbor either nonsense or frameshift mutations, generally having clinical findings that are comparable to those seen in patients with mutations in BTK. We herein report the first case of biallelic missense mutations in BLNK, Pro110Ala and Ala158Ser, with normal expression of BLNK analyzed by flow cytometry. Upon phosphorylation, non-ITAM tyrosine residues of BLNK located within a proline-rich domain serve as scaffold by assembling the BCR signalosome (56, 57). Both of our novel biallelic mutations, Pro110Ala and Ala158Ser, are located in close proximity to highly conserved tyrosine residues. We could demonstrate that the biallelic mutations in patient B result in impaired BLNK function and therefore fail to amplify PLC γ -mediated signaling. Rather than abolishing B cell signaling and causing agammaglobulinemia, our data indicate that the hypomorphic mutations in patients with selective IgM deficiency described might hamper BCR signaling.

The majority of selective IgM deficiency cases occur sporadically and only a minority of patients are described to have an aberrant B cell phenotype similar to our patients described, thus selective IgM deficiency is likely a heterogeneous disorder (17, 58). In addition to hypomorphic mutations in BCR signalosome genes, other disease mechanisms could cause selective IgM deficiency. B cells from mice with a targeted deletion of the μs cleavage polyadenylation site (pAs) do not secrete IgM but are still capable of expressing surface IgM and IgD and secreting other Ig isotypes (59). Furthermore, aberrations in phosphorylation of the RNA polymerase II (RNAP-II) and recruitment and polyadenylation of CstF factors (CstF77, CstF64, CstF50) shifts the balance to the membrane form rather to the secreted form of IgM (28, 60).

Up to now it is unknown how BCR signaling strength influences MZ and FO B cell development and homeostasis in humans. Murine models are contradictory, as mice that lack BTK show reduced total numbers of circulating B cells, while MZ B cells seemed to be less affected than the FO population (61). On the other hand, it has been shown that the presence of self-antigen-specific BCR, thus leading to strong BCR signaling, favors MZ B cell development (22). We herein describe novel hypomorphic BTK and BLNK mutations that were associated with reduced BCR signaling and a pronounced reduction in MZ B cells and an expansion of FO B cells. Our findings are supported by Tsiantoulas and colleagues, who show that low dose Ibrutinib treatment, a kinase inhibitor targeting BTK, lowers BCR signaling and promotes FO and restricts MZ B cell formation (4).

Furthermore, we could show that in patients with hypomorphic BTK and BLNK mutations BAFF-R and T-Bet, essential MZ B cell homeostasis factors are reduced. Previous reports identified that BCR signalosome signaling constitutes a positive autoregulatory loop that mediates crosstalk between BCR and BAFF-R (3).

We cannot however totally exclude that the observed reduction in MZ B cell numbers in selective IgM deficiency is a secondary phenomenon due to the lack of circulating IgM. This explanation seems unlikely as it has been demonstrated that BCR signaling is increased in $sIgM^{-/-}$ mice, and secreted IgM is known to negatively regulate BCR activation by acting as a decoy receptor for antigens that otherwise would be recognized

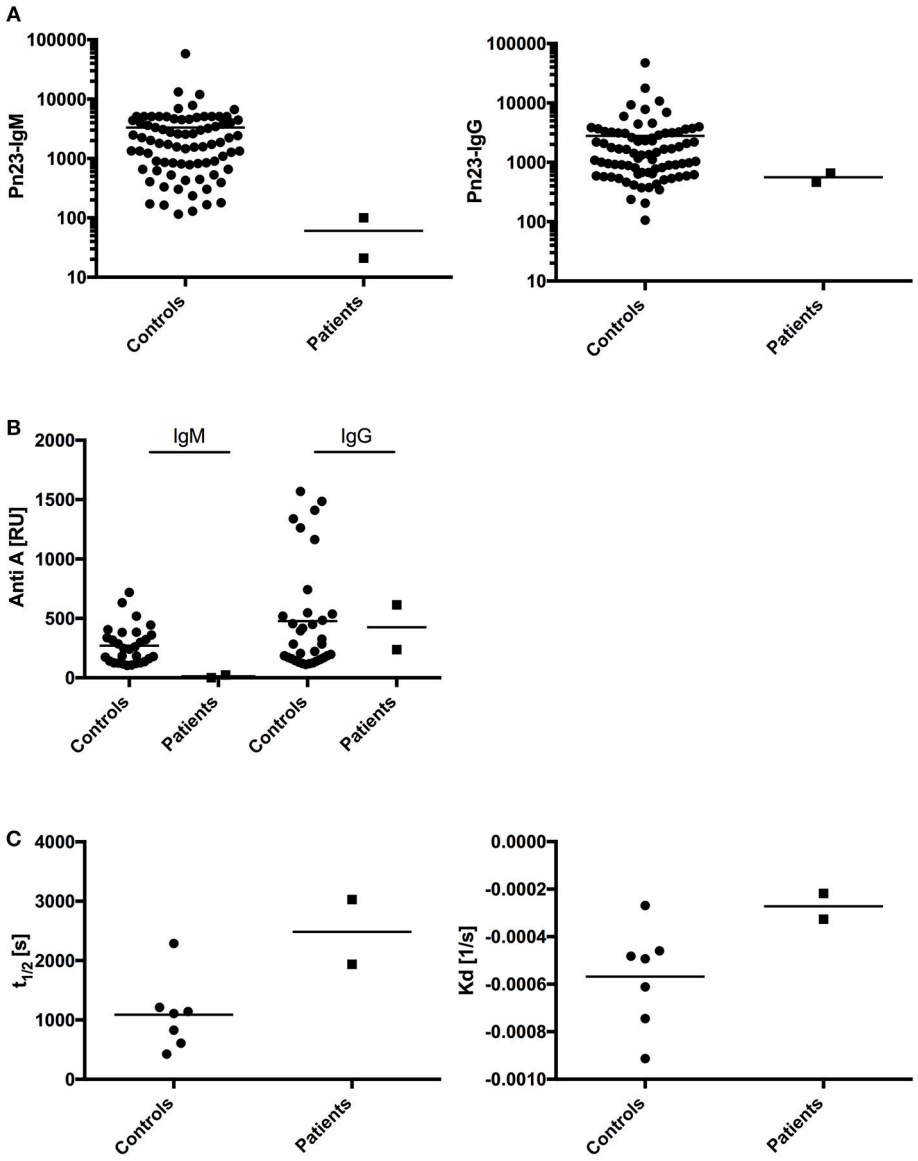

FIGURE 4 | Analysis of antibody response in patients with impaired BCR signaling.**(A)** In healthy individuals ($n = 80$, circles) and patients A and B ($n = 2$, squares) antibodies against pneumococcal polysaccharides (anti-PnPs) were determined by ELISA and presented as IgM–Pn23-antibody response (left panel) or IgG–Pn23-antibody response (right panel). Healthy controls and patient A were immunized with the PnPs vaccine Pneumo 23 Vaccine "Pasteur Merieux" (Pn23), and blood samples were drawn 4–6 weeks after vaccination. **(B**) Serum samples were diluted in HES-EP buffer (1:2) and samples were injected over the blood group A trisaccharide-coupled CM5 sensor chip. Amounts of anti-A antibodies were recorded as sensorgrams in resonance units (RU) against time in FC-I and FC-II. **(C)** Estimated affinity constant of blood group specific anti-A IgG antibodies is calculated as KD and $t_{1/2}$. Horizontal bars represent the mean.

by membrane-expressed BCR. Thus, the increased BCR signaling in $sIgM^{-/-}$ mice favors MZ B cell and restricts FO B cell development (4). In addition, EBV transformation is known to alter B- cell function by expressing LMP2A a viral protein that mimics the B-cell receptor (62). Due to limited patient's material we had to conduct experiments in EBV-LCLs, further studies in primary B-cells need to be conducted to confirm the observed alterations in BCR signalosome function in primary cells.

There is no orthologous human B-1 cell population and the phenotype of a human B subset that secrets natural IgM still remains debated (9–13). We cannot definitely pinpoint the lack of natural IgM antibodies to the impaired numbers and homeostasis of MZ-B cells found in our patients. Follow up studies need to address whether possible newly defined B1- B cell subsets are impaired in patients with hypomorphic BCR signalosome mutations. In addition, as IgG response in our patients seems to be intact, future studies should address whether there is a difference in recruitment of BTK and BLNK between the cytoplasmic tails of IgM and IgG, e.g., with ImageStream analysis or by immunostaining, as the

cytoplasmic tails of IgM BCR is shorter compared to IgG BCR (63).

In conclusion, our data indicate that selective IgM deficiency can be present in patients with hypomorphic BTK and BLNK mutations that dampen BCR signaling strength. We demonstrated that reduced BCR signaling is associated with perturbed MZ B-cell development and might impair formation of natural IgM antibodies in the blood group A/B/0 system by altering expression of essential MZ-B cell differentiation factors such as BAFF-R and T-bet.

AUTHOR CONTRIBUTIONS

CG designed the research, performed experiments, interpreted and analyzed the results, and wrote the manuscript; KS, AL-P, and IZ performed experiments, interpreted, and analyzed the results; MF and ME: interpreted and analyzed results; HW took overall responsibility for the research performed in this study and guided the writing of the manuscript. All authors have read and approved the contents of the manuscript and are accountable for all aspects of the work.

SUPPLEMENTARY MATERIAL

The Supplementary Material for this article can be found online at: https://www.frontiersin.org/articles/10.3389/fimmu.2018.02984/full#supplementary-material

Table S1 | Primary immunodeficiency genes sequenced.

Table S2 | Monoclonal fluorophore conjugated antibodies for flow cytometry.

REFERENCES

1. Rickert RC. New insights into pre-BCR and BCR signalling with relevance to B cell malignancies. *Nat Rev Immunol*. (2013) 13:578–91. doi: 10.1038/nri3487
2. Woyach JA, Johnson AJ, Byrd JC. The B-cell receptor signaling pathway as a therapeutic target in CLL. *Blood* (2012) 120:1175–84. doi: 10.1182/blood-2012-02-362624
3. Khan WN. B cell receptor and BAFF receptor signaling regulation of B cell homeostasis. *J Immunol*. (2009) 183:3561–7. doi: 10.4049/jimmunol.0800933
4. Tsiantoulas D, Kiss M, Bartolini-Gritti B, Bergthaler A, Mallat Z, Jumaa H, et al. Secreted IgM deficiency leads to increased BCR signaling that results in abnormal splenic B cell development. *Sci Rep*. (2017) 7:3540. doi: 10.1038/s41598-017-03688-8
5. Ehrenstein MR, Notley CA. The importance of natural IgM: scavenger, protector and regulator. *Nat Rev Immunol*. (2010) 10:778–86. doi: 10.1038/nri2849
6. Lobo PI. Role of natural autoantibodies and natural igm anti-leucocyte autoantibodies in health and disease. *Front Immunol*. (2016) 7:198. doi: 10.3389/fimmu.2016.00198
7. Grönwall C, Vas J, Silverman GJ. Protective roles of natural IgM antibodies. *Front Immunol*. (2012) 3:66. doi: 10.3389/fimmu.2012.00066
8. Nguyen TTT, Baumgarth N. Natural IgM and the development of B cell-mediated autoimmune diseases. *Crit Rev Immunol*. (2016) 36:163–77. doi: 10.1615/CritRevImmunol.2016018175
9. Griffin DO, Holodick NE, Rothstein TL. Human B1 cells in umbilical cord and adult peripheral blood express the novel phenotype CD20+ CD27+ CD43+ CD70-. *J Exp Med*. (2011) 208:67–80. doi: 10.1084/jem.20101499
10. Covens K, Verbinnen B, Geukens N, Meyts I, Schuit F, Van Lommel L, Jacquemin M, Bossuyt X. Characterization of proposed human B-1 cells reveals pre-plasmablast phenotype. *Blood* (2013) 121:5176–83. doi: 10.1182/blood-2012-12-471953
11. Tangye SG. To B1 or not to B1: that really is still the question! *Blood* (2013) 121:5109–10. doi: 10.1182/blood-2013-05-500074
12. Covens K, Verbinnen B, Jacquemin M, Bossuyt X. Response: extended analysis of microarray data does not contradict preplasmablast phenotype of human CD20+CD27+CD43+ cells. *Blood* (2013) 122:3693–4. doi: 10.1182/blood-2013-09-528091
13. Hu F, Zhang W, Shi L, Liu X, Jia Y, Xu L, et al. Impaired CD27+IgD+ B cells with altered gene signature in rheumatoid arthritis. *Front Immunol*. (2018) 9:626. doi: 10.3389/fimmu.2018.00626
14. Hobbs JR, Milner RD, Watt PJ. Gamma-M deficiency predisposing to meningococcal septicaemia. *Br Med J*. (1967) 4:583–6.
15. Louis AG, Gupta S. Primary selective IgM deficiency: an ignored immunodeficiency. *Clin Rev Allergy Immunol*. (2014) 46:104–11. doi: 10.1007/s12016-013-8375-x
16. Gupta S, Gupta A. Selective IgM deficiency-an underestimated primary immunodeficiency. *Front Immunol*. (2017) 8:1056. doi: 10.3389/fimmu.2017.01056
17. Chovancova Z, Kralickova P, Pejchalova A, Bloomfield M, Nechvatalova J, Vlkova M, et al. Selective IgM deficiency: clinical and laboratory features of 17 patients and a review of the literature. *J Clin Immunol*. (2017) 37:559–574. doi: 10.1007/s10875-017-0420-8
18. Cassidy JT, Nordby GL. Human serum immunoglobulin concentrations: prevalence of immunoglobulin deficiencies. *J Allergy Clin Immunol*. (1975) 55:35–48.
19. Kutukculer N, Gulez N. The outcome of patients with unclassified hypogammaglobulinemia in early childhood. *Pediatr Allergy Immunol*. (2009) 20:693–8. doi: 10.1111/j.1399-3038.2008.00845.x
20. Entezari N, Adab Z, Zeydi M, Saghafi S, Jamali M, Kardar GA, et al. The prevalence of Selective Immunoglobulin M Deficiency (SIgMD) in iranian volunteer blood donors. *Hum Immunol*. (2016) 77:7–11. doi: 10.1016/j.humimm.2015.09.051
21. Goldstein MF, Goldstein AL, Dunsky EH, Dvorin DJ, Belecanech GA, Shamir K. Selective IgM immunodeficiency: retrospective analysis of 36 adult patients with review of the literature. *Ann Allergy Asthma Immunol*. (2006) 97:717–30. doi: 10.1016/S1081-1206(10)60962-3
22. Wen L, Brill-Dashoff J, Shinton SA, Asano M, Hardy RR, Hayakawa K. Evidence of marginal-zone B Cell- positive selection in spleen. *Immunity* (2005) 23:297–308. doi: 10.1016/j.immuni.2005.08.007
23. Metzler G, Kolhatkar NS, Rawlings DJ. BCR and co-receptor crosstalk facilitate the positive selection of self-reactive transitional B cells. *Curr Opin Immunol*. (2015) 37:46–53. doi: 10.1016/j.coi.2015.10.001
24. Eibl N, Spatz M, Fischer GF, Mayr WR, Samstag A, Wolf HM, et al. Impaired primary immune response in type-1 diabetes: results from a controlled vaccination study. *Clin Immunol*. (2002) 103:249–59.
25. Geier CB, Piller A, Linder A, Sauerwein KMT, Eibl MM, Wolf HM. Leaky RAG deficiency in adult patients with impaired antibody production against bacterial polysaccharide antigens. *PLoS ONE* (2015) 10:e0133220. doi: 10.1371/journal.pone.0133220
26. Ban S a., Salzer E, Eibl MM, Linder A, Geier CB, Santos-Valente E, et al. Combined immunodeficiency evolving into predominant CD4+ lymphopenia caused by somatic chimerism in JAK3. *J Clin Immunol*. (2014) 34:941–953. doi: 10.1007/s10875-014-0088-2
27. Aspalter RM, Eibl MM, Wolf HM. Defective T-cell activation caused by impairment of the TNF receptor 2 costimulatory pathway in common variable immunodeficiency. *J Allergy Clin Immunol*. (2007) 120:1193–200. doi: 10.1016/j.jaci.2007.07.004
28. Takagaki Y, Manley JL. Levels of polyadenylation factor CstF-64 control IgM heavy chain mRNA accumulation and other events associated with B cell differentiation. *Mol Cell* (1998) 2:761–71.

29. Danner D, Leder P. Role of an RNA cleavage/poly(A) addition site in the production of membrane-bound and secreted IgM mRNA. *Proc Natl Acad Sci USA*. (1985) 82:8658–62.
30. Okoh MP, Vihinen M. Interaction between Btk TH and SH3 domain. *Biopolymers* (2002) 63:325–34. doi: 10.1002/bip.10049
31. Kabak S, Skaggs BJ, Gold MR, Affolter M, West KL, Foster MS, et al. The direct recruitment of BLNK to immunoglobulin alpha couples the B-cell antigen receptor to distal signaling pathways. *Mol Cell Biol*. (2002) 22:2524–35. doi: 10.1128/MCB.22.8.2524-2535.2002
32. Durandy A, Kracker S, Fischer A. Primary antibody deficiencies. *Nat Rev Immunol*. (2013) 13:519–33. doi: 10.1038/nri3466
33. Taguchi T, Kiyokawa N, Takenouch H, Matsui J, Tang W-R, Nakajima H, et al. Deficiency of BLNK hampers PLC-gamma2 phosphorylation and Ca2+ influx induced by the pre-B-cell receptor in human pre-B cells. *Immunology* (2004) 112:575–82. doi: 10.1111/j.1365-2567.2004.01918.x
34. Kim YJ, Sekiya F, Poulin B, Bae YS, Rhee SG. Mechanism of B-cell receptor-induced phosphorylation and activation of phospholipase C-gamma2. *Mol Cell Biol*. (2004) 24:9986–99. doi: 10.1128/MCB.24.22.9986-9999.2004
35. Fluckiger AC, Li Z, Kato RM, Wahl MI, Ochs HD, Longnecker R, et al. Btk/Tec kinases regulate sustained increases in intracellular Ca2+ following B-cell receptor activation. *EMBO J*. (1998) 17:1973–85. doi: 10.1093/emboj/17.7.1973
36. Foerster C, Voelxen N, Rakhmanov M, Keller B, Gutenberger S, Goldacker S, et al. B cell receptor-mediated calcium signaling is impaired in B lymphocytes of type Ia patients with common variable immunodeficiency. *J Immunol*. (2010) 184:7305–13. doi: 10.4049/jimmunol.1000434
37. Uslu K, Coleman AS, Allman WR, Katsenelson N, Bram RJ, Alugupalli KR, et al. Impaired B cell receptor signaling is responsible for reduced TACI expression and function in X-linked immunodeficient mice. *J Immunol*. (2014) 192:3582–95. doi: 10.4049/jimmunol.1203468
38. Huber K, Sármay G, Kövesdi D. MZ B cells migrate in a T-bet dependent manner and might contribute to the remission of collagen-induced arthritis by the secretion of IL-10. *Eur J Immunol*. (2016) 46:2239–46. doi: 10.1002/eji.201546248
39. Patenaude SI, Seto NOL, Borisova SN, Szpacenko A, Marcus SL, Palcic MM, et al. The structural basis for specificity in human ABO(H) blood group biosynthesis. *Nat Struct Biol*. (2002) 9:685–90. doi: 10.1038/nsb832
40. Milland J, Sandrin MS. ABO blood group and related antigens, natural antibodies and transplantation. *Tissue Antigens* (2006) 68:459–66. doi: 10.1111/j.1399-0039.2006.00721.x
41. Vetrie D, Vorechovský I, Sideras P, Holland J, Davies A, Flinter F, et al. The gene involved in X-linked agammaglobulinaemia is a member of the src family of protein-tyrosine kinases. *Nature* (1993) 361:226–33. doi: 10.1038/361226a0
42. Shillitoe B, Gennery A. X-Linked Agammaglobulinaemia: outcomes in the modern era. *Clin Immunol*. (2017) 183:54–62. doi: 10.1016/j.clim.2017.07.008
43. Wood PM, Mayne A, Joyce H, Smith CI, Granoff DM, Kumararatne DS. A mutation in Bruton's tyrosine kinase as a cause of selective anti-polysaccharide antibody deficiency. *J Pediatr*. (2001) 139:148–51. doi: 10.1067/mpd.2001.115970
44. Mitsuiki N, Yang X, Bartol SJW, Grosserichter-Wagener C, Kosaka Y, Takada H, et al. Mutations in Bruton's tyrosine kinase impair IgA responses. *Int J Hematol*. (2015) 101:305–13. doi: 10.1007/s12185-015-1732-1
45. Saffran DC, Parolini O, Fitch-Hilgenberg ME, Rawlings DJ, Afar DE, Witte ON, et al. Brief report: a point mutation in the SH2 domain of Bruton's tyrosine kinase in atypical X-linked agammaglobulinemia. *N Engl J Med*. (1994) 330:1488–91. doi: 10.1056/NEJM199405263302104
46. Kornfeld SJ, Haire RN, Strong SJ, Tang H, Sung SS, Fu SM, et al. A novel mutation (Cys145–>Stop) in Bruton's tyrosine kinase is associated with newly diagnosed X-linked agammaglobulinemia in a 51-year-old male. *Mol Med*. (1996) 2:619–23.
47. Lim L-M, Chang J-M, Wang I-F, Chang W-C, Hwang D-Y, Chen H-C. Atypical X-linked agammaglobulinaemia caused by a novel BTK mutation in a selective immunoglobulin M deficiency patient. *BMC Pediatr*. (2013) 13:150. doi: 10.1186/1471-2431-13-150
48. Yang W, Malek SN, Desiderio S. An SH3-binding site conserved in Bruton's tyrosine kinase and related tyrosine kinases mediates specific protein interactions *in vitro* and *in vivo*. *J Biol Chem*. (1995) 270:20832–40.
49. Drummond GB, Littlewood DG. Respiratory effects of extradural analgesia after lower abdominal surgery. *Br J Anaesth*. (1977) 49:999–1004.
50. Vihinen M, Nore BF, Mattsson PT, Bäckesjö CM, Nars M, Koutaniemi S, et al. Missense mutations affecting a conserved cysteine pair in the TH domain of Btk. *FEBS Lett*. (1997) 413:205–10.
51. López-Granados E, Pérez de Diego R, Ferreira Cerdán A, Fontán Casariego G, García Rodríguez MC. A genotype-phenotype correlation study in a group of 54 patients with X-linked agammaglobulinemia. *J Allergy Clin Immunol*. (2005) 116:690–7. doi: 10.1016/j.jaci.2005.04.043
52. NaserEddin A, Shamriz O, Keller B, Alzyoud RM, Unger S, Fisch P, et al. Enteroviral infection in a patient with BLNK adaptor protein deficiency. *J Clin Immunol*. (2015) 35:356–60. doi: 10.1007/s10875-015-0164-2
53. Lagresle-Peyrou C, Millili M, Luce S, Boned A, Sadek H, Rouiller J, et al. The BLNK adaptor protein has a nonredundant role in human B-cell differentiation. *J Allergy Clin Immunol*. (2014) 134:145–54. doi: 10.1016/j.jaci.2013.12.1083
54. Minegishi Y, Rohrer J, Coustan-Smith E, Lederman HM, Pappu R, Campana D, et al. An essential role for BLNK in human B cell development. *Science* (1999) 286:1954–1958.
55. Conley ME, Dobbs AK, Farmer DM, Kilic S, Paris K, Grigoriadou S, et al. Primary B cell immunodeficiencies: comparisons and contrasts. *Annu Rev Immunol*. (2009) 27:199–227. doi: 10.1146/annurev.immunol.021908.132649
56. Fu C, Turck CW, Kurosaki T, Chan AC. BLNK: a central linker protein in B cell activation. *Immunity* (1998) 9:93–103.
57. Chiu CW, Dalton M, Ishiai M, Kurosaki T, Chan AC. BLNK: molecular scaffolding through'cis'-mediated organization of signaling proteins. *EMBO J*. (2002) 21:6461–72. doi: 10.1093/emboj/cdf658
58. Cipe FE, Dogu F, Güloglu D, Aytekin C, Polat M, Biyikli Z, et al. B-cell subsets in patients with transient hypogammaglobulinemia of infancy, partial IgA deficiency, and selective IgM deficiency. *J Investig Allergol Clin Immunol*. (2013) 23:94–100.
59. Boes M, Esau C, Fischer MB, Schmidt T, Carroll M, Chen J. Enhanced B-1 cell development, but impaired IgG antibody responses in mice deficient in secreted IgM. *J Immunol*. (1998) 160:4776–87.
60. Takagaki Y, Seipelt RL, Peterson ML, Manley JL. The polyadenylation factor CstF-64 regulates alternative processing of IgM heavy chain pre-mRNA during B cell differentiation. *Cell* (1996) 87:941–52.
61. Cariappa A, Tang M, Parng C, Nebelitskiy E, Carroll M, Georgopoulos K, et al. The follicular versus marginal zone B lymphocyte cell fate decision is regulated by Aiolos, Btk, and CD21. *Immunity* (2001) 14:603–15. doi: 10.1016/S1074-7613(01)00135-2
62. Fruehling S, Longnecker R. The immunoreceptor tyrosine-based activation motif of Epstein-Barr virus LMP2A is essential for blocking BCR-mediated signal transduction. *Virology* (1997) 235:241–51. doi: 10.1006/viro.1997.8690
63. Liu W, Meckel T, Tolar P, Sohn HW, Pierce SK. Intrinsic properties of immunoglobulin IgG1 isotype-switched B cell receptors promote microclustering and the initiation of signaling. *Immunity* (2010) 32:778–89. doi: 10.1016/j.immuni.2010.06.006

Conflict of Interest Statement: The authors declare that the research was conducted in the absence of any commercial or financial relationships that could be construed as a potential conflict of interest.

DOI: 10.1111/jdv.14671 JEADV

ORIGINAL ARTICLE

Effect of intravenous immunoglobulin administration on erythrocyte and leucocyte parameters

A. Cicha,[1] M.B. Fischer,[2,3] A. Wesinger,[1] S. Haas,[1] W.M. Bauer,[1] H.M. Wolf,[4,5] K.M.T. Sauerwein,[4] B. Reininger,[1] P. Petzelbauer,[1] H. Pehamberger,[1] A. Handisurya[1,*]

[1]Department of Dermatology, Medical University of Vienna, Vienna, Austria
[2]Department of Health Science and Biomedicine, Danube University Krems, Krems an der Donau, Austria
[3]Department of Transfusion Medicine, Medical University of Vienna, Vienna, Austria
[4]Immunology Outpatient Clinic, Vienna, Austria
[5]Medical School, Sigmund Freud University Vienna, Vienna, Austria
*Correspondence: A. Handisurya. E-mail: alessandra.handisurya@meduniwien.ac.at

Abstract

Background Intravenous immunoglobulins (IVIG) are an attractive therapeutic tool for therapy of toxic epidermal necrolysis and severe forms of certain autoimmune diseases, including dermatomyositis, autoimmune blistering diseases, systemic vasculitis and lupus erythematodes.

Objectives Prompted by a case of IVIG-associated haemolytic anaemia, the effects of IVIG administrations on haematological parameters in patients with dermatological conditions were investigated.

Methods Erythrocyte and leucocyte parameters were retrospectively analysed in 16 patients who had received IVIG at doses from 1 to 3 g/kg bodyweight (n = 35 cycles). The influence of IVIG on leucocyte survival was determined *in vitro*.

Results Decreased absolute erythrocyte numbers, haemoglobin and haematocrit levels and a case of haemolytic anaemia were linked to transfusion of high-, but not low-dose IVIG. In contrast, leucopenia post-IVIG occurred in the vast majority of the recipients, unrelated to the administered IVIG amounts. *In vitro* investigations revealed a dose-dependent impairment of cell survival by IVIG in the neutrophil and monocyte, but not in the lymphocyte subpopulations. In several IVIG preparations, substantial amounts of blood group anti-A/anti-B antibodies were detected which could have accounted for the observed changes in the haematological parameters in our study cohort.

Conclusions IVIG products should be administered strictly according to indications. Commercially available IVIG products can contain blood group-specific antibodies that may induce haemolysis in some recipients. Monitoring of blood counts during applied IVIG therapy, especially when high doses are administered, is recommended.

Received: 26 July 2017; Accepted: 20 October 2017

Conflicts of interest

None declared.

Funding source

None declared.

Introduction

Human immunoglobulin (Ig) G concentrates are obtained from pooled plasma derived from up to 10 000 individual donors and reflect the complete spectrum of immune-specific antibodies, anti-idiotypic antibodies and natural antibodies.[1] These preparations predominantly contain purified, polyvalent IgG (>95%) with a physiological subclass distribution, but also varying trace amounts of IgA, IgM, IgE, soluble HLA-, CD4- and CD8-molecules, cytokines and adjuvants for the stabilization of Ig molecules.[1,2] The clinical use of intravenous IgG concentrates (IVIG) was initially limited to the replacement therapy in primary and secondary immunodeficiency disorders, but due to its immunomodulatory potential at higher doses, the indication was subsequently extended to the treatment of various autoimmune and inflammatory diseases.[3] In dermatology, IVIG is mainly recommended for the therapy of toxic epidermal necrolysis (TEN) and severe forms of certain autoimmune diseases, including dermatomyositis, autoimmune blistering diseases, systemic vasculitic syndromes and lupus erythematodes. Guidelines on the clinical use were developed.[4]

In general, IVIG administrations are well tolerated with mild and transient common adverse reactions, such as headache and

Table 1 Demographics of study participants

Patient No.	Age (year)/Sex	Blood group	Dermatologic conditions; concomitant diseases	IVIG dose (g/kg)	No. of IVIG administrations
1	32.3/m	B+	Ig deficiency, BD; type I allergy	1	1
2	55.3/m	AB+	CVIDS; GLILD	1	7
3	39.7/f	0+	Pemphigus vulgaris	2	3
4	65.2/f	B+	Dermatomyositis; type I allergy	2	1
5	43.1/m	n.a.	AD; type I allergy, allergic asthma, AA	2	2
6	29.5/m	A+	AD; type I allergy, allergic asthma	2	1
7	57.0/f	A+	Dermatomyositis	2	1
8	51.8/f	B+	Dermatomyositis; Hashimoto's disease	2	6
9	71.2/m	A+	Sneddon syndrome	2	1
10	31.0/m	n.a.	AD; allergic asthma	2	2
11	56.5/f	0+	Mixed connective tissue disease	2	1
12	66.3/f	B+	Bullous pemphigoid	2	1
13	61.3/f	n.a.	Epidermolysis bullosa	2	2
14	84.1/f	0+	Dermatomyositis	2	3
15	26.9/m	A+	SLE, vasculitis; psoriasis with PSA	2	1
16	53.5/m	n.a.	Toxic epidermal necrolysis	3	2

AA, alopecia areata; AD, atopic dermatitis; BD, Behçet's disease; CVIDS, common variable immunodeficiency syndrome; GLILD, granulomatous–lymphocytic interstitial lung disease; Ig, immunoglobulin; n.a., not available; PSA, psoriatic arthritis; SLE, systemic lupus erythematodes.

flu-like symptoms. In certain cases, anaphylactic symptoms, aseptic meningitis, thrombosis, renal failure, transfusion-related acute lung injury and haematological toxicities have been reported.[5] A well-documented, but under-recognized serious complication is IVIG-associated haemolysis, defined as a haemolytic episode occurring within 10 days of IVIG administration and characterized by a fall of ≥10 g/L in haemoglobin (Hb) levels, a positive direct antiglobulin test (DAT) and at least two of the following criteria: reticulocytosis, elevated levels of lactate dehydrogenase (LDH) or unconjugated bilirubin in serum, low haptoglobin, haemoglobinaemia, haemoglobinuria and the presence of spherocytosis in the absence of other possible causes of anaemia.[6] Over the past years, the worldwide incidence of IVIG-associated haemolysis has increased with rates ranging from 1.6% to 8.1%, most likely due to changes in the production technology of IVIG as well as expanded indications and more frequent application of high-dose therapy.[2,7–9]

Here, we report a case of IVIG-induced haemolytic anaemia, retrospectively evaluate the effects of high- and low-dose IVIG administration on erythrocyte and leucocyte parameters in recipients with underlying dermatologic diseases, and investigate the impact of IVIG on leucocyte survival *in vitro*.

Materials and methods

Participants′ demographics

This retrospective cohort study was approved by the Ethics Committee of the Medical University of Vienna, Austria (EK-2083/2016), and performed in accordance with the Declaration of Helsinki principles. Sixteen participants received a total of 35 IVIG cycles at cumulative doses from 1 to 3 g/kg bodyweight for various dermatologic disorders (Table 1) from January to November 2016 at the Department of Dermatology of the Medical University of Vienna. The numbers of men and women were equal, and the mean age of males (42.9 years; range 26.9–71.2 years) was lower than that of females (60.2 years; range 39.7–84.1 years). Data collected retrospectively from the medical records included patients′ age, sex, bodyweight, blood type, dermatologic conditions warranting therapy with IVIG, allergies, concomitant autoimmune and chronic inflammatory diseases, IVIG dosage and laboratory blood results routinely obtained prior to and after the IVIG administrations.

IVIG preparations

Due to the pharmacy purchasing practice of the Medical University of Vienna, all patients received the same liquid IVIG product, referred to as 'IVIG A'. An additional liquid preparation from another manufacturing company, referred to as 'IVIG B', was included in the *in vitro* experiments for comparison.

Determination of blood group-specific antibodies

The presence of blood group anti-A and anti-B antibodies in the IVIG preparations was determined using the 'LISS/Coombs' ID cards, containing polyspecific anti-human IgG, and the 'NaCl, Enzyme Test and Cold Agglutinins' ID cards, containing a neutral gel, of the DiaMed-ID Micro Typing System (DiaMed AG, Cressier FR, Switzerland).[10] Assays were performed following the manufacturer′s instructions. The IVIG samples were prepared in a twofold dilution series ranging from 1 : 2 to 1 : 512 and subsequently applied to the ID cards with either the DiaCell

ABO/I-II test cell suspension A1 or B. The titres that caused visible erythrocyte agglutination were immediately documented.

Evaluation of cell viability

Leucocytes from AB RhD-positive donors were recovered from leucoreduction system chambers of apheresis devices (TRIMA Accel®; Terumo BCT, Lakewood, CA, USA) after routine platelet apheresis. After lysis of erythrocytes by isotonic ammonium chloride, leucocytes were seeded in sextuplicates at a density of 1×10^6 in RPMI 1640, supplemented with 10% heat-inactivated fetal bovine serum, 1% penicillin/streptomycin and 30 ng/well recombinant human granulocyte colony-stimulating factor (Filgrastim; Amgen Inc., Thousand Oaks, CA, USA) and cultivated for 24 h in the absence or presence of IVIG A or B at doses ranging from 0.375 to 6 mg. For flow cytometry (FACS) analyses, cells were co-stained with anti-human CD3-APC (clone SK7), CD14-PE (clone MφP9) (both diluted 1 : 10; BD Biosciences, San Jose, CA, USA), CD15-FITC (clone SSEA-1, dilution 1 : 40; Biolegend, San Diego, CA, USA) and 7-aminoactinomycin D (dilution 1 : 10; Merck Millipore, Darmstadt, Germany). Experiments were independently repeated three times, measurements were taken using a FACSCalibur flow cytometer (BD Biosciences), and data were analysed using FlowJo v10.2 software (FlowJo; LLC., Ashland, OR, USA).

Statistical analyses

Statistical analyses (Mann–Whitney *U*-tests, two-sided *P*-value) were performed using the GraphPad Prism Software 6.00 for Windows. *P*-values of ≤0.05 were considered statistically significant.

Results

Case of haemolytic anaemia

We report on a case of a blood group A RhD-positive 26.9-year-old man who received the first cycle of IVIG in a cumulative high dose of 2 g/kg bodyweight (totalling 180 g) of IVIG product A over five consecutive days for his systemic lupus erythematodes with concomitant vasculitis. His medical history further encompassed psoriasis with psoriatic arthritis, coronary heart disease, arterial hypertension and hyperlipidaemia. Initially, the IVIG infusions were well tolerated. One day after completion of the cycle, however, the patient complained about severe headache and nausea. Subsequently, he developed haemoglobinuria, haematemesis and haematochezia. Laboratory evaluations showed a decrease of 37 g/L in Hb levels (baseline: 141 g/L; normal range [NR]: 120–160 g/L), of 1.4×10^{12}/L in absolute erythrocyte counts (RBC) (baseline: 5×10^{12}/L; NR: 3.8–5.2 $\times 10^{12}$/L) and of 11.4% in haematocrit (baseline: 41.4%; NR: 35.0–47.0%). Furthermore, increased absolute reticulocyte counts at 157×10^9/L (NR: 32–110 $\times 10^9$/L) and a positive DAT for monospecific IgG were noted. Together with elevated levels of LDH at 934 U/L (normal levels: <250 U/L) and of unconjugated and total bilirubin at 1.24 and 1.93 mg/dL (normal levels: <1 and <1.2 mg/dL), respectively, as well as low haptoglobin levels at <10 mg/dL (NR: 30–200 mg/dL), the requirements for the diagnosis of IVIG-associated haemolysis, severity grade 3, were met. Supportive treatment with systemic prednisolone for 3 days led to rapid improvement of the symptoms, and a blood transfusion was not required.

Table 2 Blood group-specific antibodies in the IVIG samples

IVIG product	Lot number	LISS/ Coombs A1	LISS/ Coombs B	NaCl A1	NaCl B
A	1	1 : 256	1 : 128	1 : 16	1 : 8
A	2	1 : 64	n.a.	1 : 4	n.a.
A	3	1 : 64	n.a.	1 : 8	n.a.
A	3	1 : 32	n.a.	1 : 4	n.a.
B	4	1 : 64	n.a.	1 : 8	n.a.

n.a., not available.

Blood group-specific antibodies in the IVIG preparations

An aliquot of the administered IVIG batch was examined for the presence of blood group-specific antibodies (Table 2) by an independent laboratory. Analysis revealed blood group anti-A1 and anti-B antibodies at titres of 1 : 256 and 1 : 128, respectively, which exceeded the allowed specifications of 1 : 64 set by the European Pharmacopoeia.[11] The regulatory authorities were notified.

Anti-A1 titres were additionally determined in two unrelated lots, in two individual flasks within the same lot, and in a different IVIG product (Table 2). In each sample, anti-A1 antibodies at titres within the specified pharmacopoeial limits were detectable. Titres of 1 : 64 and 1 : 32 measured within the same lot indicated some extent of intrabatch variability. Notably, anti-A1 titres of 1 : 4 to 1 : 8 were obtained in the native NaCl cards.

Analyses of erythrocyte parameters

Prompted by our case of haemolytic anaemia, we investigated the impact of IVIG on erythrocyte parameters in our study cohort (Table 3). A total of 35 IVIG cycles were categorized into either high-dose administrations (77.1%; $n = 27$), with cumulative doses of ≥2 g IVIG per kg bodyweight accounting for total doses of 110–240 g per cycle, or low-dose administrations (22.9%; $n = 8$), given at 1 g IVIG per kg bodyweight totalling 70–80 g per cycle.

Recipients of high-dose IVIG, compared to low-dose IVIG, exhibited significantly more often falls in Hb concentrations of ≥10 g/L, one major criterion of IVIG-associated haemolysis, and greater mean reductions from baseline ($P = 0.0088$). Similarly, decreased RBC and haematocrit levels were associated with high-, but not low-dose IVIG cycles, although the differences were insignificant ($P = 0.2718$ and $P = 0.0966$, respectively).

Table 3 Erythrocyte and leucocyte parameters after high- and low-dose IVIG administration

Parameter	High-dose IVIG		Low-dose IVIG	
	Decrease of ≥10 g/L[1] or ≥10%[2]	Mean reduction from baseline (%)	Decrease of ≥10 g/L[1] or ≥10%[2]	Mean reduction from baseline (%)
Erythrocyte parameters				
Haemoglobin	40.7% (11/27)[1]	7.5	0% (0/8)[1]	0.4
RBC	29.6% (8/27)[2]	6.3	0% (0/8)[2]	1.9
Haematocrit	25.9% (7/27)[2]	6.5	0% (0/8)[2]	0.9
Leucocyte counts				
WBC	85.2% (23/27)[2]	28.2	87.5% (7/8)[2]	25.6
Neutrophils	76.9% (10/13)[2]	20.9	71.4% (5/7)[2]	25.0
Eosinophils	61.5% (8/13)[2]	28.5	71.4% (5/7)[2]	14.5
Basophils	15.4% (2/13)[2]	15.4	14.3% (1/7)[2]	14.3
Lymphocytes	76.9% (10/13)[2]	14.3	85.7% (6/7)[2]	10.4
Monocytes	46.2% (7/13)[2]	+29.0	71.4% (5/7)[2]	22.8

The course of these parameters was monitored in more detail in a patient who had received 3 g/kg bodyweight IVIG plus 1 g/day systemic prednisolone on three consecutive days for TEN (Fig. 1a–c). After initiation of therapy, levels of Hb, RBC and haematocrit decreased from normal values to a nadir on day 2 post-IVIG, which lay below the respective lower limits of the normal reference ranges. The parameters recovered within the next 3 days after completion of the cycle, reaching normal values, and were restored to baseline around day 18.

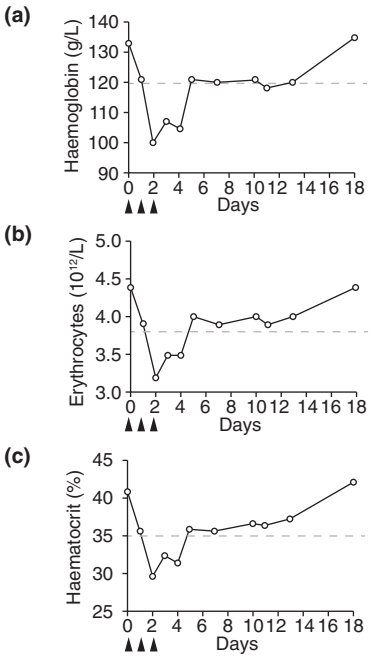

Figure 1 Course of erythrocyte parameters in a patient with toxic epidermal necrolysis after administration of a total of 240 g IVIG (3 g/kg bodyweight) over three consecutive days (indicated by arrows). Levels of haemoglobin (a), absolute erythrocyte counts (b) and haematocrit (c) were monitored over 18 days. Dashed lines depict the lower limit of the respective reference range.

In all study participants, assessment of the haemolytic parameters revealed that LDH, total and unconjugated serum bilirubin, haptoglobin and reticulocyte counts remained within normal ranges. Post-IVIG DATs were available in six cases, five of which were positive to IgG, none to complement; corresponding pre-IVIG data could not be obtained. No additional case of haemolytic anaemia occurred.

Analyses of leucocyte parameters

Absolute leucocyte counts (WBC) were decreased by ≥10% post-IVIG in the vast majority (85.7%; 30/35) of the participants. In contrast to the erythrocyte parameters, the changes were not associated with the transfused Ig amounts (Table 3), but equally affected recipients of high- and low-dose IVIG, suggesting that the impact of IVIG on leucocyte numbers is of qualitative rather than quantitative nature.

WBC differentials were available in a subset of the participants ($n = 20$), but no leucocyte subpopulation emerged as being most affected by IVIG (Table 3). Reductions of ≥10% in absolute numbers and mean decreases from baseline of the neutrophil, eosinophil, basophil and lymphocyte populations were similar after high- and low-dose IVIG administrations, and the observed differences were statistically not significant. In contrast to low-dose IVIG, high-dose administrations increased the percentage change in monocytes from baseline.

Survival of leucocyte subpopulations

Next, we investigated whether IVIG could impair leucocyte survival that could account for the marked reductions in absolute numbers. After cultivation of AB+ leucocytes for 24 h in the presence of increasing doses of IVIG, a dose-dependent decrease

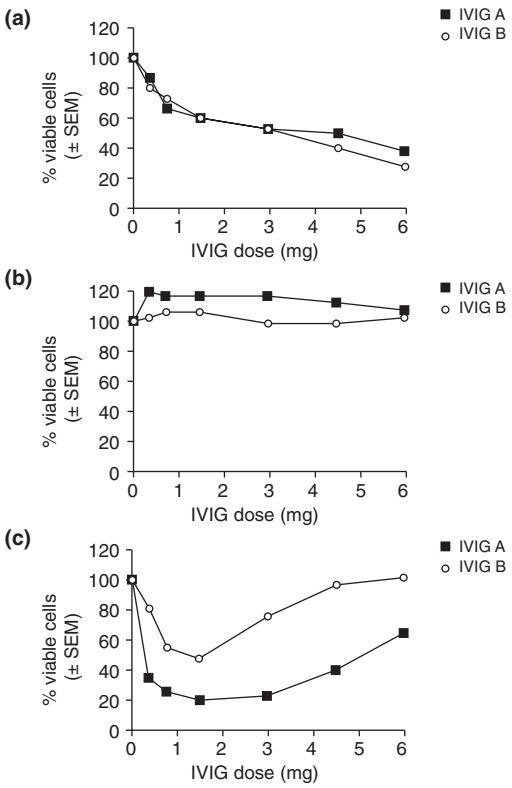

Figure 2 Effect of IVIG on the survival of leucocyte subpopulations *in vitro*. Survival of untreated cells (without IVIG) was set at 100% to exclude physiological, IVIG-unrelated cell death after cultivation for 24 h. The percentages of surviving CD15-positive neutrophils (a), CD3-positive lymphocytes (b) and CD14-positive monocytes (c) in the presence of increasing doses of IVIG A (black squares) or IVIG B (white circles) are given in relation to the respective untreated subpopulation. One representative experiment of four is shown.

in cell survival compared to non-IVIG-treated cells was predominantly observed in the neutrophil population. This effect was significant for both tested IVIG preparations (all $P < 0.01$, except for the lowest dose of 0.375 mg of IVIG A) (Fig. 2a). Less than 50% of viable cells were observed at a dose of 4.5 mg IVIG for both tested preparations compared to non-IVIG-treated cells. At the highest dose tested, 39.1% and 28.7% of the neutrophils remained viable when cultivated with IVIG A and B, respectively. Survival in the lymphocyte population, in contrast, remained relatively unaltered under the same conditions (Fig. 2b). Overall, no major differences were observed between the individual IVIG products A and B. Interestingly, IVIG were found to exert differential effects on monocyte survival that varied according to dose (Fig. 2c). In the presence of low amounts of IVIG, survival of monocytes was notably impaired compared to non-IVIG-treated cells, while at higher IVIG amounts viability gradually returned to baseline levels. The effects were observed with both IVIG preparations tested, but were more pronounced with IVIG A.

Discussion

Herein, we showed that haemolysis and leucopenia occurred in a substantial proportion of IVIG recipients with underlying dermatological disorders. Passively transferred alloantibodies against the blood group antigens A, B or Rhesus present in the IVIG products are thought to represent the major causative factor for IVIG-associated haemolytic reactions.[12–14] These antibodies have the potential to activate complement and to initiate intra- and/or extravascular destruction of erythrocytes.[15–17] Here, we demonstrated blood group anti-A and anti-B antibodies with titres exceeding the pharmacopoeial limits in the respective IVIG batch (Table 2; product A, lot 1) that had caused haemolytic anaemia in our blood type A-positive patient. Further screening of different IVIG preparations revealed the presence of blood group-specific anti-A antibodies, albeit within the regulatory levels, which could have accounted for the incidence of abnormal erythrocytic values in our study population, especially after administration of larger IVIG quantities (≥2 g/kg bodyweight) to recipients of blood types non-O. Although the frequency of blood group O approximates 40%–50% in the general population, only sporadic reports exist on IVIG-associated haemolysis in blood type O individuals.[7,14] Interestingly, we found signs of haemolysis in a substantial proportion (about 33%) of individuals with blood group O (data not shown), which pointed to additional factors present in polyvalent Ig preparations that may have exerted unexpected haemolytic activity. In this respect, we could demonstrate that the IVIG samples tested induced erythrocyte agglutination in the native NaCl DiaMed system (Table 2). The mechanism whereby IVIG directly induces erythrocyte agglutination is unknown; whether IgG dimers formed in pooled IVIG preparations could play a role, as these molecules could possibly facilitate bridging the gap between two or more erythrocyte antigens, a prerequisite to agglutination and subsequent complement activation, remains to be determined.[16] Along the line, variable amounts of IgG dimers were reported in commercially available IVIG products that can be influenced by manufacturing processes, excipients and storage conditions.[18,19] No association was found between a history of allergy or atopy and changes in erythrocyte parameters, in particular decreased haemoglobin levels, after low- and high-dose IVIG administrations.

Previous reports associated IVIG administrations with reduced leucocyte counts, particularly affecting neutrophils, but also monocytes and lymphocytes.[20–24] Certain antibodies, such as antineutrophil, atypical antineutrophil cytoplasmic, anti-Siglec-9 and anti-CD95 antibodies, present in IVIG were proposed to cause neutropenia in the recipients.[25–29] Furthermore, Ig aggregates, which display immune complex-like activity, were

shown to alter the expression of complement receptor 3 (CD11b/CD18) or Fcγ receptors (CD32, CD16) on neutrophil surfaces.[30] These antigens are involved in the induction of neutrophil oxidative burst and degranulation and contribute to the adherence to vascular endothelial cells, all together reducing the number of circulating cells. Previously, IVIG was shown to induce neutrophil degranulation *in vitro* already at low doses, however, in the presence of dimeric and polymeric IgG the effects were more pronounced.[31] The IgG dimers present in our IVIG products could have participated in and even promoted the observed decrease in WBC in our study cohort that occurred in low- and high-dose IVIG recipients. Furthermore, we could show marked induction of neutrophil death *in vitro* at IVIG doses that were reported to be achieved *in vivo*.[32] In our assays, significant neutrophil cell death was observed already at low IVIG concentrations, while in a previous study significant neutrophil death was observed only at higher doses.[29] However, the death-inducing effect of IVIG on neutrophils observed in both studies offers a plausible explanation for the low WBC counts in our study cohort, where post-IVIG serum IgG levels were measured at high concentrations of 28–52 mg/mL (data not shown).

In human monocytic cell lines as well as in purified blood monocytes, IVIG were previously reported to induce apoptosis via the Fas death receptor signalling pathway and activation of the caspase family of proteases.[33–35] Here, we found varying amounts of IVIG to differentially modulate monocyte survival, either decreasing cell viability at lower doses or promoting survival at higher doses. It is conceivable that higher amounts of IVIG induce changes in the phenotype (e.g. the receptor repertoire) and/or activation status of the monocytes that desensitize the cells to IVIG-induced apoptosis. Alternatively, alterations in the preponderance and/or activity of either agonistic or antagonistic anti-Fas antibodies and stabilizers in the IVIG products could preserve monocyte viability. However, as monocytes constitute a small fraction (up to 10%) of the total leucocyte population, the observed effects may not crucially affect overall leucocyte numbers.

In contrast to previously IVIG-induced apoptosis reported in human T lymphoblastoid cell lines, we did not observe impaired survival of the lymphocyte subpopulation *in vitro* in the presence of IVIG.[33,34] However, apart from differences specific to the respective IVIG products employed in the studies, these discrepancies could have resulted from diverging assay conditions, as we have not isolated the individual fraction from blood, but cultivated the whole leucocyte population in the presence of IVIG and discriminated the individual subpopulations by FACS analyses.

Taken together, several causative factors exist that could account for abnormal haematological values observed after IVIG administration. Predisposing factors can either be specific to the recipients, such as non-O blood types, underlying immune-mediated and inflammatory conditions, genetic determinants (secretor status, Fcγ or complement receptor polymorphisms, antigen density on erythrocytes) or the activation status of target cells, as well as to the transfused IVIG product. Product-related factors that can affect haematological parameters encompass the presence and levels of blood group-specific antibodies, of non-blood group antibodies and the conformational status of the Ig. In addition, characteristics of antibodies present in the IVIG products (ratio between agonistic and antagonistic activity, variable affinities for an antigen) and the use of certain excipients and impurities may influence the effects on erythrocyte and leucocyte populations in recipients. Therefore, patients should be monitored for alterations in their blood cell counts after IVIG administrations. While IVIG represent a valuable therapeutic tool, applications should be made with caution in the light of the possible severe side-effects and restricted to the recommended indications.[4]

Acknowledgement

We thank Lisa Weidner, MD, for the excellent technical assistance.

References

1 Kazatchkine MD, Kaveri SV. Immunomodulation of autoimmune and inflammatory diseases with intravenous immune globulin. *N Engl J Med* 2001; **345**: 747–755.
2 Barahona Afonso AF, João CM. The production processes and biological effects of intravenous immunoglobulin. *Biomolecules* 2016; **6**: 15.
3 Sewell WA, Kerr J, Behr-Gross ME, Peter HH, Kreuth Ig Working Group. European consensus proposal for immunoglobulin therapies. *Eur J Immunol* 2014; **44**: 2207–2214.
4 Enk AH, Hadaschik EN, Eming R *et al.* European Guidelines (S1) on the use of high-dose intravenous immunoglobulin in dermatology. *J Eur Acad Dermatol Venereol* 2016; **30**: 1657–1669.
5 Späth PJ, Granata G, La Marra F, Kuijpers TW, Quinti I. On the dark side of therapies with immunoglobulin concentrates: the adverse events. *Front Immunol* 2015; **6**: 11.
6 Canadian Blood Services. Important information regarding IVIG associated hemolysis. [WWW document] 2009. URL: http://www.bloodservices.ca/CentreApps/Internet/UW_V502_MainEngine.nsf/resources/CustomerLetters09/$file/CL_2009-02.pdf (last accessed: 26 July 2017)
7 Daw Z, Padmore R, Neurath D *et al.* Hemolytic transfusion reactions after administration of intravenous immune (gamma) globulin: a case series analysis. *Transfusion* 2008; **48**: 1598–1601.
8 Kahwaji J, Barker E, Pepkowitz S *et al.* Acute hemolysis after high-dose intravenous immunoglobulin therapy in highly HLA sensitized patients. *Clin J Am Soc Nephrol* 2009; **4**: 1993–1997.
9 Desborough MJ, Miller J, Thorpe SJ, Murphy MF, Misbah SA. Intravenous immunoglobulin-induced haemolysis: a case report and review of the literature. *Transfus Med* 2014; **24**: 219–226.
10 Fischer MB, Wolfram W, Binder CJ *et al.* Surface plasmon resonance analysis shows an IgG-isotype-specific defect in ABO blood group antibody formation in patients with common variable immunodeficiency. *Front Immunol* 2015; **6**: 211.
11 European Directorate for the Quality of Medicines and Healthcare. Human normal immunoglobulin for intravenous administration. European Pharmacopoeia. 7th Monograph 0918 ed. Council of Europe, Strasbourg, France, 2011: 4166–4168.
12 Gaines AR. Acute onset hemoglobinemia and/or hemoglobinuria and sequelae following Rh(o)(D) immune globulin intravenous

administration in immune thrombocytopenic purpura patients. *Blood* 2000; **95**: 2523–2529.
13 Quinti I, Pulvirenti F, Milito C *et al.* Hemolysis in patients with antibody deficiencies on immunoglobulin replacement treatment. *Transfusion* 2015; **55**: 1067–1074.
14 Bellac CL, Hottiger T, Jutzi MP *et al.* The role of isoagglutinins in intravenous immunoglobulin-related hemolysis. *Transfusion* 2015; **55**: S13–S22.
15 Padmore R. Possible mechanisms for intravenous immunoglobulin-associated hemolysis: clues obtained from review of clinical case reports. *Transfusion* 2015; **55**: S59–S64.
16 Flegel WA. Pathogenesis and mechanisms of antibody-mediated hemolysis. *Transfusion* 2015; **55**: S47–S58.
17 Kessary-Shoham H, Levy Y, Shoenfeld Y, Lorber M, Gershon H. In vivo administration of intravenous immunoglobulin (IVIg) can lead to enhanced erythrocyte sequestration. *J Autoimmun* 1999; **13**: 129–135.
18 Bleeker WK, Teeling JL, Verhoeven AJ *et al.* Vasoactive side effects of intravenous immunoglobulin preparations in a rat model and their treatment with recombinant platelet-activating factor acetylhydrolase. *Blood* 2000; **95**: 1856–1861.
19 Farrugia A, Poulis P. Intravenous immunoglobulin: regulatory perspectives on use and supply. *Transfus Med* 2001; **11**: 63–74.
20 Koffman BM, Dalakas MC. Effect of high-dose intravenous immunoglobulin on serum chemistry, hematology, and lymphocyte subpopulations: assessments based on controlled treatment trials in patients with neurological diseases. *Muscle Nerve* 1997; **20**: 1102–1107.
21 Berkovitch M, Dolinski G, Tauber T, Aladjem M, Kaplinsky C. Neutropenia as a complication of intravenous immunoglobulin (IVIG) therapy in children with immune thrombocytopenic purpura: common and non-alarming. *Int J Immunopharmacol* 1999; **21**: 411–415.
22 Matsuda M, Hosoda W, Sekijima Y *et al.* Neutropenia as a complication of high-dose intravenous immunoglobulin therapy in adult patients with neuroimmunologic disorders. *Clin Neuropharmacol* 2003; **26**: 306–311.
23 Niebanck AE, Kwiatkowski JL, Raffini LJ. Neutropenia following IVIG therapy in pediatric patients with immune-mediated thrombocytopenia. *J Pediatr Hematol Oncol* 2005; **27**: 145–147.
24 Lemos S, Jacob CM, Pastorino AC, Castro AP, Fomin AB, Carneiro-Sampaio MM. Neutropenia in antibody-deficient patients under IVIG replacement therapy. *Pediatr Allergy Immunol* 2009; **20**: 97–101.
25 Tam DA, Morton LD, Stroncek DF, Leshner RT. Neutropenia in a patient receiving intravenous immune globulin. *J Neuroimmunol* 1996; **64**: 175–178.
26 Jolles S, Deacock S, Turnbull W *et al.* Atypical C-ANCA following high dose intravenous immunoglobulin. *J Clin Pathol* 1999; **52**: 177–180.
27 Jarius S, Eichhorn P, Albert MH *et al.* Intravenous immunoglobulins contain naturally occurring antibodies that mimic antineutrophil cytoplasmic antibodies and activate neutrophils in a TNF alpha-dependent and Fc-receptor-independent way. *Blood* 2007; **109**: 4376–4382.
28 Von Gunten S, Schaub A, Vogel M, Stadler BM, Miescher S, Simon HU. Immunologic and functional evidence for anti-Siglec-9 autoantibodies in intravenous immunoglobulin preparations. *Blood* 2006; **108**: 4255–4259.
29 Altznauer F, von Gunten S, Späth P, Simon HU. Concurrent presence of agonistic and antagonistic anti-CD95 autoantibodies in intravenous Ig preparations. *J Allergy Clin Immunol* 2003; **112**: 1185–1190.
30 Voice JK, Lachmann PJ. Neutrophil Fc gamma and complement receptors involved in binding soluble IgG immune complexes and in specific granule release induced by soluble IgG immune complexes. *Eur J Immunol* 1997; **27**: 2514–2523.
31 Teeling JL, De Groot ER, Eerenberg AJ *et al.* Human intravenous immunoglobulin (IVIG) preparations degranulate human neutrophils in vitro. *Clin Exp Immunol* 1998; **114**: 264–270.
32 Bayry J, Lacroix-Desmazes S, Donkova-Petrini V *et al.* Natural antibodies sustain differentiation and maturation of human dendritic cells. *Proc Natl Acad Sci U S A* 2004; **101**: 14210–14215.
33 Prasad NK, Papoff G, Zeuner A *et al.* Therapeutic preparations of normal polyspecific IgG (IVIg) induce apoptosis in human lymphocytes and monocytes: a novel mechanism of action of IVIg involving the Fas apoptotic pathway. *J Immunol* 1998; **161**: 3781–3790.
34 Reipert BM, Stellamor MT, Poell M *et al.* Variation of anti-Fas antibodies in different lots of intravenous immunoglobulin. *Vox Sang* 2008; **94**: 334–341.
35 Gille C, Dreschers S, Spring B *et al.* Differential modulation of cord blood and peripheral blood monocytes by intravenous immunoglobulin. *Cytometry B Clin Cytom* 2012; **82**: 26–34.